UCLouvain

École polytechnique de Louvain

Development of a method of encapsulation of bacteria in polysaccharide nanotubes

Author: **Louise DUPONT**
Supervisors: **Alain JONAS, Karine GLINEL**
Readers: **Charles-André FUSTIN, Sophie DEMOUSTIER-CHAMPAGNE**
Academic year 2019–2020
Master [120] in Biomedical Engineering

Abstract

Bacteria evolving on the skin like *S. epidermidis* are currently considered as potential components for skin-care products because of the beneficial effects they provide. However, considering the risks associated with their proliferation, it is crucial to think of solutions, such as encapsulation, to enjoy the full clinical potential of these bacteria while controlling their development and limiting the risks of adverse outcomes. The encapsulation method used in this thesis was based on the use of bicompartmentalized microtubes having a sacrificial outer compartment erasable in order to liberate the inner microtube compartment. Such bicompartimentalized microtubes were fabricated by LBL deposition, on the pores of a porous track-etched membrane, of synthetic polyelectrolytes PVCL/PMAA for the outer compartment and a pair of oppositely charged polysaccharides ALG/CHI for the inner compartment. The ALG/CHI microtubes were then released by filtering NaCl aqueous solution at pH 6.5 through the membrane, causing the desintegration of the PVCL/PMAA sacrificial compartments. Finally, microtubes were collected by filtering the filtrate containing released microtubes on a porous support.

The first part of this thesis consisted in the optimization of the encapsulation method of fluorescent latex microparticles modelling bacterial cells. Different parameters were studied in order to increase the fraction of encapsulated microparticles. Results showed a larger fraction of encapsulated microparticles when using membranes with larger pore size. However, this parameter decreased the encapsulation efficiency of microtubes by making difficult or even impossible to close microtubes at their extremities. The deposition of a negatively charged ALG layer as last layer in the inner wall of microtubes allowed microparticles to penetrate deeper in the pores, increasing the amount of microparticles encapsulated. Despite the formation of a cake and aggregates of microparticles, the forced filtration process is easier, more rapid and more efficient to load the microparticles inside the pores of the membrane compared to the passive diffusion. The filtration conditions leading to the best results in terms of fraction of encapsulated microparticles were obtained for the filtration of 50mL of a microparticle suspension at the concentration of 3×10^6 microparticles/mL in 5 steps (5×10mL).

After establishing the optimal parameters for the encapsulation of microparticles, the second part of this thesis consisted in transposing and adapting this method on bacterial cells. The bacterial cells chosen for this study were *S. epidermidis* bacteria because of the large range of beneficial effects they provide to their hosts. Results of the first conducted assays showed very few microtubes containing bacteria, with many bacteria outside the microtubes. Few experiments could unfortunately be carried out for this part because of the health crisis (COVID-19). This part will therefore be the subject of a further study.

Aknowledges

First and foremost, I would like to thank the UCLouvain. Despite the unprecedented situation linked to the health crisis (COVID-19), the University organized itself rapidly to protect students from the spread of the virus while ensuring the completion of this academic year through the implementation of teaching activities in distance learning mode. The University has shown remarkable communication, ingenuity and support for its students. I am proud to belong to UCLouvain.

Then, I would like to express my very profound gratitude to my supervisors : Prof. Sophie Demoustier-Champagne, Prof. Karine Glinel and Prof. Alain Jonas ; who gave me the opportunity to work on this research project. I thank them for their help, for the time they have devoted to me and for their enlightened supervision throughout the writing of the thesis. Their advice and support helped me to carry out this research project and to write this thesis.

I would also like to acknowledge Wanlin Xu for her daily support, the planning of the work and her patience. She was a pillar for me to carry out this research project. She was always benevolent and tolerant of my mistakes. Thanks to her for sharing with me her passion, experience and knowledge for the research. It was a real pleasure to work with her on this research project and I wish her much success in pursuing her PhD. Finally, I thank her for reading my thesis. Her comments on this thesis were particularly valuable.

I would also like to thank the experts who contributed to the realization of this research project. They were competent, friendly, and open-minded. In particular, I express my gratitude to Marie-Christine Eloy for the confocal microscopy and Delphine Magnin for the SEM. Discussions with them were interesting and their words always friendly and reassuring.

Thanks also to the other Master and PhD students with whom I had the pleasure of sharing many moments in the laboratory. I especially thank Pierre for his good humor, his motivation and his enthusiasm for research. I also wish him much success in his thesis.

Finally, my further gratitude goes to my family : my mother Nathalie, my stepfather Philippe, my brother Julien, my sister Camille and my grandparents Viviane and Marc. I thank them for their love, support, and patience.

List of Figures

List of Tables

List of Abreviations

ALG : Alginate

CHI : Chitosan

CLSM : Confocal Laser Scanning Microscope

DCM : Dichloromethane

HA : Hyaluronan

HFIP : Hexafluoroisopropanol

LbL : Layer-by-Layer

MES : 2-(N-morpholino)ethanesulfonic acid

MT : Microtube

OD : Optical Density

PAA : Poly(acrylic acid)

PAH : Poly(allylamine hydrochloride)

PC : Polycarbonate

PDMS : Polydimethylsiloxane

PE : Polyester

PEG : Poly(ethylene glycol)

PEI : Poly(ethylenimine)

PEO : Poly(ethylene oxide)

PET : Poly(ethylene terephthalate)

PLL : Poly(L-lysine)

PMAA : Poly(methacrylic acid)

PNIPAAM : Poly(N-isopropyl-acrylamide)

PSS : Poly(styrene sulfonate)

PVCL : Poly(N-vinyl caprolactam)

PVPON : Poly(vinylpyrrolidone)

PVA : Poly(vinyl alcohol)

Rh : Rhodamine

SEM : Scanning Electron Microscopy

UV : Ultraviolet

Contents

Introduction

Context

Many distinct microbial communities, including fungi, viruses, protists and bacteria, exist in and on the human body and are known as the human microbiota. Specific microbiotae include the gastrointestinal, urogenital and respiratory tracts, the mouth and nasal cavities, and the skin. Each microbial community is characterized by its own structure and ecosystem determined by the body environment in which it exists. For instance, a gut community with a high biodiversity is related to a healthy state while a poor biodiversity of microbes is observed in patients presenting diseases such as Crohn's disease. However, the vagina microbiota of healthy individuals has a lower biodiversity compared to patients with vaginosis. The microbiota plays an important role in the human health state because it protects its host by preventing the colonization of pathogenic agents through the secretion of antimicrobial molecules, by sheer niche occupation or by regulating the host immune system. Moreover, the microbiota allows and facilitates host biological functions [5].

Disturbance to human microbiota can cause several pathologies, allergies and inflammatory disorders. The microbiota can be controlled by inhibiting the growth of pathogenic bacteria but also by promoting symbiotic bacteria. A typical example of treatment used to restore a healthy gut microbiota consists of delivering probiotics to the gastrointestinal tract. However, there are important challenges limiting the delivery of live-probiotics to the gut microbiota. Indeed, probiotic bacteria have to survive in an unfavourable environment due to acidic stomach conditions and presence of bile salts that are capable of deactivating probiotics. This can be achieved by encapsulating the probiotics [6]. Regarding the skin microbiota, there is an increasing interest in the use of living commensal skin bacteria as active components in skin-care products. In particular, many beneficial effects of the *Staphylococcus epidermidis* (*S. epidermidis*) have been highlighted in recent years. However, this commensal bacterium can also become dangerous when its growth is not controlled. Therefore, the realization of products designed to be interfaced with skin, including *S. epidermidis* or other living skin bacteria, requires the development of methods that allow bacteria to maintain their activity without risk of unwanted proliferation. One such method is the encapsulation of bacteria in a nanoporous material, so that nutrients and products can diffuse whereas the bacterial growth is delayed [7, 8].

Different strategies of cell encapsulation were explored and microorganisms so far encapsulated include yeast cells but also bacteria such as *Bacillus subtilis*, *Allochromatium vinosum*, *Lactobacillus acidophilus*, *Escherichia coli*, *Alcaligenes faecalis*, *Micrococcus luteus*, and *Bacillus coagulans*. Al-

though capsules composed from soft organic materials are the most widespread for cell encapsulation, capsules of hard materials such as gold, silica and calcium carbonate were also proposed [8]. In a typical encapsulation process, cells are trapped by solidifying or freezing droplets of a liquid solution in which the cells are suspended. Other interesting methods for cell encapsulation are coating and Layer-by-Layer (LbL) assembly [9]. The shape and the structure of the capsules play an important role because these properties can affect the survival of trapped cells. Among these, microtubes are particularly promising in the field of medicine because they constitute a suitable platform to support cell attachment and maintain enzymatic activity. Moreover, they have a high surface-to-volume ratio and good diffusion properties. Microtubes also enable to obtain a high cell internalization rate. Finally, microtubes are easily produced compared to other microstructures. For instance, they can be obtained by performing LbL deposition inside the pores of a porous membrane that acts as a template and released by dissolving the template [10]. This approach is called template-assisted LbL assembly and has become a popular method to produce various sorts of microtubes [11].

Given the importance of microbiota and the explosive development of microtechnologies, many researches are conducted to develop products containing encapsulated living microorganisms. For clinical applications, the encapsulation process has to be precisely mastered.

Objective and strategy

The objective of this thesis was to develop a method for the encapsulation of commensal skin bacteria, namely *S. epidermidis*, in polymeric microtubes able to preserve the metabolic activity of bacteria while reducing the risks of bacterial proliferation and bacterial infection. These microtubes were constructed inside the pores of a microporous membrane by combining hard templating with LbL assembly. Briefly, hard templating is based on the use of preformed templates on which a desired material is deposited. Subsequently, the template is removed, revealing the geometry of the templating structure in the deposited material [12]. Regarding LbL assembly, this approach consists of the successive adsorption of complementary materials interacting through electrostatic or nonelectrostatic interactions [11].

In order to achieve this objective, the following strategy was followed. First, the encapsulation method was optimized by using microparticles mimicking bacterial cells. Different experimental parameters were tested and their effects on the encapsulation process were analysed using a variety of characterization tools. Once optimized, the encapsulation method was applied and adapted on *S. epidermidis* bacteria.

Report structure

The first chapter deals with a bibliographic study on microbiota and especially on skin microbiota with a particular attention on *S. epidermidis* which was used in this project. Then, health benefits provided by *S. epidermidis* are described, as well as its evolution as a pathogen under certain conditions. Afterwards, most popular encapsulation methods for living microorganisms are presented. Among the methods described in this chapter, the emphasis is on the LbL assembly technique which was combined with hard templating in this study to construct the microtubes. Finally, this chapter ends with a brief presentation of the polymers used.

The second chapter details the experimental protocols for the fabrication of microtubes and the optimization of the encapsulation process to entrap polymer latex microparticles. In this chapter, the influence of different experimental parameters such as the diameter and the wall composition

of the microtubes, as well as the technology and conditions used to load microparticles into the microtubes, are presented and the encapsulation performance is analysed.

The third chapter deals with the transposition of the encapsulation method to bacterial cells. This chapter presents the results of a first attempt to encapsulate *S. epidermidis*, the problems encountered and the experiments which would potentially be interesting to carry out in the future to overcome the problems identified.

Finally, this report ends with a conclusion, which develops the improvements required for the encapsulation method before real-life application. This conclusion also critically analyses the method developed in this thesis and proposes eventual strategies to explore in the future to achieve the objective of this thesis.

CHAPTER 1

State of the art

The objective of the first section of this chapter is to briefly describe the skin microbiota and its roles, to present the driving forces of human skin microbiota diversity, to outline its positive and negative effects and lastly, to present some challenges related to the skin microbiota. Then, a second section is devoted to the purposes of cell encapsulation, to the different parameters to integrate in an effective encapsulation technique, and to an overview of the most popular encapsulation methods available for living microorganisms, with their respective advantages and limitations. The third section aims to describe the LbL assembly technique more in details. Finally, the last section of this chapter outlines the general properties and characteristics of the polymers used for the fabrication of microtubes in this study in which microparticles and bacteria will be entrapped. This section is especially important to better understand the experimental conditions selected at each step of the development of the encapsulation process.

1.1 Skin microbiota

All humans harbor a complex and dynamic population of microorganisms mainly composed of bacteria but also viruses, fungi and protists. These microorganisms form what is called the "microbiota". The microbiota composition varies according to the colonized surfaces, leading to different types of microbiotae : the intestinal microbiota, the skin microbiota, the urogenital microbiota, the respiratory microbiota, and the microbiota of the mouth and nasal cavities [8].

Skin, the largest human organ, is an important ecological niche inhabited by a multitude of microorganisms. The skin microbiota fulfits important functions in human health and is involved in the prevention of the entry of foreign pathogens and the regulation of the immune system [13]. The initial microbiota of an individual is formed from birth and depends on the mode of delivery. The vaginally-delivered babies have a microbiota more similar to their mother's vaginal microbiota while cesarean-delivered babies have a microbiota more similar to their mother's skin microbiota. The skin microbiota then evolves progressively, varying from one individual to another according to host demographics and genetics, human behavior, environmental characteristics and transmission events. This means that each individual has an unique skin microbiota. Furthermore, the skin microbiota differs within the same individual depending on its location on the body. Indeed, the surface of the skin is very diverse and can be seen as a set of different microenvironments with distinct pH, temperature, moisture, sebum content and topography [14]. Studies of discrete skin sites demonstrated that skin physiology, either moist, dry, or sebaceous, determines the mode of organization of microorganism communities [13]. This is why the skin microbiota of the hands is not the same as the face, underarms, feet or genitals ones. Regarding demographic characteristics, a greater bacterial diversity was found on the hand skin of women compared to men, which could be attributed to the fact that women are most often in contact with children and more frequently use cosmetic products.

Moreover, differences in hormones, sweat, sebum production and skin pH are also explanations for age and gender related differences. Genetic variations in the human genome can also play a role in skin microbiota composition. These genetic variations are for instance nucleotide deletion or insertion [15]. Behavioral characteristics including the use of medications and cosmetics, hygiene practices, diet and smoking are also able to influence the skin microbiota. In particular, excessive personal hygiene practices can reduce the diversity of microorganisms present on the skin and alter skin condition itself by changing its resistance, composition and pH. These changes have the consequence of disrupting the microbial community structure as well as the trade-off between its microbial colonizers and competitors [15]. Environmental factors such as temperature, moisture, and sun exposure have also been reported as having the capacity to alter skin microbiota. Seasons have been shown to cause some skin diseases, probably as a result of skin microbiota alterations in response to climate change. In addition, ultraviolet (UV) radiation can have microbiocidal effects on the skin microbiota and alter the skin condition. Finally, direct contact with other individuals or indirectly via objects in the environment can transmit transient microorganisms likely to disrupt the dynamics between resident microorganisms of skin microbiota [15].

All these microorganisms exploit their host for nutrients present on skin surface. More recent work has revealed that skin microorganisms interact to maintain the physical and immune barrier of skin under healthy homeostatic conditions [16]. The presence of commensal bacteria protects the host against pathogenic agents via two mechanisms. On the one hand, they compete for nutrients and available space, therefore reducing the risk that invasive pathogens proliferate. On the other hand, they can also produce bacteriocins, compounds able to kill other bacterial species. In addition to limiting pathogenic microbial invasion, the skin microbiota also promotes the expression of various immune factors. Consequently, any imbalance of skin microbiota, called "dysbiosis", would lead to skin disorders such as psoriasis, atopic dermatitis and acne. Skin dysbiosis results either from an increase or a reduction of microorganism diversity, which promotes the emergence of pathogenic agents and/or a disruption of immune responses. It is in this context that emerged the idea of promoting certain type of bacteria to restore the skin equilibrium and treat certain dermatological diseases [13].

While many microorganisms of the skin are beneficial, commensal or neutral, some can become pathogenic. This is especially the case of *S. epidermidis*, a highly important commensal bacterium of the skin. Examples of beneficial functions induced by *S. epidermidis* include the ability to regulate inflammation after injury, to enhance expression of host innate antimicrobial peptides and mature T cell response, to secrete antimicrobial compounds such as acidic substances that reduce skin pH, to prevent colonization of highly pathogenic bacteria like *Staphylococcus aureus* and even to counteract the influenza virus [8, 17]. However, *S. epidermidis* is also known as an important opportunistic pathogen and is one of the most frequent cause of nosocomial infections associated with catheters and other medical devices [18]. Indeed, *S. epidermidis* is a permanent and ubiquitous colonizer of human skin, which increases the probability of medical device contamination during insertion. Although infections caused by *S. epidermidis* only rarely develop into life-threatening diseases, they remain extremely difficult to treat because of their resistance to antibiotics and the formation of biofilms that promote virulence of this bacterial species and therefore further enhance their resistance to antibiotics and mechanisms of host defense [19].

1.2 Encapsulation methods of living microorganisms

1.2.1 Overview

Encapsulation refers to the process of entrapping a substance in a material. A large variety of methods exist for the encapsulation of biological microorganisms. The primary objective of the encapsulation is to protect microorganisms from their surroundings. This can be for additional protection against harsh conditions such as extreme pH, oxidizing media and UV radiation to preserve cell functionality. For instance, encapsulation of probiotic bacteria aims to protect them against acidic stomach conditions and bile salts which are able of deactivating probiotics [6]. In addition to provide cell protection, encapsulation can provide new magnetic, electrical or mechanical properties for the encapsulated microorganisms [20]. Another reason for which encapsulation is useful is to control release of the encapsulated active elements over an extended timescale. In this case, encapsulation is particularly interesting for pharmaceutical applications such as drug delivery. In the case of bacteria encapsulation, the objective is to alleviate the problem of contamination by controlling the metabolic activity and growth of encapsulated bacteria. Indeed, remember that the purpose of the thesis is to develop microtubes able to preserve the metabolic activity of bacteria while reducing the risks of bacterial proliferation and bacterial infection [9, 7].

The choice of materials used for encapsulation is crucial because they affect the properties of trapped microorganisms. The capsules can have different chemical compositions ranging from hard materials to soft organic materials. Hard materials include silica [21], calcium carbonate [22], calcium phosphate [23], gold [1] and metal-organic frameworks [24]. Regarding soft materials, the polymers that are generally used for encapsulation can be natural or synthetic. Natural polysaccharides include alginate (ALG), carrageenans, agar/agarose, gellan gum, guar gum, acacia gum, starch, starch-based materials, cellulose, pectin, chitosan (CHI), polypeptides such as poly(L-lysine) (PLL), proteins like gelatin, lipids or other biopolymers like lignin [9, 25]. Among these, ALG is generally used for biomedical applications because of its simple and rapid gelation process, its excellent biocompatibility and biodegradability [26]. Besides, a large range of synthetic polymers are well known to be suitable encapsulating materials such as polyurea, polyurethanes, polyamides, polyesters, polyvinylalcohol, polyacrylates, silica-based polymers as well as co-polymers [9, 25]. All these materials are distinguished by several characteristics that are of particular importance for the application of encapsulation methods to microorganisms. These characteristics can be divided in three categories : the physico-chemical properties, the economic factors, and the safety and quality. Physico-chemical properties include molar mass and distribution, counter ions, gelation mechanism, pH, viscoelastic properties, hydrophobicity, as well as primary, secondary and tertiary structures of the polymers. Economic factors refer to costs which mostly depend on the intended application. Safety and quality include toxicity, degradability, FDA or EPA approval and source of the material used for encapsulation [9]. Depending on their nature, polymers can respond to a large number of parameters of their physico-chemical environment such as pH, temperature, salts, sugars, solvents, CO_2, light, electric current, magnetic fields, etc. These factors must also be taken into account because they affect characteristics and properties of polymers [9].

Depending on the encapsulation method, the capsule used to trap living microorganisms can have different structures. Among these, the spherical design is the most popular shape because of its high surface/volume ratio which minimizes the diffusion path between microorganisms and external environment. The capsule can also have multiple walls and be compartmentalized. The thickness and shape of the capsule are important parameters that affect the survival of encapsulated microorganisms. The membrane of the capsule has to be sufficiently resistant to not break under mechanical stresses. The capsule thickness also influences the diffusion mechanisms essential for maintaining mi-

croorganisms viability. Thin membranes have the advantage of facilitating the diffusion of nutrients, oxygen and waste but remain very fragile and require careful handling. Thick capsules are more resistant but tend to have a central necrotic area due to nutritional deficiencies caused by the long diffusion path [25].

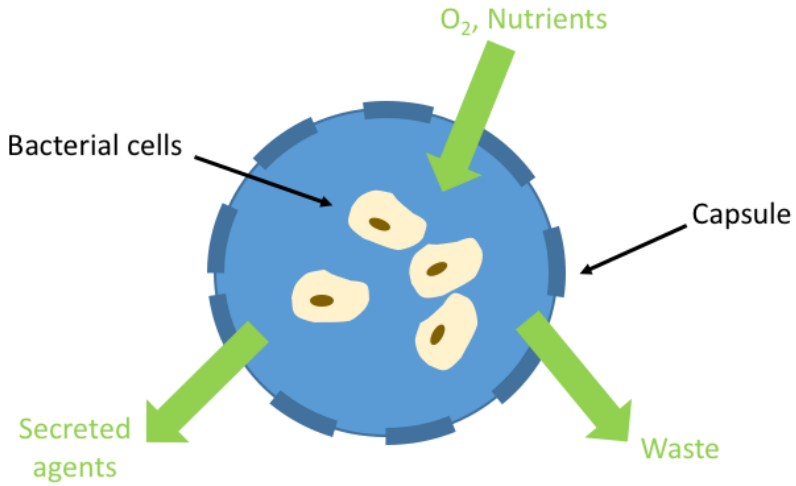

Figure 1.1: Encapsulation of living microorganisms.

1.2.2 Dripping

Dripping is a very simple encapsulation method that consists of extruding a polymer solution in which microorganisms are dispersed through a nozzle, leading to the formation of droplets. Then, the droplets are hardened via diverse gelation mechanisms depending on the encapsulating material. Thermally sensitive gels such as gelatin or agarose are formed through a temperature change [9]. In this case, a heated polymer solution containing the living microorganisms is dropped into a cold collecting solution. The decrease of temperature allows the gelation of the polymer droplet and subsequently the formation of a capsule surrounding the living microorganisms. Figure 1.2 shows the dripping principle based on thermal gelation.

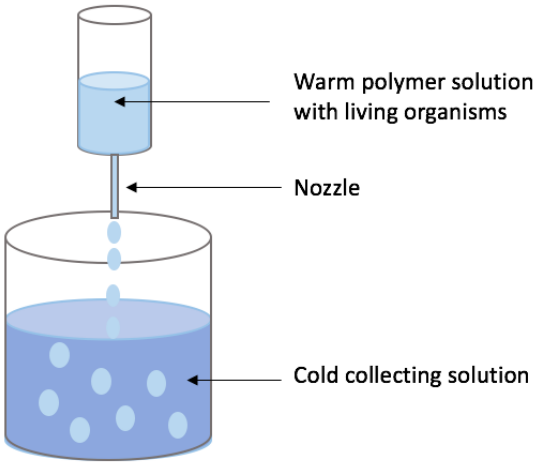

Figure 1.2: Dripping based on thermal gelation.

As for photoresistive materials such as modified poly(ethylene glycol) (PEG), they harden under UV light exposure which causes the crosslinking of the material [25]. Unfortunately, both thermal and photocuring process can affect the viability or physiology of the encapsulated microorganisms. This is why safer gelation methods for the encapsulation of living microorganisms have been developed such as ionic gelation. The principle consists of dropping a polymer solution containing microorganisms into a solution containing ionic crosslinking agents, for instance tripolyphosphate anions (for cationic polymer) or calcium cations (for anionic polymer) [27, 28]. These crosslinkers crosslink the charged polymer chains in order to form a physical gel. Due to the diffusion of the crosslinking agents, the crosslinking occurs from the outside to the inside of the droplet and allows the formation of full beads of gel, as shown in figure 1.3. For instance, calcium ALG beads produced by ionic gelation were used for the encapsulation and delivery of diverse microorganisms, mainly fungi (*Alternaria*, *Fusarium*, *Phyllosticta spp.*, *Trichoderma*, *Gliocladium*, *Talaromyces* and *Penicillium spp.*) but also bacteria (*Pseudomonas* and *Bacillus spp.*) in order to control pathogen agents and nematodes [29]. Lifeng Qi et al. prepared CHI nanoparticles based on the ionic gelation of CHI with tripolyphosphate anions in order to evaluate the antibacterial activity of CHI nanoparticles against *Escherichia coli*, *Salmonella choleraesuis*, *Salmonella typhimurium*, and *Staphylococcus aureus* [30].

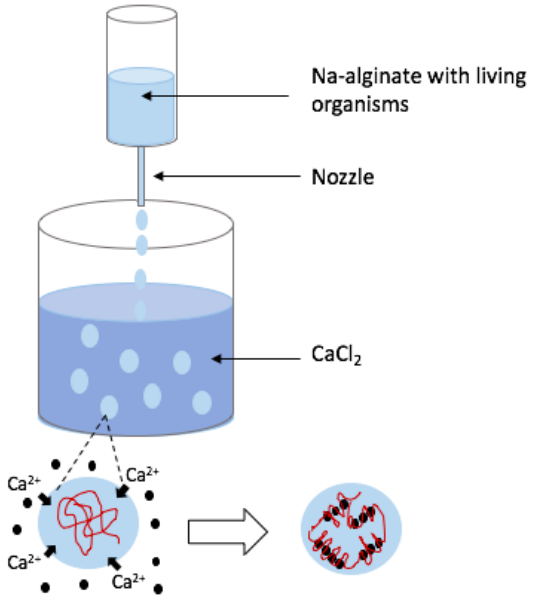

Figure 1.3: Ionic gelation : crosslinking from the outside to the inside.

It is also possible to fabricate hollow beads by simply interchanging the solutions, i.e., the crosslinking solution is dropped into the solution containing microorganisms. In this case, the crosslinkers diffuse from the core to the surface and the crosslinking occurs from the inside to the outside [9], as illustrated in figure 1.4. Patel and Vorlop used this method to encapsulate an entomopathogenic nematode into calcium ALG hollow beads [31].

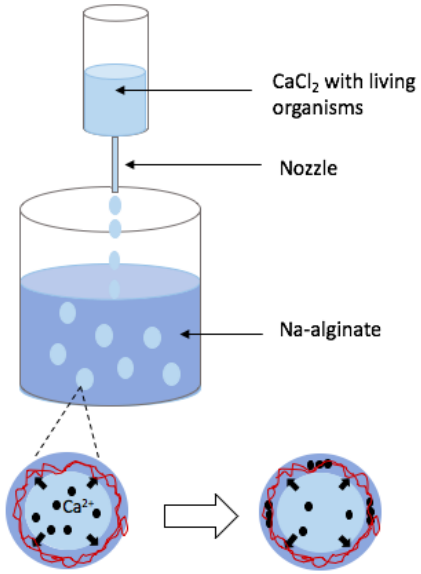

Figure 1.4: Ionic gelation : crosslinking from the inside to the outside.

Dripping has numerous advantages, in particular its experimental simplicity and the possibility to get a narrow distribution of particle sizes. However, dripping has the drawback to be dependent on

the diameter of the needle used to form droplets, resulting in relatively large beads. In addition, the speed of droplet formation is a significant limiting factor regarding the production capacity [32].

1.2.3 Spray-drying

Spray-drying is a method requiring both a strict selection of the encapsulating materials and an optimization of the operating conditions. In this technique, represented in the figure 1.5, a liquid containing the microorganisms to encapsulate is sprayed in the form of small droplets into a hot air stream which allows evaporation of the solvent, thereby leaving a dried particle. The liquid feeding the sprayer can be a solution, a suspension or an emulsion. Carbohydrates (starches, corn syrup solids, maltodextrins, etc), polysaccharides (gum arabic, ALG, carragenans, etc) and proteins (gelatin, milk proteins, etc) are typical materials used for encapsulation by spray-drying [33]. Although spray-drying is highly reproducible and allows a high capacity of production, this method has many drawbacks from the viewpoint of biological control such as the variability in particle shape and size distribution, high temperatures and fast drying rates that are not compatible with the survival of living microorganisms sensitive to high temperature and drying [9]. However, it was reported that incorporation of protectants in the solution prior to drying improves microorganism survival [34]. For instance, the addition of trehalose, non-fat milk solids and/or adnitol, growth promoting factors including diverse probiotic/prebiotic combinations and granular starch have been reported to enhance culture viability after drying [35]. In order to obtain an effective encapsulation, optimal spray-drying conditions must be used. The main parameters to optimize in spray-drying include the feed temperature, air inlet temperature and air outlet temperature. In addition to process parameters, the biology of microorganisms to be encapsulated (species and strain type, adaptation to heat, etc) is also important. In their study, Gardiner et al. demonstrated a strain-dependent decline of viable counts of *Lactobacillus paracasei NFBC* and *Lactobacillus salivarius UCC* as the outlet temperature increased, the latter strains being the most temperature sensitive [36]. As an alternative, freeze drying can be used to reduce thermal damage but it is less advantageous in terms of cost, energy, and throughput than spray-drying [37].

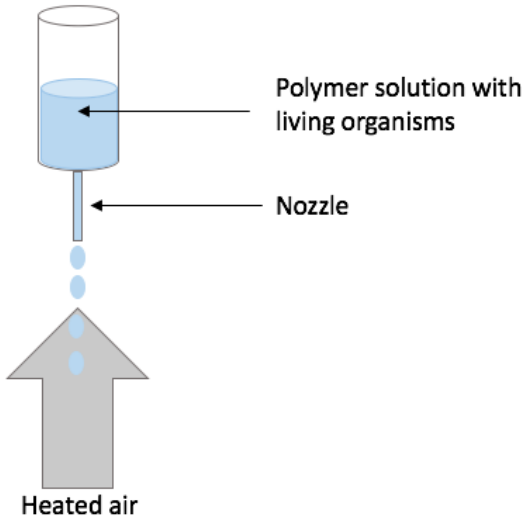

Figure 1.5: Scheme of the spray-drying method.

1.2.4 Emulsification

An emulsion is a heterogeneous mixture of two non-miscible liquids, one being dispersed as small droplets in the other. These two substances do not mix spontaneously but one of them is dispersed in the second phase in the form of droplets through specific operations (agitation, mixing, addition of emulsifiers). These droplets are solidified by different gelation mechanisms. The encapsulating materials typically used for emulsification are hydrocolloids [34]. In the case of thermal gelation, an aqueous solution of a thermoresponsive polymer such as κ-carrageenan, agarose or agar, containing living microorganisms is emulsified in hot oil. Then, the temperature is decreased, which causes the gelation of the polymer and consequently, the hardening of the droplets formed by emulsion [38]. Ionic gelation can also be used to solidify droplets formed by emulsion. In this case, a mixture of polymer, typically sodium ALG, living microorganisms and an insoluble calcium salt are emulsified in an oil phase. Then, the pH of the emulsion is decreased by addition of acetic acid, leading to the release of calcium ions from the salt and the subsequent crosslinking of the polymer [39]. Hardening of droplets can be also achieved by polymerization reaction. The principle of interfacial emulsion polymerization consists of emulsifying living microorganisms and a hydrophilic monomer in an organic phase containing an emulsifier. Then, a hydrophobic monomer and a initiator are added, which induces a polymerization reaction at the liquid/liquid interface and forms a wall on the surface of droplets [40]. Emulsification has the advantages of being easy to scale-up and producing smaller particles compared to dripping. Capsule sizes ranging from a few micrometers to 1 millimeter can be produced but with a high dispersion. The main drawbacks of emulsification technique for biological control include the use of emulsifying agents and/or monomers and sometimes reaction conditions which are often toxic to microorganisms [9, 27]. Examples of bacteria strains encapsulated include *Lactobacillus rhamnosus*, *Lactobacillus paracasei*, *Lactobacillus delbrueckii ssp. Bulgaricus*, *Lactobacillus acidophilus*, *Bifidobacterium lactis*, *Bifidobacterium infantis*, *Lactobacillus casei* and *Bifidobacterium bifidum* [35].

1.2.5 Micromolding

Capsules entrapping living microorganisms can be fabricated by replication of a micromold, typically based on polydimethylsiloxane (PDMS, in soft polymer) stamp. Several micromolding methods are available. In the micropatterning approach, a photosensitive polymer, for instance hyaluronic acid (HA) modified with photoreactive methacrylates [1], containing the microorganisms to encapsulate, is placed onto a methacrylated glass slide. Then, the PDMS mold is brought into contact with the solution and gently pressed. Finally, the PDMS micromold is exposed to UV light, which causes the crosslinking of the polymer. After exposure, the PDMS micromold is peeled from the surface, leaving an array of regularly shaped microstructures containing microorganisms inside (for instance, square blocks as shown in figure 1.6) [9, 1].

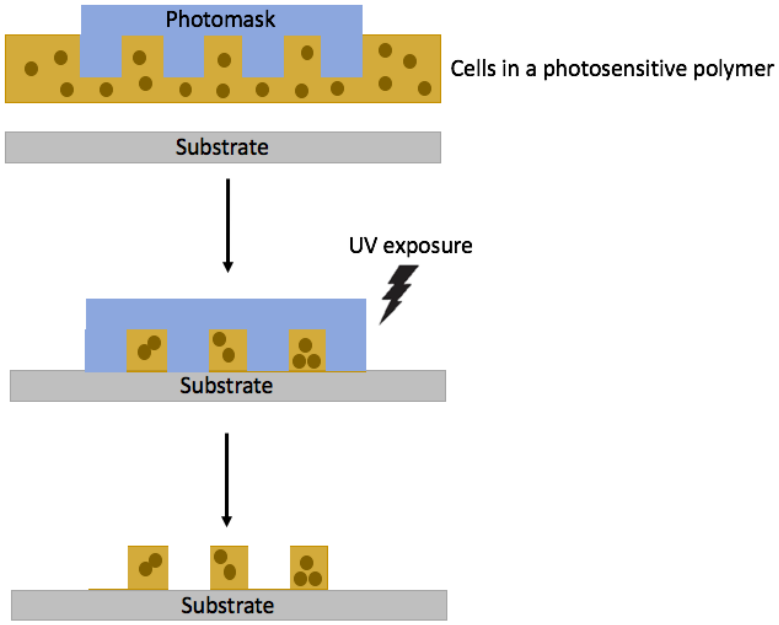

Figure 1.6: Scheme of the micropatterning process. Adapted from [1].

1.2.6 Electrospinning

Electrospinning has been exploited to encapsulate living microorganisms. This technique consists of using an electric force to generate ultrafine fibers of polymers with diameters varying from less than 100nm to more than 1μm. In this method, a polymer solution is supplied from a spinneret and forms a pendant droplet at the spinneret exit. When an electrical field is applied, the droplet becomes charged and electrostatic repulsion counteracts the surface tension, which causes the stretching of the droplet. At a critical point, a jet emerges in a nearly straight line. Due to an electrically-induced bending instability, the bent sections of the jet elongate. The solvent evaporates, the jet dries and solidifies, resulting in as-spun fibers that are deposited on the counter electrode [41]. Electrospinnable polymeric materials include natural polymers such as CHI, collagen, gelatin, elastin, HA and cellulose but also synthetic polymers like poly(lactic acid), polycaprolactone, polyvinyl alcohol (PVA) and polyethylene oxide (PEO) [42]. The selection of an appropriate solvent is crucial because it influences the physical properties of the polymer solution, including surface tension, electrical conductivity, and viscosity. The solvent must respond to the following requirements : (i) it must be able to dissolve the polymer to form a solution with a suitable concentration and viscosity, (ii) it must be volatile enough to allow a massive evaporation before the electrospun fibers reach the collector and (iii) it must be able to carry electrical charges. Generally, natural polymers like collagen, CHI and cellulose are combined with hexafluoroisopropanol (HFIP) or tetrafluoropropanol as a solvent for electrospinning while synthetic biodegradable polymers use solvents such as dichloromethane (DCM), acetone, dimethylformamide and HFIP. The residual solvent remaining in the electrospun fibers must be as small as possible because most of solvents that are generally used for electrospinning of polymeric materials are toxic to cells. Zussman et al. studied the encapsulation of bacteria (*Escherichia coli*, *Staphylococcus albus*) and viruses (T7, T4, λ) in nanofibers by electrospinning a mixture of bacteria and viruses suspension and PVA in water solution [43]. In their study, it was demonstrated that viruses and bacteria remain viable after the electrospinning process.

1.2.7 Sol-gel

Sol-gel is a method consisting in the chemical transformation of a system from an inorganic colloidal suspension (sol) into a three-dimensional gelatinous network structure (gel). Then, the obtained gel is subjected to drying process to obtain the final material. The use of inorganic matrices offers several advantages over other polymeric matrices used for the encapsulation of microorganisms, including high mechanical and thermal resistance and low cost. Moreover, they are chemically inert and are not affected by contact with organic solvents and/or microbial attacks [44]. Nevertheless, microorganisms encapsulated by sol-gel are exposed to stresses due to gel formation and the drying process that can lead to the shrinkage of the matrix and damage the trapped microorganisms [45]. Coiffier et al. immobilized bacteria in silica gels and demonstrated that they conserved their enzymatic activity [46]

1.2.8 Layer-by-layer assembly

The LbL assembly technique consists of forming multilayer films by the successive adsorption of diverse materials on a substrate, occurring either via electrostatic or nonelectrostatic interactions. The materials can be deposited on the substrate through diverse approaches such as dip-coating, spraying, and spin-coating. The LbL process using dip-coating is shown in figure 1.7. Each deposition is followed with rinsing steps in order to remove excess of materials that have not been adsorbed. The deposition cycles are repeated as many times as desired. Electrostatic interactions between oppositely charged materials such as polycations and polyanions are the most important driving force in LbL assembly. Moreover, the deposited polymer chains can also interact via hydrogen bond, covalent bond, and biospecific interactions among a variety of functional groups. In addition, it is possible to control the structure and properties of LbL films by changing the assembly conditions such as the nature of the solvent, pH and ionic strength. Among the main advantages of LbL assembly technique, we can cite its experimental simplicity, its low cost, as well as its compatibility with biological entities because of the use of aqueous solutions [47]. Finally, LbL assembly can be combined with the hard-templating technique, for instance, by performing deposition on supports such as porous substrates to form tubular structures [10]. Because the microtubes developed in this study to encapsulate *S. epidermidis* are fabricated by membrane-templated LbL assembly, we describe this method in more detail in the section 1.3.

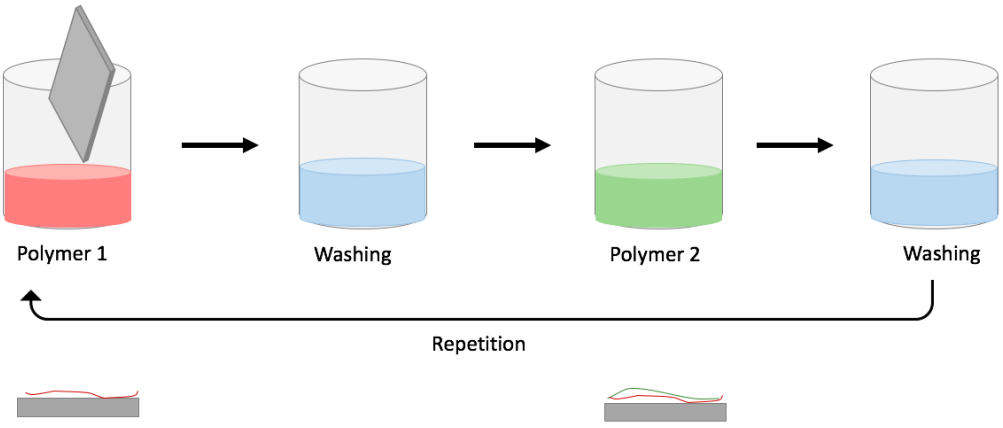

Figure 1.7: LbL assembly based on dip-coating.

1.3 Layer-by-Layer assembly

1.3.1 Overview

LbL assembly is a cyclic process to fabricate multilayer films with well-defined thickness, composition and structure onto a large range of substrates. The main advantages of LbL assembly are its simplicity, efficacy, reproductibility, flexibility and versatility. LbL assembly can be applied on a large variety of substrates including planar and porous surfaces, colloidal particles, and cylindrical structures. Moreover, LbL assembly is suitable for a large range of surface chemistry. Lastly, a wide range of building blocks can be incorporated into the multilayer films including polymers, clays, dyes, metal oxides, and other components such as living cells, which allows the addition of new functionalities and properties. It is also important to mention that LbL assembly is based on the use of aqueous solutions and therefore is compatible with living entities. LbL assembly is based on the successive adsorption of interacting materials on a surface, occurring either via electrostatic or nonelectrostatic interactions. Each deposition of a material layer is followed with rinsing steps in order to remove the excess of polymers (or other compounds) not adsorbed on the surface. These deposition cycles can be reiterated until obtaining the desired number of layers. LbL multilayer assemblies can be prepared through a wide range of deposition methods such as dip-coating, spin-coating and spraying. Among these methods, dip-coating is extensively used because it allows to coat any type of substrates with complex shapes. The principle consists of the immersion of a substrate into a series of aqueous polymer or particle solutions and rinsing solutions. Nevertheless, dip-coating has some drawbacks including the use of large amount of materials for each deposition step and its long process time which becomes critical for the fabrication of assemblies of many layers. Spin-coating consists of the deposition of a coating material on a rotating substrate on which the material is spread over the entire surface by centrifugal force. Regarding the spraying method, films are deposited on the surface with a sprayer. Spin-coating and spraying approaches avoid the limitations related to dip-coating and can be used at the industrial scale because of their large production capacity at faster rate [48].

1.3.2 Molecular interactions driving the LbL multilayer assemblies

The LbL assembly of multilayers is based on various driving molecular interactions but the most commonly used is the electrostatic interaction. Experimentally, the substrate is dipped into successive polyanion-polycation aqueous solutions, with intermediate rinsing steps. The polyelectrolytes adsorb on the surface of the substrate because of the electrostatic interactions between them and counterions are released in the solutions. The restriction of electrostatic LbL assembly to charged and water-soluble materials has stimulated researchers to investigate other driving forces for the incorporation of many uncharged materials into multilayers. These nonelectrostatic interactions include hydrogen bonding, hydrophobic interactions, change-transfer interactions, host-guest interactions, biologically specific interactions, coordination chemistry interactions, covalent bonding and stereocomplexation [48]. Thereafter, only the case of LbL films produced from polyelectrolyte chains will be treated.

1.3.3 Parameters influencing the LbL assembly process

By adjusting parameters such as temperature, ionic strength, concentration, solvent nature, pH of the solutions, adsorption time and number of layers deposited during the process, it is possible to control the composition of the film, layer thickness, topography and intermixing of neighboring layers. However, given the very high number of influencing parameters on LbL assembly process, it is difficult to define and establish a priori the best assembly conditions to obtain a desired film structure [48, 49]. Because some of the parameters previously mentioned influence only slightly the

architecture and characteristics of multilayer films, only the two most important parameters are developed in this section : the ionic strength and the number of layers deposited.

Effect of ionic strength

Usually, the film thickness increases as the salt concentration increases until a critical salt concentration at which the multilayer completely dissociates. This commonly observed trend means that an increase of the ionic strength decreases the intramolecular electrostatic repulsions in the polyelectrolyte chains leading them to adopt a more loopy conformation. This leads to thicker layers compared to layers obtained at low ionic strength for which the chains are in an extended conformation and tend to adsorb flat on the substrate. Nevertheless, when the ionic strength is too high, the intermolecular attractive interactions between oppositely charged polyelectrolytes are screened with the consequence of a desorption of the layers. There is indeed a competition between polyelectrolyte pairs and external salt ions [50, 48]. In addition to salt concentration, researchers also investigated the effect of salt type and concentration on the thickness. For instance, Boulmedais et al. examined the influence of salt type on the buildup and structure of poly(styrene sulfonate) (PSS)/poly(allylamine hydrochloride) (PAH) films. In their study, they varied the nature of the anions by following the Hofmeister series from osmotropic to chaotropic anions (F^-, Cl^-, NO^{3-}, ClO^{4-}) and demonstrated a larger interaction between anions and polyelectrolytes for chaotropic anions, related to thicker films compared to those obtained with osmotropic anions [51].

Effect of the number of layers

For many LbL films, the thickness increases linearly with the number of layers deposited. However, there are some systems of polyelectrolytes for which the film thickness and amount of adsorbed polyelectrolytes increase more rapidly than linearly with the number of deposition cycles. This is particularly true for systems containing weak polyelectrolytes such as PLL/ALG, PLL/HA or PLL/poly(glycolic acid). Such LbL systems exhibit an exponential growth. This exponential thickening phenomenon is the consequence of an "in and out" diffusion mechanism. Indeed, the adsorption of the polyelectrolyte chains not only occurs on the film surface but they also interpenetrate into inner layers for charge overcompensation, leading to an exponential increase of the total film thickness. While the thickness of one polyelectrolyte layer in the linear growth regime is typically several nanometers, it can reach up to hundreds of nanometers after deposition of only one polyelectrolyte layer in the exponential growth regime [52].

1.3.4 Hydrogen bonding-based LbL films

Originally introduced for pairs of oppositely charged polymers, the LbL assembly technique has been extended to LbL films based on hydrogen bonding which is a weak bond. A key feature of this type of hydrogen bonded films is that they are stable up to the point where altered pH or other environmental stimulus introduces an unacceptably large electrical charge within them [53]. This increased ionization results in a weakening of the hydrogen-bond-donating ability with a simultaneous increase of electrostatic repulsions causing the delamination of the film. Such behavior has been largely demonstrated for the polyacids poly(acrylic acid) (PAA) and poly(methacrylic acid) (PMAA) and for the polybases poly(vinylpyrrolidone) (PVPON) and poly(ethylene oxide) (PEO) in D_2O [54]. The chemical structure of these polymers is shown in figure 1.8a and a scheme of a hydrogen bonding-based LbL film constructed with PAA and poly(vinylpyridine) is shown in figure 1.8b.

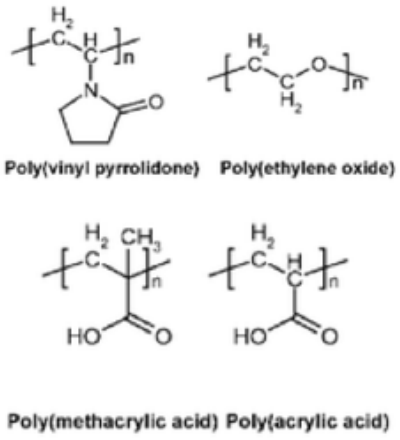

(a)

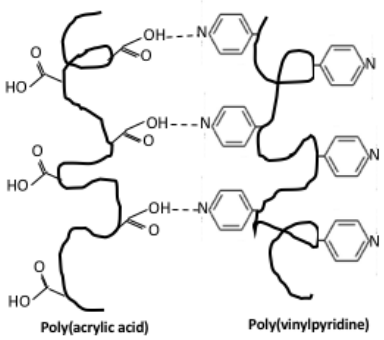

(b)

Figure 1.8: (a) Chemical structures of hydrogen bonding-based polymers. Polyacids: PAA and PMAA. Polybases: PVPON and PEO [2]. (b) Scheme of a hydrogen bonding-based system composed of PAA and poly(vinylpyridine) [3]

The new properties associated with hydrogen bonding-based LbL films allow to produce films responsive to environmental conditions. In particular, the pH and ionic strength environments considerably affect the physicochemical properties of these films in solution [55].

Influence of the pH

A polymer chain containing acidic groups such as carboxylic acid groups (-COOH), becomes on average negatively charged when the pH is higher than the pKa of the polymer. The electrostatic repulsions between these negative charges, as well as the breaking of hydrogen bonds cause the swelling of the polymer and the delamination of the film. A polymer containing basic groups such as amine groups ($-NH_2$) becomes positively charged and exhibits a swelling behavior and a desorption of the film from the surface when the pH decreases below the pKa of the polymer [53]. This mechanism is illustrated in figure 1.9. Therefore, depending on the multilayer system, there exists a critical pH at which the film starts to become unstable. For example, PAA/PEO multilayers are characterized by a critical pH of 3.3. This low pH value can be explained by the weak hydrogen bonds established between PAA and PEO at low pH. By using polyacids having a higher pKa such as PMAA, and/or more hydrophobic neutral polymers such as poly(N-isopropyl-acrylamide) (PNIPAM), it is possible to obtain higher critical pH values. Regarding poly(N-vinylcaprolactam) (PVCL)/PMAA films, they start to disintegrate at pH of 6.5, making this system promising for biological applications for which neutral pH conditions are required [10].

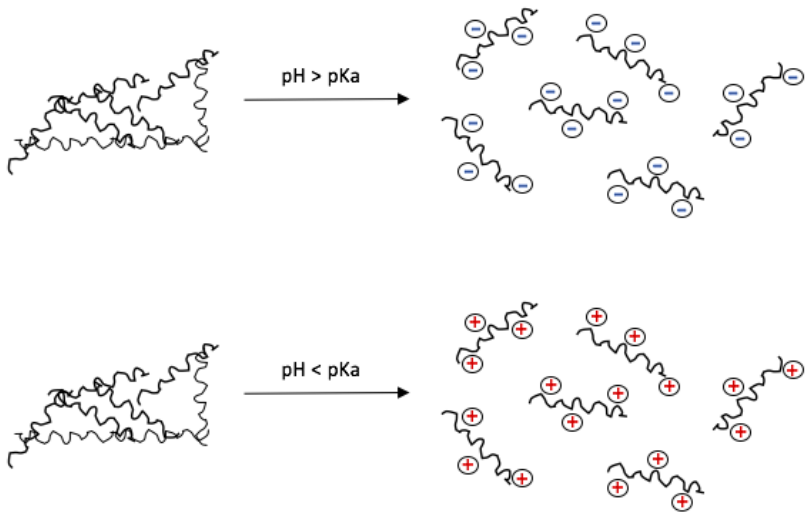

Figure 1.9: Influence of the pH on the stability of hydrogen bonding-based LbL films.

Influence of the ionic strength

The ionic strength is another parameter that affects the multilayer stability. For instance, Sukhishvili et al. reported in 150mM NaCl a decrease by 0.5 pH units of the critical pH for film disintegration of polyphenol/neutral polymer systems such as tannic acid (TA)/PEO and TA/PNIPAAM [56]. The effect of NaCl concentration on the stability of PVCL/PMAA multilayers was also examined. In this study, PVCL/PMAA layers were deposited on poly(ethylenimine) (PEI)-modified Si wafers at pH 2.0 in 0, 50, or 150mM NaCl solutions. It was shown that the critical pH for disaggregation strongly depended on salt concentration, with pH values of 7.1, 6.6, and 6.1 for 0, 50, and 150mM NaCl, respectively. The decrease of the critical pH and hydrogen bonds weakening in the presence of salts was due to increase of polymer ionization, change of polymer solubility and hydration [10].

1.3.5 LbL for cell encapsulation

In comparison to other techniques for cell encapsulation, the LbL assembly method is particularly promising because of its versatility and tunability to form various multilayer capsules with adjustable compositions and structures. The advantages of the LbL assembly approach in encapsulation of cells include a precise control of the capsule thickness and the ability to control permeability properties which is particularly important as cell viability strongly depends on the diffusion of oxygen and nutrients through the capsule [57]. Numerous LbL assembly strategies for cell encapsulation have been developed for different cell species, including bacteria, yeasts, stem cells, erythrocytes, platelets, tumor cells, pancreatic islets, etc. Many materials have been tested for the LbL encapsulation of cells. The most popular synthetic polymers include PSS, PAH, PLL, poly(dimethyldiallylammonium chloride), PEI, PNIPAM, PAA, PMAA and poly(vinylsulfate). Among natural polymers, the most commonly used for cell encapsulation are CHI, ALG, HA, heparin, cellulose sulfate, dextran sulfate, and carboxymethylcellulose [58]. For instance, LbL assembly approach was used to encapsulate *Bacillus coagulans* (BC) probiotics in CHI and ALG multilayers in order to protect encapsulated probiotics from gastrointestinal tract insults and to facilitate adhesion, growth and proliferation on intestinal surfaces. Results demonstrated an enhanced survival and persistence of LbL-BC probiotics

compared to plain-BC probiotics [6].

Despite successful application of the LbL-based cell encapsulation, cytotoxicity of the polycations can pose eventual limitations of this approach for cell encapsulation. Indeed, it was reported that the positive charge of cationic polyelectrolytes can cause the cell membrane perforation, subsequently causing cell damage and cell death. For instance, a study revealed the extreme toxicity of PLL/ALG multilayers on human pancreatic islets, causing their instant death [20]. However, natural cationic polyelectrolytes have shown an excellent cytocompatibility with no detectable cytotoxicity [57]. Glinel et al. encapsulated *S. epidermidis* in shells either composed of a pair of synthetic polyelectrolytes PAH/PSS or a pair of oppositely charged polysaccharides ALG/CHI by perfoming LbL assembly. They showed that the bacterial growth was strongly delayed or even entirely arrested when ammonium groups of the polycations were not paired with carboxylic groups of the polyanions. However, the delay of bacterial growth decreased as an additional polyanionic layer was deposited on the shell because of the addition of an excess of innocuous negatively charged carboxylic acid groups [8]. In addition, it is possible to reduce the cytotoxicity of synthetic polycations by incorporation of neutral chains, such as PEG in the polyelectrolyte structure in order to decrease the charge density [58].

1.3.6 Membrane-templated LbL assembly

Microtubes are particularly interesting for biological applications because of numerous advantages. They can be fabricated by combining LbL assembly with hard-templating methods based on porous membranes having cylindrical-shaped pores. This combination allows the formation of cylindrical tubes with well-defined and tunable diameter, length and composition, by depositing a material within the pores of a membrane. The pore diameter and the membrane thickness determine the morphology of the tubes and the number of LbL layers deposited determines the wall thickness of the tubes. For LbL deposition, the membrane is successively immersed in polymer solutions, followed by intermediate rinsing steps. This cycle is repeated until the desired number of layers deposited is achieved in the system. During the LbL process, a polymer multilayer crust forms on the top and bottom surfaces of the membrane, thereby limiting the access to the pores. This is why it is necessary to decrust the top and bottom surfaces of the membrane in order to eliminate this adherent layer. Then, the tubes are released by dissolving the membrane [11]. In general, the templating membrane is dissolved in an organic solvent such as DCM when using polycarbonate (PC) membrane, which is particularly harmful for living microorganisms. Consequently, the dissolution step is a major concern and represents an obstacle for biological applications. The challenge is thus to find a strategy to efficiently extract microtubes from the membrane in conditions that not denature or kill the biological components contained inside [10]. Figure 1.10 shows the general principle of membrane-templated LbL assembly to fabricate microtubes.

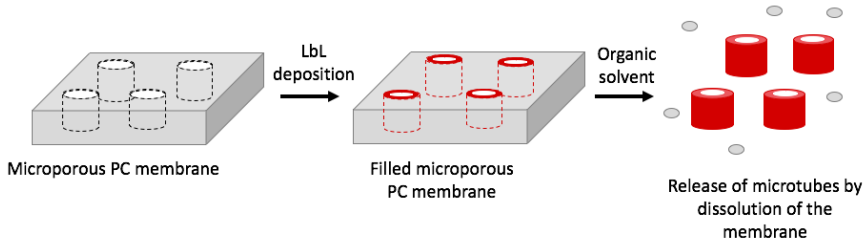

Figure 1.10: Membrane-templated LbL assembly where the templating membrane is dissolved in an organic solvents.

Porous membranes

The two membrane types most commonly used for hard-templating are track-etched polymeric membranes and porous alumina membranes. Each membrane type has its advantages and disadvantages. On the one hand, track-etched membranes are available in a wide range of pore sizes and templating materials including PC, polyester (PE), polyethylene terephthalate (PET) or polyimide, but have low pore densities and a random distribution of pores across the membrane surface. The pore sizes and pore densities of track-etched membranes can cover a range from a few nanometers to tens of micrometers, and 10^{10} pores/cm^2, respectively. On the other hand, alumina membranes allow higher pore densities, up to 10^{11} pores/cm^2, and a regular distribution of pores in a hexagonal array but these exist commercially in only a very limited number of pore sizes. The selection of the membrane type depends on the targeted application. PC track-etched membranes can easily be dissolved with a wide range of solvents while alumina membranes require extreme pH values and are very resistant to organic solvents and high temperatures [4]. Figure 1.11 shows PC (**A** and **B**) and alumina (**C** and **D**) templating membranes.

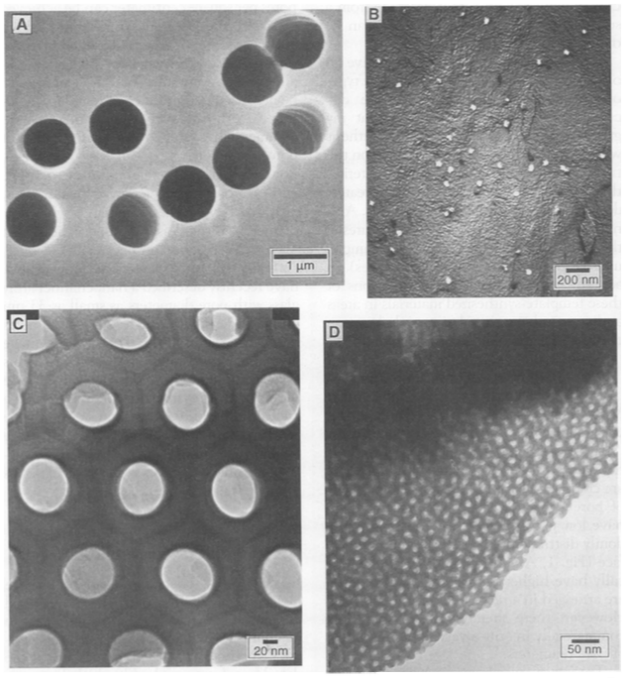

Figure 1.11: Electron micrographs of PC (**A** and **B**) and alumina (**C** and **D**) templating membranes. A and C are images of larger pore membranes (1μm and 70nm in diameter respectively) in order to better observe pore characteristics. B and D are images of a membrane with very small pores (30nm and 10nm in diameter respectively) [4].

Track-etched membranes. As suggested by their name, these membranes are fabricated by a track-etched method. It consists of bombarding a nonporous polymer sheet of the desired material (PC, PET,...) with heavy ions of high energy and accelerated in a cyclotron in order to produce damage tracks in the material. These damages result from the deterioration of the polymer chains in the membrane. Then, the tracks are chemically etched into well-defined pores. This chemical etching allows to remove the damaged zone of a latent track and to transform it into a hollow channel. This step determines the pore size and pore shape of the track-etching technology. The pore size and pore density are parameters that can be controlled independently during the production process. Pore size ranges from a few nanometers to tens of micrometers and can be controlled by varying etching

solution concentration, temperature, pH and reaction time with the solvent. Pore density depends on the number of ions bombarding the membrane and can reach up to 10^{10} pores/cm^2 with membrane thicknesses between 5 and 50μm. Because the etching also affects the template thickness, the range of available pore densities is limited [4, 59].

Alumina membranes. The fabrication of alumina membranes is based on two-step anodic oxidation of aluminium metal in certain acid electrolytes such as sulfuric acid and phosphoric acid electrolytes. The first one allows to create regular honeycomb-like structures in depth. These structures are the pore nuclei and are intended to guide the growth of pores. The second anodization consists of uniformly increasing the diameter and the depth of the pores. Pore size and pore density are controlled by the anodizing voltage and the acid electrolytes selected whereas the membrane thickness depends on the rate of charge transferred. Pore sizes from 10 to 250nm can be achieved and pore densities can reach up to 10^{11} pores/cm^2 [60].

1.4 Polymers used in this research project

1.4.1 Alginate

ALG is a natural polysaccharide typically derived from brown algae. ALG is a linear copolymer containing blocks of 1,4 linked β-D-mannuronic acid (M) and α-L-guluronic acid (G) residues. ALG can be easily solubilized in aqueous solution because of the presence of many carboxylic groups on both monomers. The blocks consist of consecutive G residues (GGGGGG), consecutive M residues (MMMMMM), and alternating M and G residues (GMGMGM). The content of M and G residues, as well as the length of each block depend on the species of algae from which the ALG is extracted. ALG is a polymer extremely used for cell encapsulation because of its favorable properties, including biocompatibility both with host and enclosed cells, biodegradability and ease of gelation [26, 61, 62].

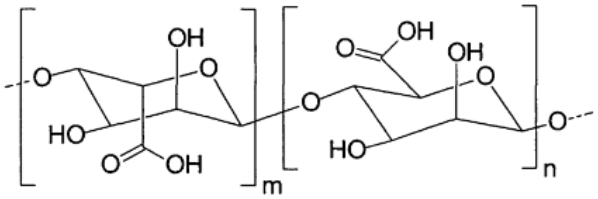

Figure 1.12: Structure of ALG.

1.4.2 Chitosan

CHI is a partially deacetylated polymer of N-acetyl glucosamine and is generally obtained from chitin, a natural polysaccharide derived from various natural sources including crustaceans, fungi and insects. CHI is a cationic polymer because of the amine residues that are mostly protonated below pH 6.5. CHI is also known for its antibacterial properties against various bacteria. In a study conducted by Riccardo Muzzarelli et al., they demonstrated that CHI was especially active against gram-positive bacteria including strains of *Staphylococcus aureus* and *S. epidermidis*. The growth of the strains tested was inhibited and most of them were killed in presence of a thin pad of CHI. The origin of the antimicrobial activity of CHI is complex and goes beyond the scope of this thesis. Nevertheless, this is probably due to its polycationic nature which disrupts the membrane functions of certain bacteria [63, 64]. Because the materials used have to be be gentle and non-toxic

for the encapsulation of viable cells, the antibacterial activity of CHI limits its use. However, the antimicrobial properties of CHI tend to decrease by electrostatic complexation with ALG [8].

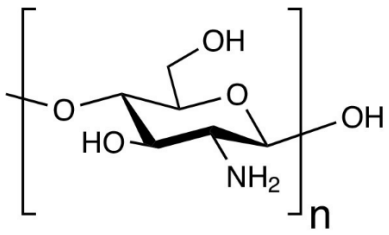

Figure 1.13: Structure of CHI.

1.4.3 Poly(methacrylic acid)

PMAA is an ionizable hydrophilic polymer composed of methacrylic acid (MAA) residues. PMAA can be solubilized in aqueous solution because of the deprotonation of many MAA groups in the chains at neutral pH. Due to the ionization of the carboxylic group with pH increasing above pKa, PMAA shows a pH-responsive behavior. When the pH is lower than approximately 5.5, the carboxylic acid groups are not ionized and the PMAA chains are in a collapsed state but when the pH increases above 5.5, carboxylic acid groups are ionized and the PMAA chains swells because of the repelling of the charged carboxylic acid groups [65].

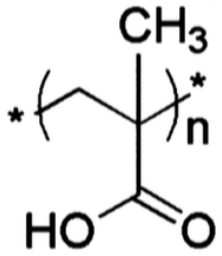

Figure 1.14: Structure of PMAA.

1.4.4 Poly(N-vinylcaprolactam)

PVCL is a cationic linear polymer obtained by polymerization of N-vinyl caprolactam residues. PVCL is a water soluble polymer that responds to external stimuli such as pH and temperature. The low critical solution temperature of PVCL is around 32-34°C which is near to the physiological temperature while its critical pH is around 6.0 when associated with PMAA in a 150mM NaCl solution [10]. These conditions are close to the physiological media, making PVCL particularly interesting for biological applications requiring responsive polymers. Moreover, PVCL exhibits other favorable properties including biocompatibility, nontoxicity and stability to hydrolysis [66, 53].

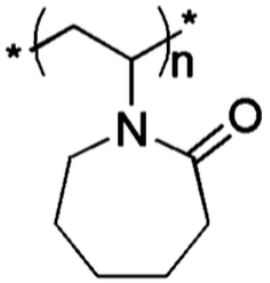

Figure 1.15: Structure of PVCL.

CHAPTER 2

Fabrication of polymer microtubes entrapping microparticles

This chapter describes in detail the experimental protocols for the fabrication of microtubes and the encapsulation of microparticles mimicking bacterial cells of *S. epidermidis* in these microtubes. The influence of different experimental parameters on the effectiveness of the encapsulation method is studied in order to select the optimal conditions for the encapsulation process.

2.1 Objective and strategy

As a reminder, the objective of this thesis is to encapsulate bacterial cells in polymer microtubes under biocompatible conditions. A well-known approach to construct such microtubes is the deposition of LbL films inside the pores of a microporous polymer membrane [11]. In general, structures fabricated by membrane-templated LbL assembly are collected by dissolving the polymer membrane in an organic solvent. However, the use of organic solvent is particularly adverse for biological applications involving microorganisms and creates safety problems. Because microorganisms are living entities, they have to be treated with non-harmful experimental methods to preserve their functions. A biologically compatible approach to produce polymer microtubes was developed by Xu et al. [10]. This approach is based on the fabrication of bicompartmentalized microtubes. The external compartment is a sacrificial layer intended to be erased from the wall of the released microtubes by a pH variation close to the physiological pH. The internal compartment is the one that is supposed to hold living entities and has to be stable at this same pH value. They found as most promising systems fitting these requirements, the PVCL/PMAA system for the sacrificial compartment and the ALG/CHI system for the internal compartment (see (a) in the figure 2.1). Indeed, PVCL/PMAA bilayers were reported to remain stable at pH lower than 6.0 in a 150mM NaCl solution but disintegrate at pH 6.5 in 10mM phosphate buffer. Regarding ALG/CHI bilayers forming the inner compartment, they remain stable under these pH conditions, and therefore maintain their ability to form the walls of the released microtubes.

This chapter explores the use of such microtubes for the fabrication of hybrid systems comprising microparticles mimicking bacterial cells. To achieve this objective, the strategy developed by Xu et al. was carried out. First, PVCL/PMAA sacrificial compartments were deposited by LbL assembly into the pores of a microporous PC membrane. Then, the inner ALG/CHI compartments were deposited in the same way in the pores of the membrane containing the sacrificial compartments. After that, microparticles were loaded into the microtubes by filtration through the pores of the membrane and the pores were closed through the deposition of ALG/CHI bilayers on the top surface of the membrane. Finally, the release and collection of the inner ALG/CHI compartments were performed by disaggregating the sacrificial compartments in a pH 6.5 buffer solution while pushing the inner compartments outside the pores of the membrane by filtration. Figure 2.1 is a schematic

illustration of the strategy followed for (**a.**) the fabrication of bicompartmentalized microtubes, (**b.**) the release and (**c.**) the collection of the inner microtubes in biologically compatible conditions.

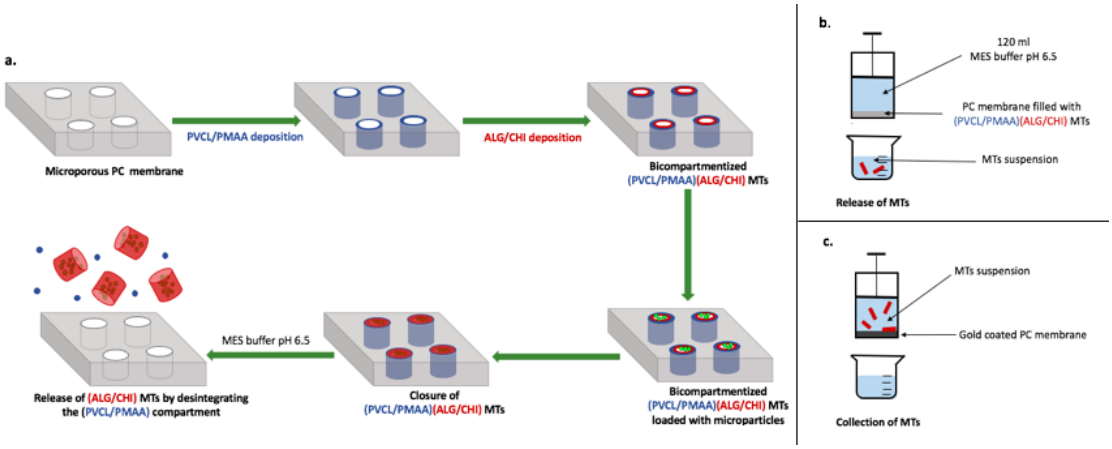

Figure 2.1: Schematic illustration of (**a.**) the fabrication of bicompartmentalized MTs, (*b.*) the release and (**c.**) the collection of the inner MTs in biocompatible conditions.

2.2 Materials

Polymers PMAA of average molar mass 100kg/mol was purchased from Polysciences and PVCL of average molar mass 1.8kg/mol was purchased from Polymer Source Inc. Branched polyethylenimine (bPEI) of average molar mass 750kg/mol and sodium ALG were purchased from Sigma-Aldrich. Rhodamine-labelled poly(allylamine hydrochloride) (PAH-Rh) (1:392 mol:mol monomer ratio in dye) of average molar mass 15kg/mol was purchased from Surflay Nanotec GmbH. CHI of average molar mass 50-150kg/mol and deacetylation degree >90% was obtained from NovaMatrix. Polymer solutions were prepared at 1mg/mL, except for PAH-Rh (0.5mg/mL) and bPEI (0.5mg/mL). The NaCl concentration of all polymer solutions was fixed to 150mM. The chemical structure of the polymers used to form the microtubes is shown in figure 2.2.

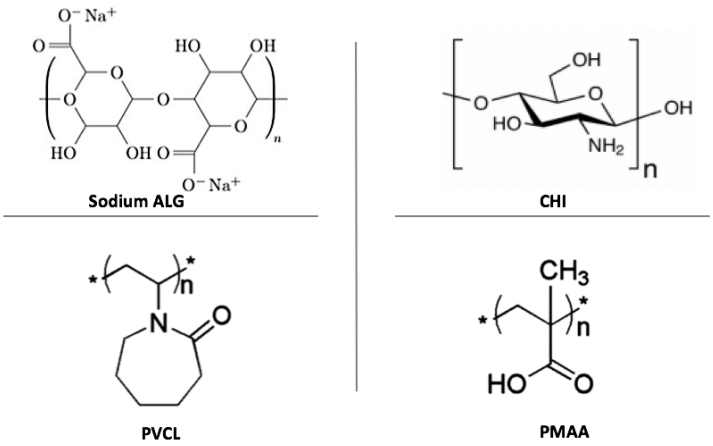

Figure 2.2: Chemical structure of ALG, CHI, PVCL and PMAA.

Track-etched membranes Track-etched membranes were provided by It4ip (Belgium). Track-etched membranes were used either as template for LbL deposition of microtubes or as filter for collecting microtubes. In the case of a template, a 6x6cm^2 square of the membrane was used whereas in the case of a filter, a disk of 12mm in diameter was used. The characteristics, i.e., pore diameter, pore density and thickness, of each track-etched membrane used are shown in Table 2.1.

Material	**Pore diameter** [μm]	**Pore density** [cm^{-2}]	**Thickness** [μm]
PC	1.6	1×10^7	24
PC	2.0	2×10^6	23
PC	3.0	1.6×10^6	22
PC	5.0	8×10^5	21
PC	0.8	4×10^7	24
PET	0.8	4×10^7	24

Table 2.1: Track-etched membranes used during the encapsulation process of microparticles.

Latex particles suspension Aqueous suspension of latex particles of 1μm in diameter was purchased from Sigma-Aldrich. Particles were composed of carboxylate-modified polystyrene (PS) and tagged with yellow-green fluorescent dye. Their excitation wavelength λ_{ex} was around 470nm while their emission wavelength λ_{em} was around 505nm.

Water and other solvents Milli-Q water, also called ultrapure water, was obtained from a Merck Millipore system and used in all experiments. Milli-Q water was characterized by a resistivity of 18.2MΩ·cm. 2-(N-morpholino)ethanesulfonic acid (MES) monohydrate (98%, Alfa Aesar, molar mass of 213.248g/mol) was purchased from Thermo Fischer Scientific and used as buffering agent.

2.3 Characterization techniques

It is essential to characterize the microtubes fabricated, i.e., to analyze their properties and morphology. The purpose of this section is to briefly explain the characterization techniques used in the frame of this thesis.

2.3.1 Epifluorescence microscopy

Fluorescent tagged microtubes and fluorescent microparticles were observed with an Olympus IX71 inverted epifluorescence microscope. The red channel was used to observe the microtubes while the green channel was chosen to visualize the microparticles. Epifluorescence microscope is an optical microscope based on the fluorescence phenomenon. The term "epi" refers to the fact that both the illuminated and emitted light travel through the same objective lens. Such an arrangement allows to obtain a high signal-to-noise ratio. The main components of a fluorescence microscope are a light source, an excitation filter for illuminated light, a dichroic beamsplitter or a mirror, an emission filter for emitted light and a camera system. The principle consists of illuminating a sample with light of a specific wavelength. This wavelength is selected by placing a filter just after the light source. Afterwards, the light hits a dichroic mirror (or beam splitter), causing the reflection of the light through the objective lens and the sample. The light is then absorbed by the fluorescent molecules within the sample and re-emitted at a longer wavelength. This emitted fluorescent light is collected

by the objective lens before passing through the dichroic mirror (or beam splitter). Finally, the emitted light is detected by the CCD camera [67].

2.3.2 Confocal microscopy

Since epifluorescence microscopy only provides images of the tips of the microtubes, the filled membranes were also observed with a confocal laser scanning microscope (CLSM). CLSM is an optical microscope able to produce images of very narrow depth of field. Like the wide-field fluorescence microscope, the CLSM is an imaging method that uses the phenomenon of fluorescence. CLSM overcomes some limitations of conventional fluorescence microscopes for which all parts of the sample are excited at the same time by the light source, causing blurring effect on the images due to the disturbing fluorescent light from unfocused background part and other regions of the sample. To surpass this issue, a defined point of the sample at a specific depth is illuminated by a laser beam instead of illuminating the whole sample at once. Then, the emitted light hits a series of mirrors to amplify the signal gain and is focused onto a pinhole that removes out-of-focus light. This allows only the fluorescence light from the illuminated spot to enter into the light detector. In addition, the reconstruction of a three-dimensional representation of the sample can be obtained by stacking several two-dimensional images from different depths in the sample [68].

2.3.3 Fluorescence spectroscopy

Fluorescence spectroscopy was used to quantify the concentration of microparticles in suspensions by measuring the optical density (OD) of these suspensions. The OD is proportional to $\log_{10}(I/I_0)$ where I is the intensity of light absorbed at a specific wavelength by a cuvette containing the sample to analyze and I_0 the intensity of light passing through an empty cuvette (reference measurement) [69]. The percentage of absorbed light was proportional to the concentration of microparticles. The spectrometer used was a Tecan plate reader Infinite M Nano$^+$ PRO and the OD was measured at a wavelength of 540nm.

2.3.4 Scanning electron microscopy

Morphology of microtubes was observed by scanning electron microscopy (SEM). The principle of SEM is based on the scanning of a surface with a focused beam of electrons to produce an image. The interactions between electrons and atoms in the sample produce different signals giving information on the surface morphology and composition of the sample. Electrons are generated by an electron gun (field emission). Afterwards, electrons are accelerated by a potential difference and travel through a combination of lenses and apertures to generate a focused beam which hits the surface of the sample and penetrates inside to a depth of a few microns. The interactions between the electrons and the surface produce several signals including secondary electrons, backscattered electrons and X-rays. Secondary electrons are collected by detectors and used to create images. Backscattered electrons can also be used for imaging but the resolution is not as good as secondary electrons. Finally, X-rays can be used to identify the distribution of elements in a sample, a technique named "energy-dispersive X-ray spectroscopy". Compared to an optical microscope, SEM can achieve a very high resolution. However, samples have to be conductive in order to be analyzed by SEM. Therefore, to increase the electrical conductivity of the samples, they need a specific preparation that consists of depositing a thin layer of metal, typically gold or chrome [70]. Here, the membranes filled with LbL microtubes were coated by a 20nm thick layer of sputtered gold. The SEM was a JSM-7600F JEOL and the voltage was fixed at 5kV for a distance of 8mm between the sample and the electron gun.

2.4 Methods

To fabricate the microtubes and encapsulate the microparticles, several steps were necessary:

- Preparation of polymer and rinsing solutions
- Modification of the surface of PS microparticles
- Fabrication of PVCL/PMAA sacrificial compartments by LbL assembly
- Fabrication of ALG/CHI microtubes by LbL assembly
- Loading of microparticles into the microtubes
- Closure of microtubes
- Release and collection of microtubes

The experimental protocol for each of these steps is developed in the following sections.

2.4.1 Preparation of the solutions

A large number of solutions were necessary for the encapsulation process. The preparation of these solutions had to be performed accurately since their intrinsic properties, such as concentration, temperature, pH and salt concentration, influence the physicochemical properties like the thickness, stiffness, composition, structure, roughness, wettability, and swelling/shrinking behaviour of the LbL assembled multilayer films. Moreover, a sodium chloride concentration of 150mM is typical for biological applications [10]. Therefore, the final concentration of polymer and rinsing solutions was set to 150mM NaCl.

- Solution of PVCL (1mg/mL, 150mM NaCl, pH 2.0) for the fabrication of sacrificial compartments
- Solution of PMAA (1mg/mL, 150mM NaCl, pH 2.0) for the fabrication of sacrificial compartments
- Solution of ALG (1mg/mL, 150mM NaCl, pH 4.0) for the fabrication of microtubes
- Solution of CHI (1mg/mL, 150mM NaCl, pH 4.0) for the fabrication of microtubes
- Solution of ALG (1mg/mL, 150mM NaCl, pH 6.0) for the closure of microtubes
- Solution of CHI (1mg/mL, 150mM NaCl, pH 6.0) for the closure of microtubes
- Solution of PAH-Rh (0.5mg/mL, 150mM NaCl, pH 4.0) for the labelling of microtubes
- Solution of bPEI (0.5mg/mL, 150mM NaCl, pH 4.0) for the surface modification of microparticles
- Solution of ALG (1 mg/mL, 150mM NaCl, pH 4.0) for the surface modification of microparticles
- Buffer solution (20mM MES, 150mM NaCl, pH 6.5) for the release of microtubes
- Rinsing solutions (150mM NaCl, pH 2.0, 4.0, and 6.0) for the different deposition cycles by LbL assembly

For the preparation of PVCL and PMAA solutions, 250mg of polymer and 2.19g NaCl (58.4g/mol) were mixed in 250mL ultrapure water and stirred at 400 rpm for 2 hours in order to obtain the complete dissolution of the polymer. Then, the pH of the solution was measured with a pH-meter and adjusted to the desired value by the addition of small amounts of hydrochloric acid (HCl) or sodium hydroxide (NaOH) solutions. Figure 2.3 is a schematic representation of the experimental procedure to apply for the preparation of the solutions.

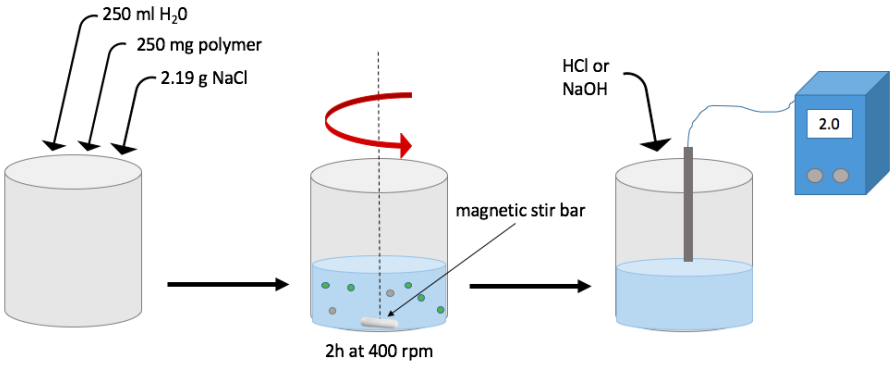

Figure 2.3: Scheme of the preparation of PVCL and PMAA solutions.

In the case of ALG and CHI solutions, the experimental protocol was a bit different because these two polymers are more difficult to dissolve in salt solution. For these two particular cases, 100mg polymer were mixed with 85mL ultrapure water and stirred at 200 rpm for 4 hours. Then, the pH of the solution was adjusted to the desired value and stirred for 12 more hours. When the pH value was stable, 15mL of a 1M NaCl solution were added and the solution was stirred for 1 to 2 hours. Lastly, the value of the pH was measured again and re-adjusted. This process is illustrated in figure 2.4.

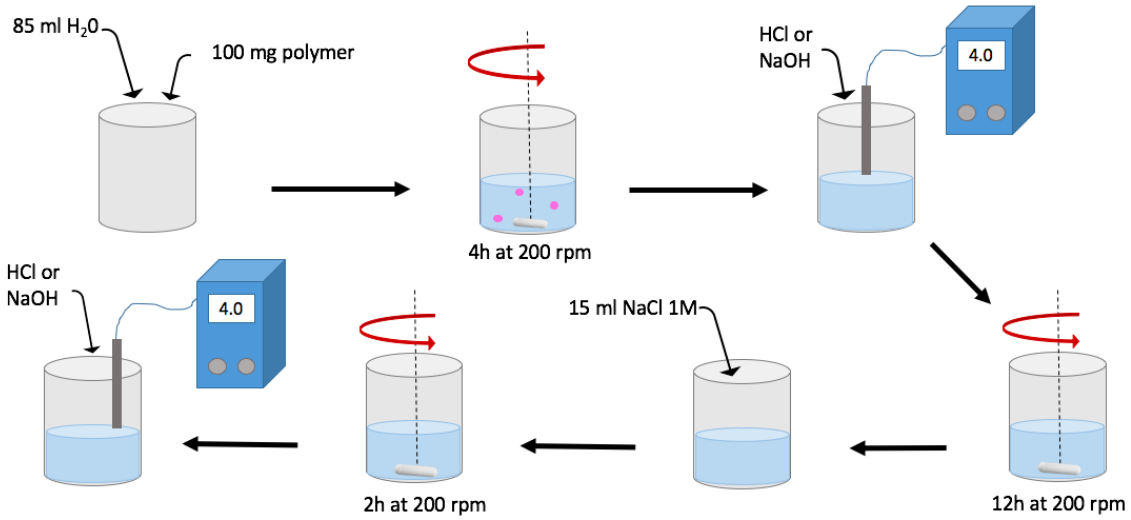

Figure 2.4: Scheme of the preparation of ALG and CHI solutions.

Rinsing solutions were prepared like PVCL and PMAA ones, except that they were mixed for a shorter time because salt dissolves much easier in water compared to polymers. In this case, 2.19g NaCl were dissolved in 250mL ultrapure water for 10 minutes at 400 rpm. Then, the pH of the solution

was set to 2.0, 4.0 or 6.0 depending on the conditions used for the polyelectrolyte deposition.

Finally, the MES/NaCl buffer solution used for the liberation of microtubes should have a final concentration of 20mM MES and 150mM NaCl. This was obtained by adding 1.066g MES (203.2g/mol) and 2.19g NaCl in 250mL ultrapure water and stirring the mixture at 400 rpm for 10 minutes. Then, the pH was adjusted to 6.5.

When the solutions were ready, they were either used directly or stored in the fridge for later use, in which case the temperature, as well as the pH value were measured and eventually re-adjusted just before use to meet the experimental conditions.

2.4.2 Surface modification of PS microparticles

In order to enhance the attraction and penetration of microparticles into microtubes and simulate better the wall of bacteria, microparticles were coated with one bilayer of bPEI/ALG by LbL assembly at pH 4.0 (fig. 2.5).

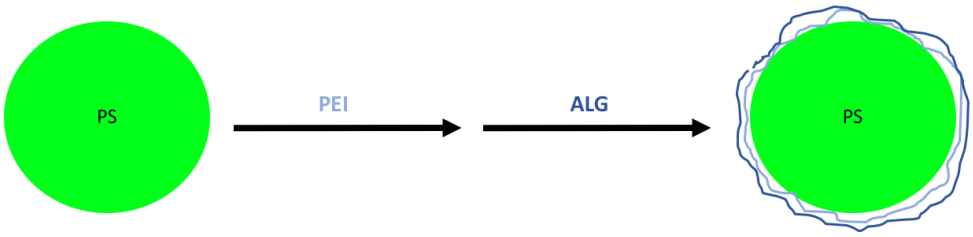

Figure 2.5: microparticles coated with one bPEI/ALG bilayer.

The experimental protocol is shown in figure 2.6. 14μL of a solution of microparticles were added to 486μL water (pH 4.0) in a tube. The mixture was then vortexed and sonicated for 30 secondes in order to well disperse the microparticles. After addition of 500μL bPEI solution (0.5mg/mL, 150mM NaCl, pH 4.0) in the tube, the resulting suspension was vortexed, sonicated and left to stand for 10 minutes to allow bPEI chains to adsorb onto the surface of microparticles. Next, the suspension was centrifuged for 10 minutes at 12,000 rpm and the supernatant (bPEI liquid) was removed and replaced by ultrapure water to rinse the microparticles and remove the excess of bPEI which had not adsorbed on the microparticles. For this, 1mL ultrapure water was added into the tube. The solution was vortexed and sonicated for 30 secondes to ensure complete dispersion of microparticles in water. Afterwards, the mixture was centrifuged for 10 minutes at 12,000 rpm and the supernatant (water) was removed. This rinsing process was repeated two times. After that, 1mL of sodium ALG solution (1mg/mL, 150mM NaCl, pH 4.0) was added in the tube and the same experimental protocol as described above was reiterated. Finally, 1mL ultrapure water was added into the tube and the final concentration of microparticles was measured by fluorescence spectroscopy. This concentration had to be ca. 1.5×10^8 microparticles/mL, corresponding to 3,300 a.u by fluorescence spectroscopy according to a calibration curve (see figure 2.7).

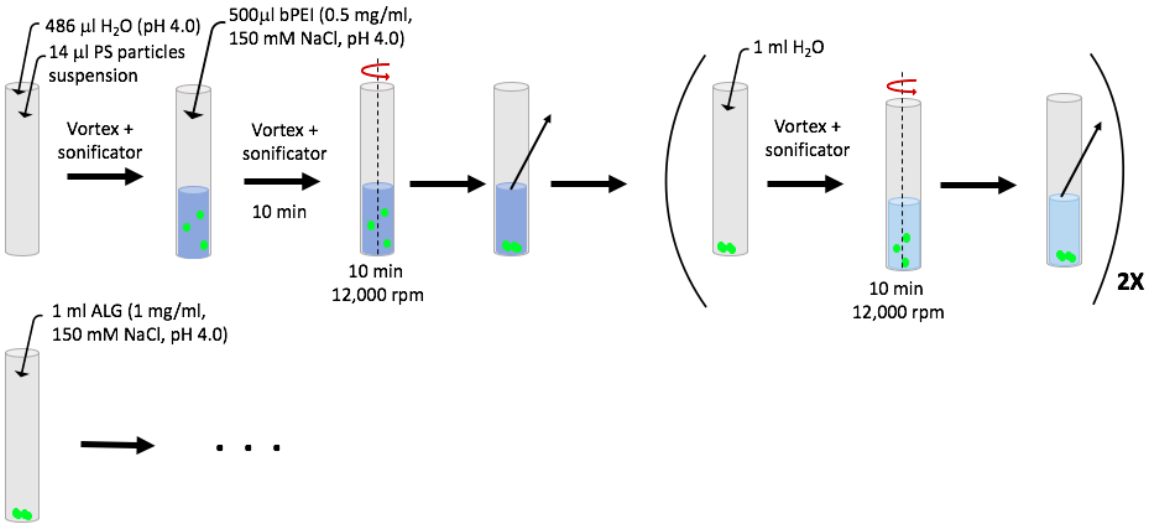

Figure 2.6: Scheme of the experimental protocol for microparticle surface modification.

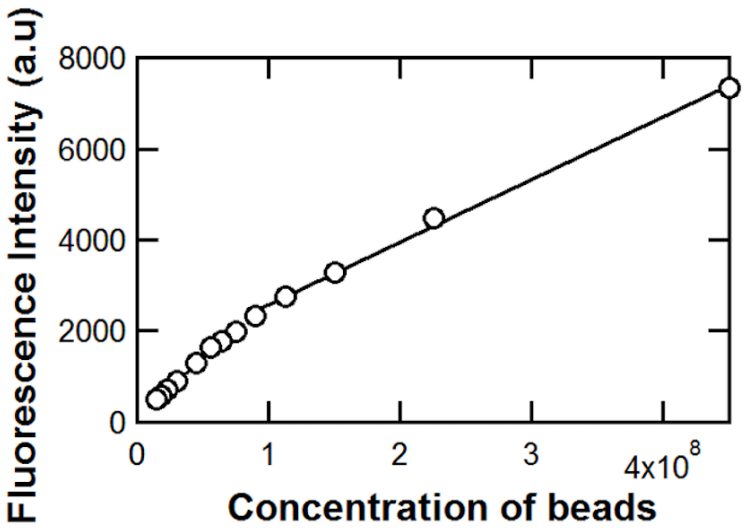

Figure 2.7: Correlation between the concentration of microparticles in suspension and the fluorescence intensity.

2.4.3 Fabrication of the PVCL/PMAA sacrificial compartment

The sacrificial compartment aims to be dissolved, so that the microtubes can be extracted from the membrane without using organic solvent. The sacrificial compartment was deposited using the LbL assembly technique. As a reminder, this technique consists of alternately depositing diverse complementary materials on a substrate, each deposition step being separated by rinsing steps. For the sacrificial compartment, the materials deposited were PVCL and PMAA. This pair of polymers are able of forming hydrogen bonds [10]. The procedure followed for the preparation of the sacrificial compartment is described below and represented in figure 2.8. Each circle corresponds to a culture dish filled with a given solution.

1. The PC membrane was dipped in a PVCL solution (1mg/mL, 150mM NaCl, pH 2.0) for 20 minutes during the first cycle, then 10 minutes for the following cycles.

2. The PC membrane was dipped in a rinsing solution R1 (150mM NaCl, pH 2.0,) for 2 minutes.
3. The PC membrane was dipped in a rinsing solution R2 (150mM NaCl, pH 2.0) for 2 minutes.
4. The PC membrane was dipped in a PMAA solution (1mg/mL, 150mM NaCl, pH 2.0) for 20 minutes during the first cycle, then 10 minutes for the following cycles.
5. The PC membrane was dipped in a rinsing solution R3 (150mM NaCl, pH 2.0) for 2 minutes.
6. The PC membrane was dipped in a rinsing solution R4 (150mM NaCl, pH 2.0) for 2 minutes.
7. The cycle was repeated until the desired number of bilayers was reached.

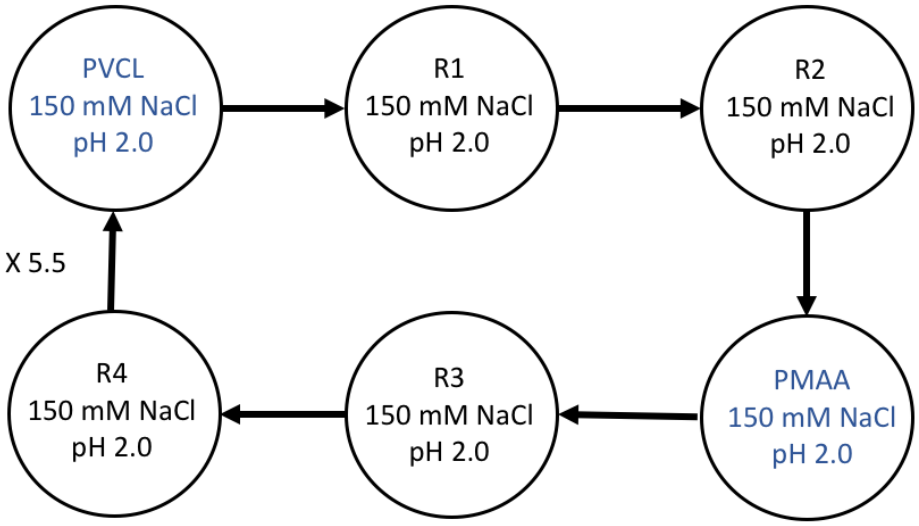

Figure 2.8: Scheme of the typical deposition cycle followed for the fabrication of sacrificial compartments.

After the two successive rinsing steps, the membrane was wiped with an absorbent paper in order to remove the liquid adhering to the membrane. In addition, every second cycle, the bottom surface of the membrane was decrusted with a cotton swab in a rinsing solution (pH 2.0, 150mM) in order to remove the LbL film present on the surface of the membrane so as only the interior of the pores was modified by the LbL film, but also to close the end of the pores with this excess of material which was displaced. Figure 2.9 represents the objectives of the decrusting process.

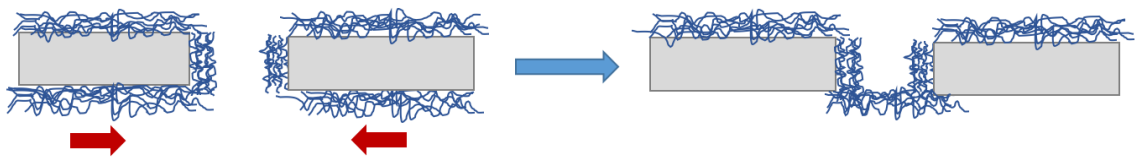

Figure 2.9: Decrusting of the bottom surface of the membrane to remove the LbL film adhered on the surface of the membrane and to close the pores with the LbL film. This process was performed every second PVCL/PMAA deposition cycle.

The cycle was repeated 5.5 times. Indeed, to prevent the adsorption of microtubes on the membrane during the release process, the external surface of the microtubes had to be negatively charged like

the surface of the bare membrane. By depositing 5.5 bilayers of PVCL/PMAA, the last layer of the sacrificial compartment was PVCL which allowed to deposit ALG as a first layer to build up the wall of the microtubes. As a result, the external surface of the microtubes obtained after dissolution of the sacrificial compartment will be negatively charged in order to limit the electrostatic interactions with the bare membrane during the release process.

2.4.4 Fabrication of ALG/CHI microtubes

Based on previous studies on the coating of *S. epidermidis* by polyelectrolyte multilayers, CHI and ALG were selected as polycation and polyanion, respectively, to form the wall of the microtubes. Indeed, the ALG/CHI system has already been used for the encapsulation of bacterial cells and has shown to maintain their activity [7, 8]. The ALG/CHI microtubes were produced by the LbL assembly technique onto the pores of the membrane in which the PVCL/PMAA sacrificial compartments had been previously deposited. The procedure was exactly the same as described in the section 2.4.3, except for the polymers deposited, the pH of the solutions and the number of cycles carried out. The assembly of the ALG/CHI bilayers is ensured by the electrostatic interactions between the positively charged CHI chains and the negatively charged ALG chains. The procedure followed for the preparation of microtubes is described below and represented in figure 2.10.

1. The PC membrane was dipped in an ALG solution (1mg/mL, 150mM NaCl, pH 4.0) for 10 minutes.
2. The PC membrane was dipped in a rinsing solution R1 (150mM NaCl, pH 4.0) for 2 minutes.
3. The PC membrane was dipped in a rinsing solution R2 (150mM NaCl, pH 4.0) for 2 minutes.
4. The PC membrane was dipped in a CHI solution (1mg/mL, 150mM NaCl, pH 4.0) for 10 minutes for all cycles, except the last two cycles for which the CHI solution was replaced by a PAH-Rh solution[1] (0.5mg/mL, 150mM NaCl, pH 4.0).
5. The PC membrane was dipped in a rinsing solution R3 (150mM NaCl, pH 4.0) for 2 minutes.
6. The PC membrane was dipped in a rinsing solution R4 (150mM NaCl, pH 4.0) for 2 minutes.
7. The cycle was repeated until the desired number of bilayers was reached.

[1] To be able to observe the microtubes by CLSM and epifluorescence microscopy.

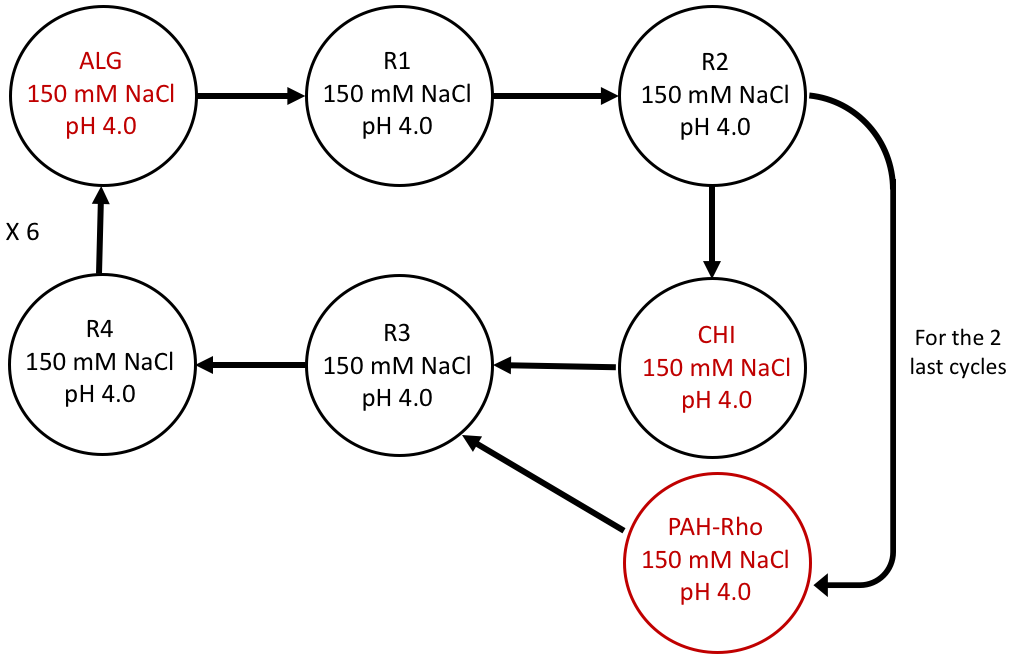

Figure 2.10: Scheme of the typical deposition cycle followed for the fabrication of ALG/CHI microtubes.

It was also necessary to perform a decrusting of the bottom surface of the membrane every two cycles in order to close the pores, as shown in figure 2.11.

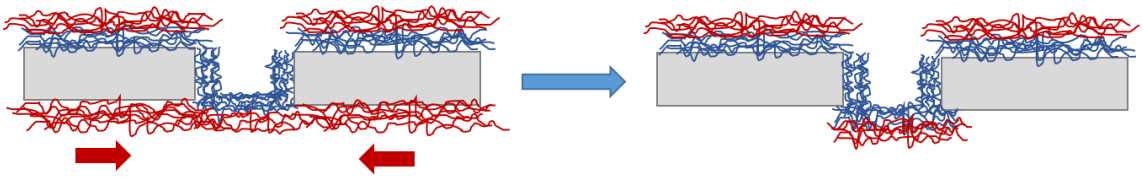

Figure 2.11: Decrusting of the bottom surface of the membrane. This process is performed every two ALG/CHI deposition cycles.

After repeating the CHI/ALG deposition cycle 6 times, the top surface of the membrane was dipped in a 3M NaCl solution for 1 minute and then a decrusting of the top surface with a cotton swab was performed for 1 minute. Such a treatment caused the removal of the LbL film deposited on the top surface of the membrane. During this treatment, it should be ensured that the membrane only floated on the salt solution rather than being fully immersed in order to limit the contact of the solution with the bottom side of the membrane, for which the pores had to be kept closed for the encapsulation of the PS microparticles. Then, the membrane was turned over and decrusted rapidly so that the bottom surface did not have time to be attacked by the solution. The principle of this decrusting step is described in figure 2.12.

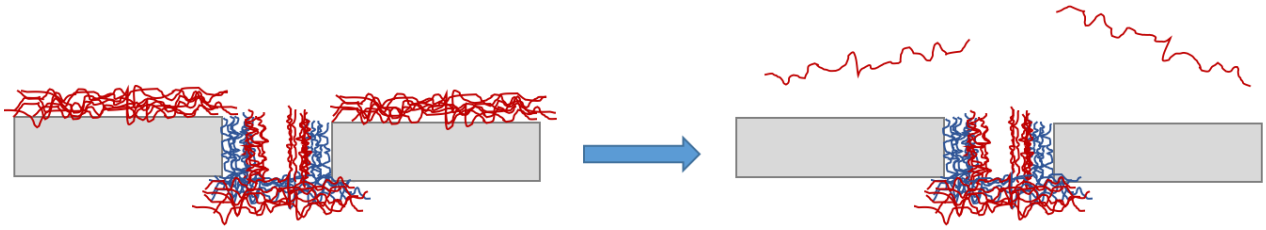

Figure 2.12: Decrusting of the top surface in a 3M NaCl solution.

Finally, the membrane was rinsed twice in ultrapure water for 1 minute and dried with an absorbent paper in order to remove the salt solution. Regarding the storage conditions of the membrane, it was kept in the fridge (4°C) and wrapped in an aluminum foil to protect it from light.

2.4.5 Loading of modified PS microparticles in the microtubes

The next step consisted of loading modified PS microparticles into the microtubes built into the pores of the membrane. The loading of microparticles into the microtubes was based on the filtration technology. A sample of circular shape (12mm in diameter) was carefully cut in the modified membrane and placed in a filtration unit, called "Swinny filter". This consists of a syringe-operated filter holder composed of two metal parts designed to accommodate plastic rings. These plastic rings help to seal the membrane at this junction. Generally, a metal grid is inserted to support the membrane, i.e., to prevent it from breaking or deforming under pressure. The upper metal part allows to insert a syringe in order to pour the desired solution. Figure 2.13a shows the different components of the Swinny filter and figure 2.13b shows the Swinny filter mounted with the syringe.

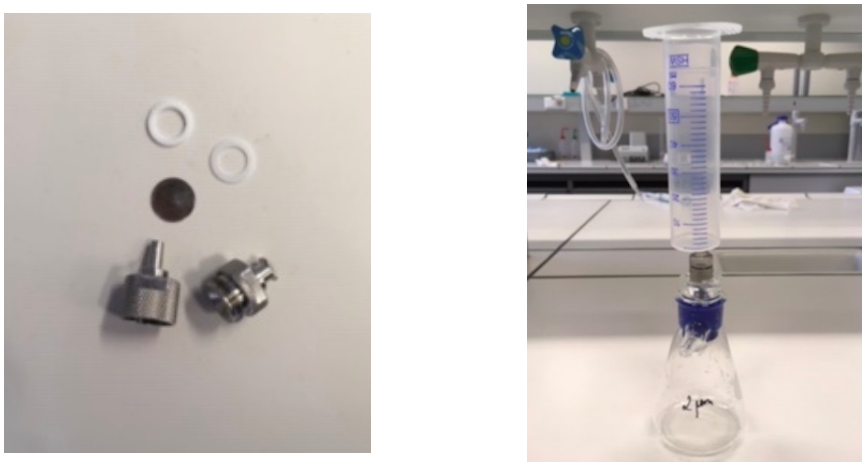

(a) Components of the Swinny filter.

(b) Complete assembly.

Figure 2.13: Filtration setup used to load the PS microparticles in the microtubes.

Here, 1mL of modified PS microparticle suspension, corresponding to 1.5×10^8 microparticles, was pushed through the membrane by using a syringe, thereby forcing the penetration of microparticles into the microtubes deposited in the pores of the membrane, as shown in figure 2.14.

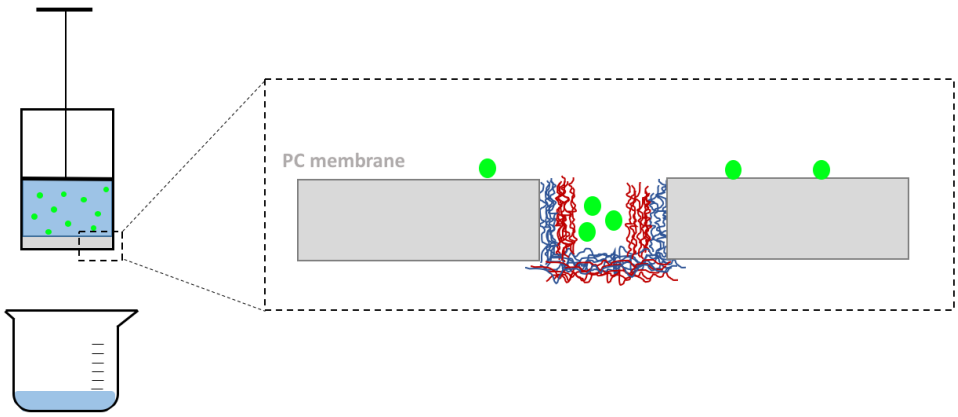

Figure 2.14: Loading of PS microparticles by filtration in the microtubes formed in the pores of a membrane.

Then, the circular membrane sample was removed from the Swinny filter and decrusted on both sides with a cotton swab in ultrapure water in order to remove the "free microparticles" adhered on the surfaces of the membrane. This rinsing process, illustrated in figure 2.15, was repeated three times.

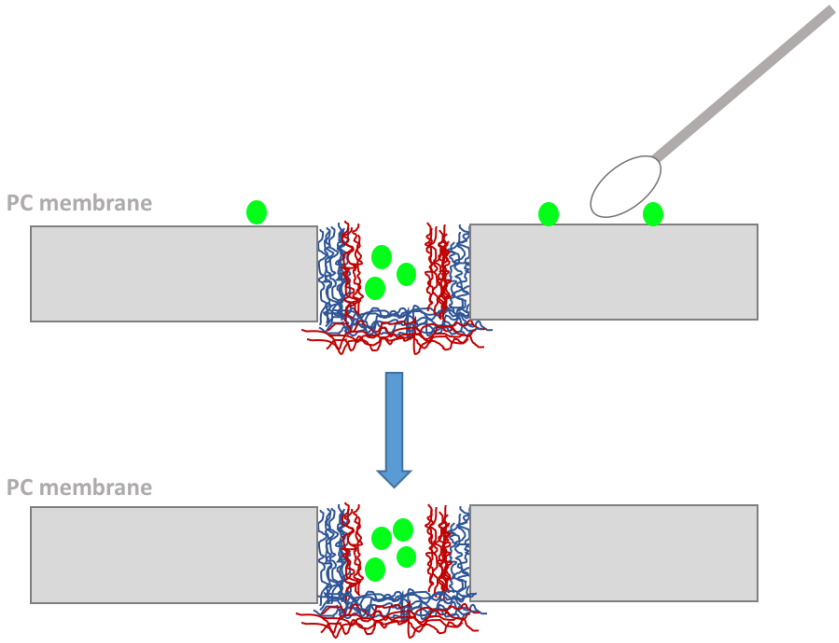

Figure 2.15: Decrusting of one side of the membrane in order to remove microparticles sticking on the surface.

2.4.6 Closure of the microtubes

In order to prevent the release of microparticles from the top end of the pores, ALG/CHI bilayers were deposited on the top side of the membrane, thereby blocking the pores. During the deposition process, the top surface of the membrane was deposited alternately in ALG and CHI baths (1mg/mL, 150mM NaCl, pH 6.0) for 3 minutes, with two intermediate rinsing steps (150mM NaCl, pH 6.0) for 30 secondes. This process was repeated 10 times and the membrane was decrusted every two cycles on the top surface. For the two last deposition cycles, the CHI solution was replaced by PAH-Rh

solution for the observation of the microtubes by fluorescence microscopy. The immersion time in the polyelectrolyte solutions was rapid because the adsorption of polyelectrolyte chains had to be done only on the surface and not inside the pores of the membrane. The pH value of the ALG and CHI solutions, as well as rinsing solutions was set to 6.0 in order to ensure both the stability of the sacrificial compartments but also the viability and functionality of bacteria that will subsequently be encapsulated instead of microparticles. Figure 2.16 shows the objective of the top layer deposition.

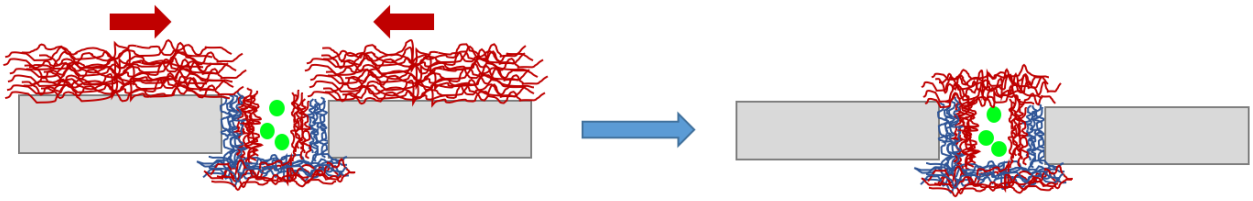

Figure 2.16: Closure of pores on top surface by depositing and decrusting $(ALG/CHI)_{10}$ bilayers.

2.4.7 Release and collection of microtubes

The experimental protocol for the release of microtubes is represented in figure 2.17. A circular-shaped (12mm in diameter) sample of the membrane containing microtubes was fixed in a Swinny filter and 100mL of a buffer solution (20mM MES, 150mM NaCl, pH 6.5) were filtered through the membrane to disintegrate the sacrificial compartments and to release the microtubes into the filtrate. For the observation by SEM of the membrane after the release of microtubes, 20mL of ultrapure water were filtered through the membrane in order to remove salt crystals. In order to collect microtubes, the filtrate containing the released microtubes was filtered through a track-etched PC membrane (pore size 0.8μm, pore density 4×10^7cm^{-2}) covered with a thin layer of gold[2] (20nm thick). Finally, the PC membrane with the collected microtubes was rinsed three times with 5mL of ultrapure water in order to eliminate residues of salt and dried in a desiccator for 4 hours.

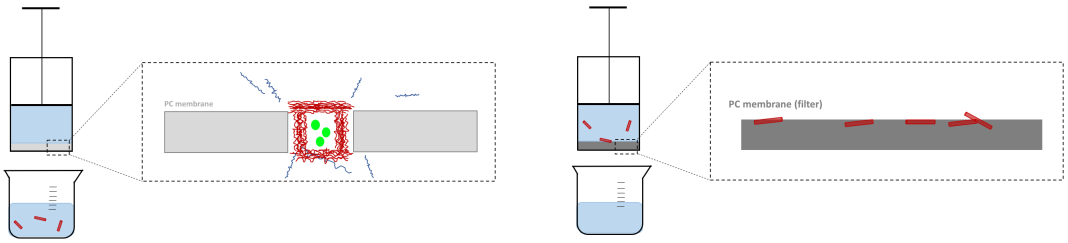

(a) Release of the microtubes. (b) Collection of the microtubes.

Figure 2.17: Experimental setup used to (a) release and (b) collect microtubes by disintegration of the sacrificial compartment at pH 6.5.

To characterize the microtubes surrounded by a PVCL/PMAA sacrificial shell, the PC membrane modified with $(PVCL/PMAA)_{5.5}(ALG/CHI)_6$ was dissolved in an organic solvent in order to release the whole microtubes. For this, the filled PC membrane was dissolved in 5mL of DCM. After 10 minutes, the microtubes suspension was sonicated for 3 secondes to promote the full dissolution of the PC membrane. The released microtubes were then collected by filtering the suspension through a PET membrane (pore size 0.8μm, pore density 4×10^7cm^{-2}) coated with a 20nm layer of gold.

[2]For SEM observation.

Then, the PET membrane was rinsed three times with 5mL of "fresh" DCM to remove PC traces. Finally, the PET membrane with the microtubes was dried for 4 hours in a desiccator.

2.4.8 Nomenclature

Microtubes built with n bilayers of PVCL/PMAA, then m bilayers of ALG/CHI are designated as : $(\text{PVCL/PMAA})_n(\text{ALG/CHI})_m$.

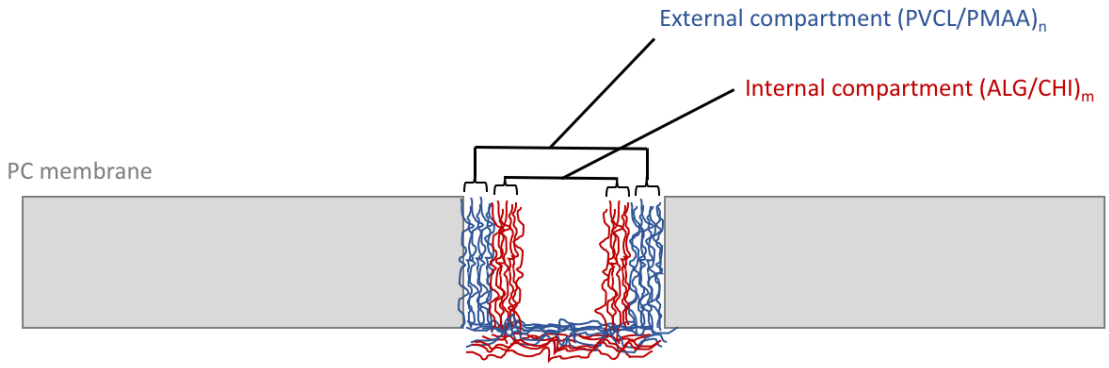

Figure 2.18: Nomenclature used to describe the microtubes.

2.5 Results and discussion

The objective of this work was to start from the method developed by Xu et al. [10] for the fabrication and release of microtubes under biologically compatible conditions and to use these microtubes to entrap bacteria. For this, bacteria cells were replaced by microparticles of same size. In order to optimize the encapsulation process, the influence of different parameters was studied. These parameters were : (i) the size of the pores of the membrane used as a template, (ii) the electrostatic interactions between the internal wall of the microtubes and the surface of microparticles, (iii) the loading technology and (iv) the parameters of the filtration process.

2.5.1 Pore size

The pore size of the membrane used for the fabrication of microtubes is a very important parameter because it determines their final morphology and dimensions. Indeed, LbL deposition into the pores of the membrane results in the formation of polymer microtubes that replicate the porosity of the membrane. The larger the pore size, the larger the diameter of the microtubes and conversely the smaller the pore size, the smaller the diameter of the microtubes. Since these microtubes are intended to encapsulate bacteria, they have to be large enough to allow the passage of bacteria and at a high rate. In general, bacteria of the *Staphylococcus* family of which *S. epidermidis* is a member, have diameters ranging from 0.5 to 1μm [71]. In addition, we intend to use these microtubes for biomedical applications. Consequently, it is necessary to close the microtubes at their extremities after having filled them with bacteria in order to mitigate the risk of causing safety problems if bacteria manage to escape from the microtubes.

During the LbL assembly process for the deposition of PVCL/PMAA sacrificial compartment and ALG/CHI internal compartment, a multilayer crust formed on the top and bottom surfaces of the

PC template. To close the microtubes, the membrane was decrusted every two deposition cycles in a saline (150mM) solution at a given pH depending on the polymer deposited. The objective of the decrusting process was twofold. First, it removed the multilayer crust adhering to the surface so that only the interior of pores of the membrane was modified. Secondly, the decrusting process pushed this excess of LbL film in the entrance of the pores of the membrane, which had the consequence of closing the ends of the microtubes. Figure 2.19a shows the top surface of the membrane for which no decrusting was carried out whereas figure 2.19b shows the bottom surface of the membrane for which a decrusting was performed every two cycles in a saline solution (150mM). On these figures, we can observe that the pores are closed on the bottom surface but all the pores on the top surface are open.

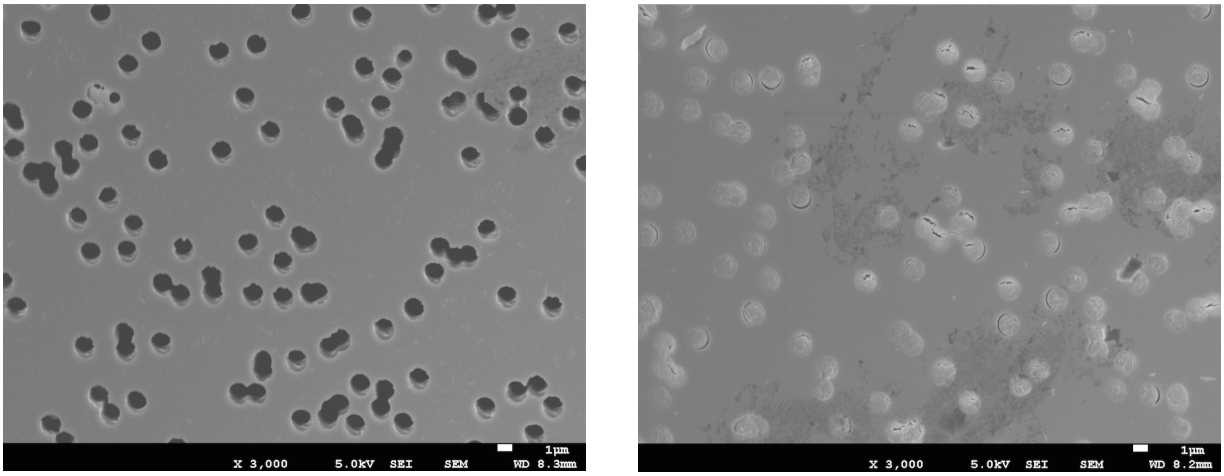

(a) Top surface. (b) Bottom surface.

Figure 2.19: SEM images of the top (left) and bottom (right) surfaces of the membrane after LbL deposition. The top surface was never decrusted while the bottom surface was decrusted every two deposition cycles.

The effectiveness of the decrusting treatment to close the pores of the membrane depends on the size of the pores of the membrane and the number of layers deposited during the LbL assembly process. Indeed, the larger the pores, the more layers have to be deposited to have a crust thick enough to close the entire diameter of the pores on the surface. In order to find a pore size that meet the criteria of the intended application, namely (i) the possibility of loading enough bacteria and (ii) the possibility of closing the microtubes, membranes of different pore sizes were used to fabricate microtubes. The pore sizes tested were 1.6, 2.0, 3.0 and 5.0μm. Then, microparticles of same diameter size than *S. epidermidis* were loaded into these different membranes by filtration. For each membrane, a sample was taken and observed by CLSM. Orthogonal views xz and yz are respectively at the bottom and on the side of the primitive Z-stack of xy-images. In order to facilitate the understanding of the images obtained by CLSM, figure 2.20 represents a scheme of the sections of the membrane corresponding to each view.

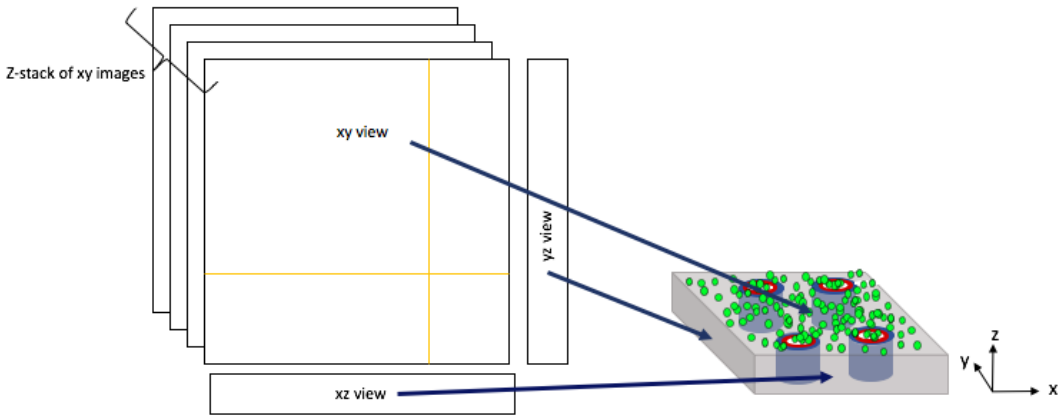

Figure 2.20: Scheme of the sections of the membrane corresponding to each view obtained by CLSM.

On CLSM images, microtubes labelled with PAH-Rh appear in red while microparticles appear in green. The figure on the left corresponds to one section of the top surface of the membrane while the figure on the right corresponds to one section of its bottom surface. Results shown in figures 2.21, 2.22 and 2.23 reveal that the fraction of encapsulated microparticles increases as the pore size increases.

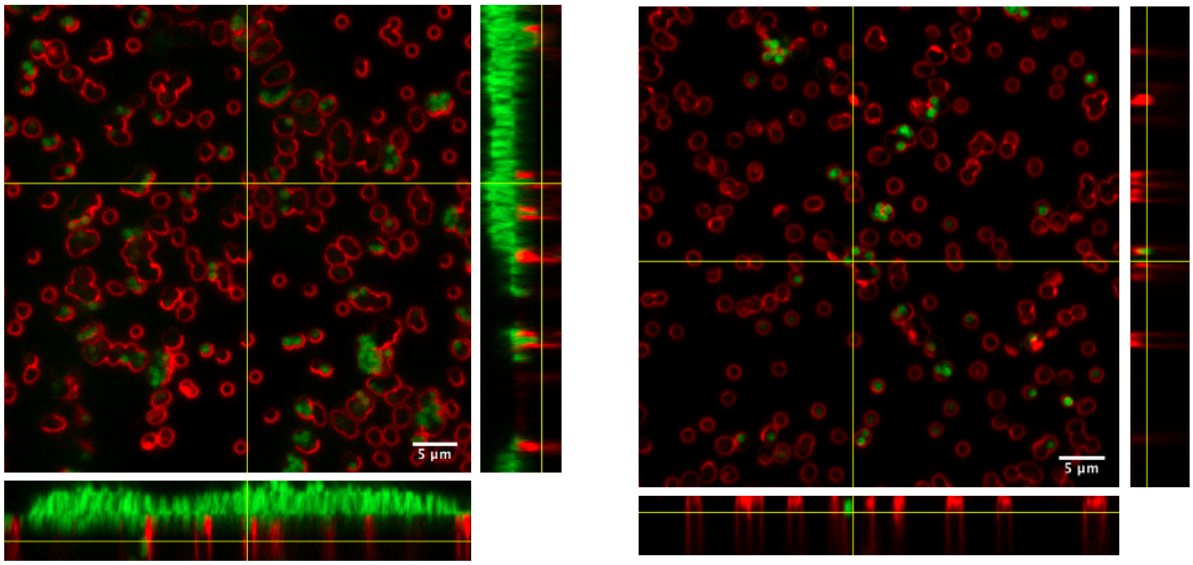

Figure 2.21: Top (left) and bottom (right) surfaces of the membrane with pores of 1.6μm in diameter. Orthogonal views xz, at the bottom, and yz, on the side. Each view corresponds to a section of the Z-stack of xy images, taken at the location of the crosshair.

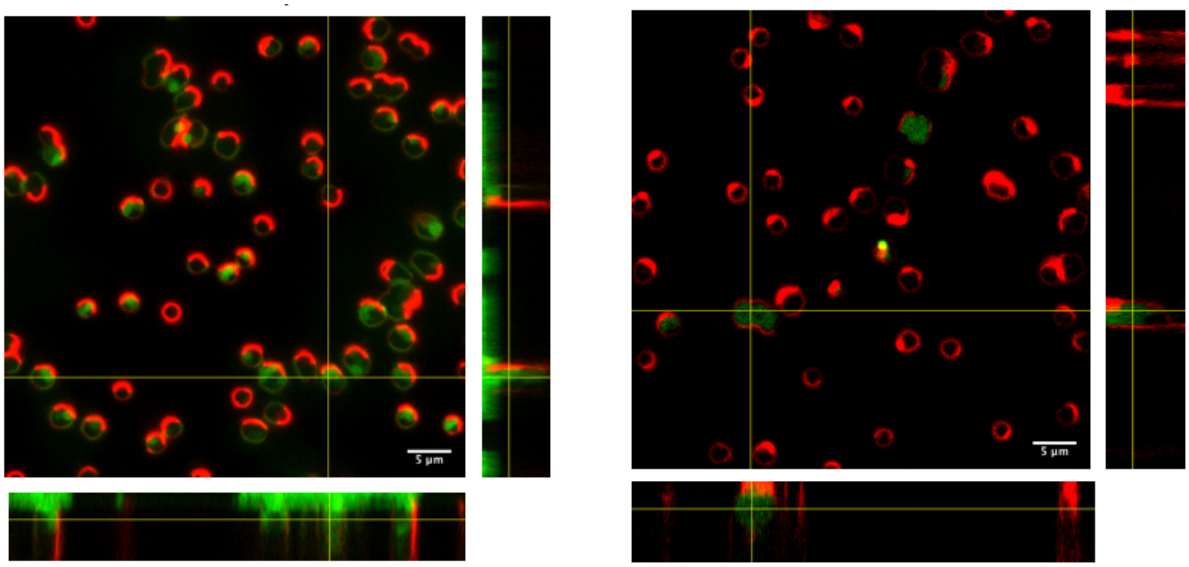

Figure 2.22: Top (left) and bottom (right) surfaces of the membrane with pores of 2.0μm in diameter. Orthogonal views xz, at the bottom, and yz, on the side. Each view corresponds to a section of the Z-stack of xy images, taken at the location of the crosshair.

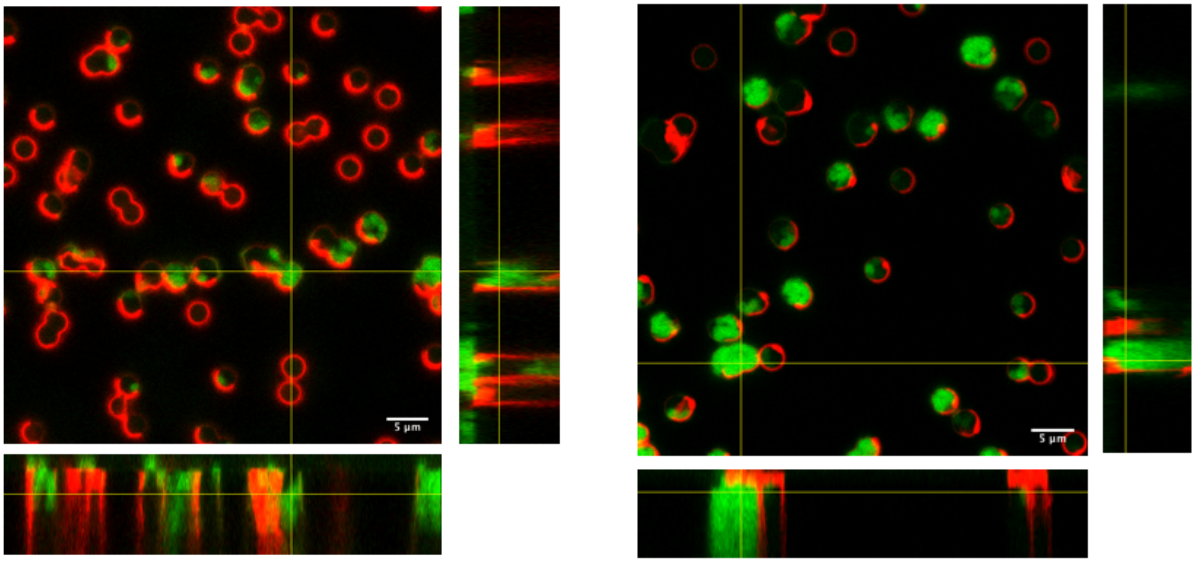

Figure 2.23: Top (left) and bottom (right) surfaces of the membrane with pores of 3.0μm in diameter. Orthogonal views xz, at the bottom, and yz, on the side. Each view corresponds to a section of the Z-stack of xy images, taken at the location of the crosshair.

Although the use of a larger pore membrane improved the fraction of encapsulated microparticles, it required depositing more layers to have enough material to close the pores. For example, for the membrane with pores of 1.6μm in diameter, 5.5 PVCL/PMAA bilayers and 6 ALG/CHI bilayers had to be deposited to close the lower end of the microtubes by decrusting every two deposition cycles, and 10 ALG/CHI bilayers had to be deposited on the top surface to close the upper end of the microtubes by decrusting. For the membrane with pores of 2.0μm in diameter, the number of bilayers deposited remained the same for PVCL/PMAA deposition but increased to 8 for ALG/CHI

deposition to close the lower end of the microtubes and to 16 for ALG/CHI deposition on the top surface to close the upper end of the microtubes. These values are listed in Table 2.2.

	Sacrificial compartment $(PVCL/PMAA)_x$	Internal compartment $(ALG/CHI)_y$	Top layer $(ALG/CHI)_z$
1.6μm pore size	$x = 5.5$	$y = 6$	$z = 10$
2.0μm pore size	$x = 5.5$	$y = 8$	$z = 16$

Table 2.2: Number of layers deposited to close the pores as a function of pore size.

The number of layers deposited is intimately related to the time required to fabricate the microtubes. For instance, the deposition of 16 ALG/CHI bilayers with a dipping time for 3 minutes and two rinsing steps for 30 secondes, lasted approximately 2 hours 30 minutes during which the membrane was dipped in salt solution at pH 6.0. Such a long exposure at such a pH could affect the stability of the PVCL/PMAA compartment and eventually denature or kill the bacteria loaded into the microtubes. Table 2.3 shows the time required to fabricate the various compartments of the microtubes and to close them by depositing multilayers on the top surface.

	Sacrificial compartment $(PVCL/PMAA)_x$	Internal compartment $(ALG/CHI)_y$	Top layer $(ALG/CHI)_z$
1.6μm pore size	3h	3h	1h30
2.0μm pore size	3h	4h	2h30

Table 2.3: Approximate duration required for the deposition of the sacrificial compartment, the internal compartment and the top layer depending on the pore size membrane.

In addition, figure 2.24a obtained by epifluorescence microscopy and figure 2.24b obtained by SEM show that even by depositing 16 bilayers on the top surface of a membrane with a pore size of 2.0μm, the microparticles still manage to escape from microtubes, hence the need to further increase the number of layers to be deposited.

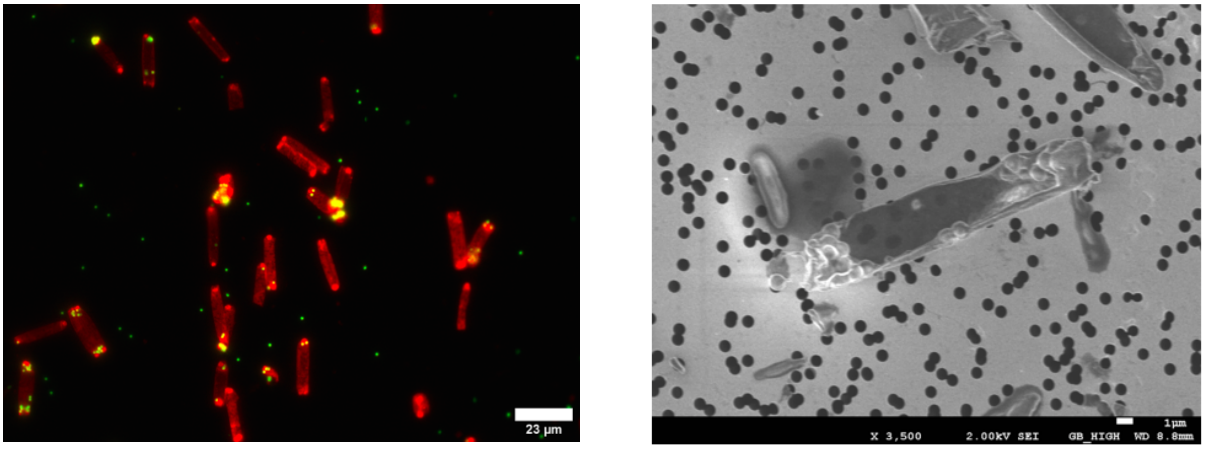

(a) (b)

Figure 2.24: Released $(PVCL/PMAA)_{5.5}(ALG/CHI)_8$ microtubes labelled with PAH-Rh and loaded with green microparticles (which appear yellow when superposed on red). The microtubes were prepared with a membrane with pore size of 2.0μm. (a) Image obtained by epifluorescensce microscopy. (b) Image obtained by SEM.

In conclusion, the use of a larger pore membrane improves the encapsulation rate but requires to deposit additional bilayers, which is time consuming and can affect the morphology of microtubes and probably the viability and functionality of the bacteria that will be encapsulated. After the analysis of these results, it was decided to use a membrane with pore size of 1.6μm in diameter to fabricate the microtubes since these pores are large enough to allow the passage of microparticles and small enough to be able to block them.

2.5.2 Interactions between microtube wall and microparticles

During the fabrication process of microtubes, the first layer deposited to form the microtube wall was ALG in order to get microtubes with a negatively charged external surface. This negative charge contributed to limit the interactions between the microtubes and the PC membrane which was also negatively charged, during the release process at pH 6.5. Moreover, to study the influence of the charge of the inner part of microtubes on the entrapment of microparticles which were surface modified with negatively charged ALG, CHI or ALG was used as the last deposited layer to form the microtubes.

In order to examine the effect of the charge of the inner part of the microtubes on the penetration efficiency of microparticles, two samples of microtubes were prepared. These samples were prepared in the same conditions (same pore size, same pore density, same conditions of preparation) except the nature of the last deposited layer forming the inner wall. The internal compartment of the first sample ended with a CHI layer in order to have positively charged internal microtubes. For the second sample, an additional layer of ALG was deposited in the pores of the membrane in order to get microtubes with a negatively charged inner wall. Then, bPEI/ALG coated microparticles were loaded into these different microtubes by filtration and the top and bottom surfaces of the membranes were observed by CLSM.

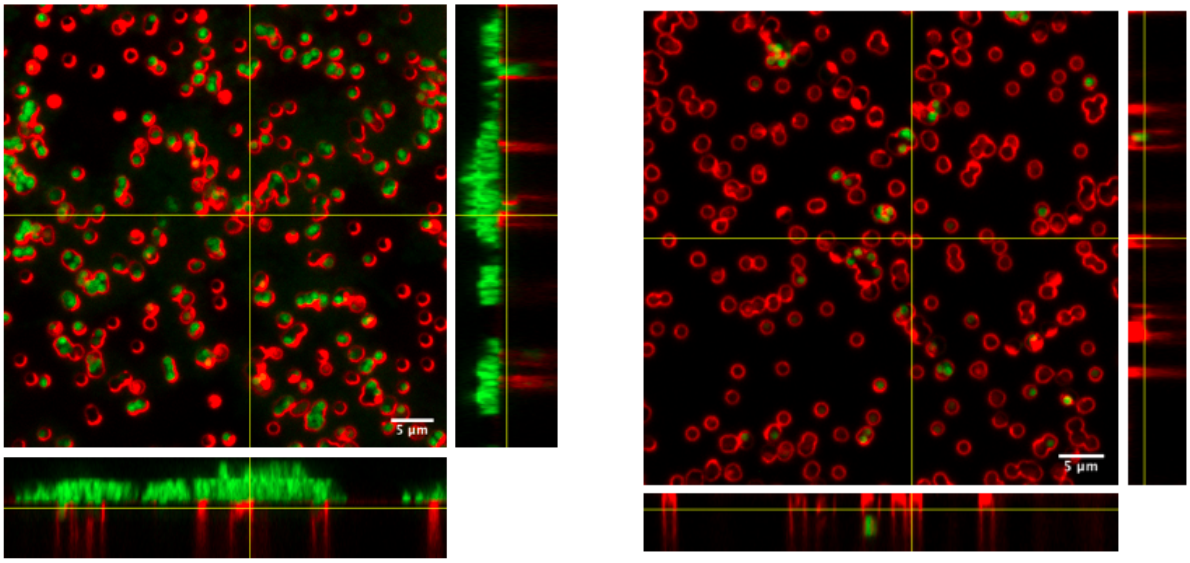

Figure 2.25: Top (left) and bottom (right) surfaces of the membrane containing positively charged internal microtubes (last layer deposited : CHI). Orthogonal views xz, at the bottom, and yz, on the side. Each view corresponds to a section of the Z-stack of xy images, taken at the location of the crosshair.

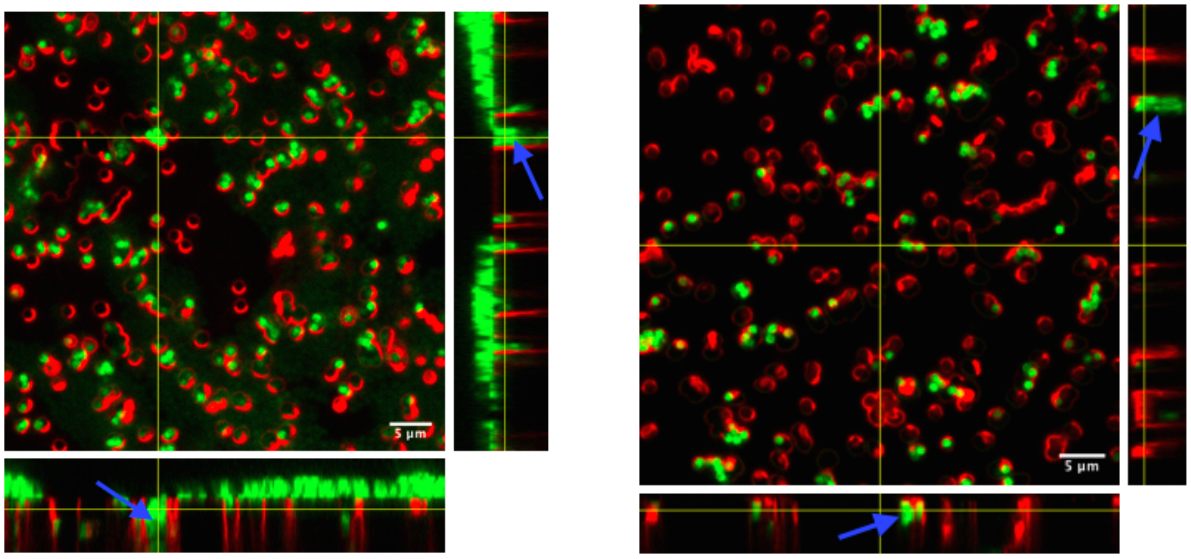

Figure 2.26: Top (left) and bottom (right) surfaces of the membrane containing negatively charged internal microtubes (last layer deposited : ALG). Orthogonal views xz, at the bottom, and yz, on the side. Each view corresponds to a section of the Z-stack of xy images, taken at the location of the crosshair. The blue arrows highlight the microparticles that are inside the microtubes.

Figures 2.25 and 2.26 show the top (left) and bottom (right) surfaces of membranes containing microtubes with inner wall composed by CHI and ALG, respectively. Whatever the internal charge of the microtubes, we observe the formation of microparticle aggregates and a thick filter cake of microparticles on the top surface of the membranes. These two effects were caused by the filtration process and limited the passage of microparticles into the pores of the membrane, resulting in a low

encapsulation rate. However, when the inner part of the microtubes was ended by an ALG layer, a larger fraction of encapsulated microparticles entered into the microtubes. This is because the electrostatic interactions between the inner wall of the microtubes and the surface of the microparticles decreased. As a result, microparticles adhered less to the walls of microtubes and more of them could penetrate more deeply and reach the bottom of the microtubes.

From now on, the images that will be shown in the following experiments will only concern negatively charged microtubes inside.

2.5.3 Loading technology

In order to increase the fraction of microparticles trapped into the microtubes, two loading methods were tested: filtration by application of pressure and passive diffusion. For the filtration process, a microparticle suspension was added in a syringe connected to a Swinny filter and the suspension was filtered through the membrane by pressing the syringe plunger, thereby forcing the passage of the microparticle suspension into the pores of the membrane. For the passive diffusion, the membrane was dipped in a diluted microparticle suspension for 12 hours and the microparticles were left to freely diffuse into the pores of the membrane.

For each loading process, the top and bottom surfaces of the membranes were observed by CLSM and compared in order to determine which one allowed to obtain the higher fraction of encapsulated microparticles into the pores. Figures 2.27 and 2.28 show the top (left) and bottom (right) surfaces of membranes for microparticles loaded by forced filtration and by passive diffusion, respectively.

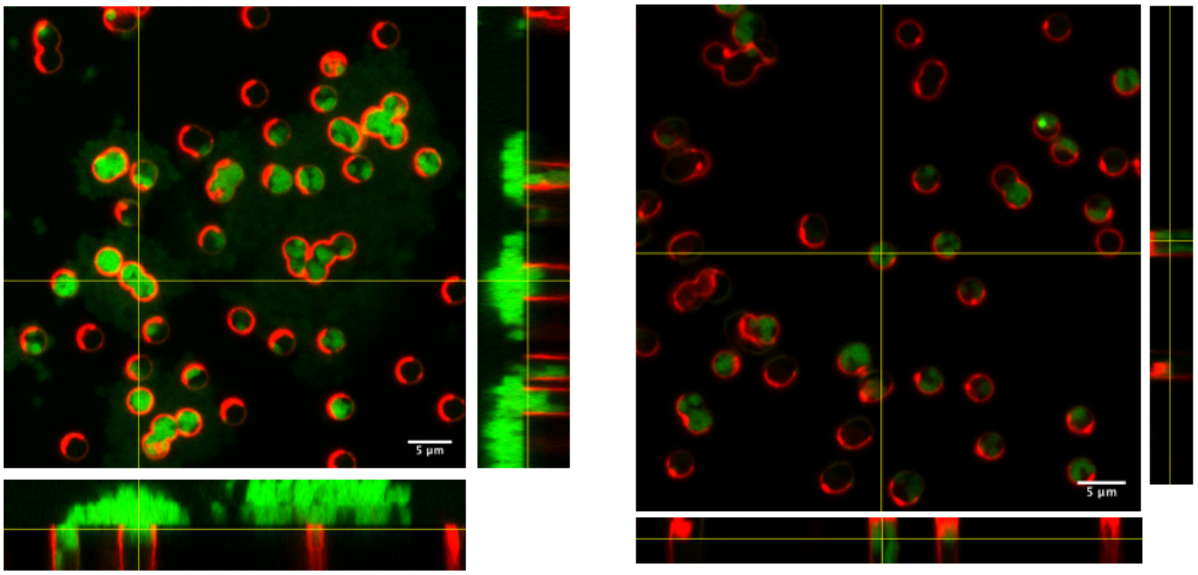

Figure 2.27: Top (left) and bottom (right) surfaces of the membrane for the forced filtration process. Orthogonal views xz, at the bottom, and yz, on the side. Each view corresponds to a section of the Z-stack of xy images, taken at the location of the crosshair.

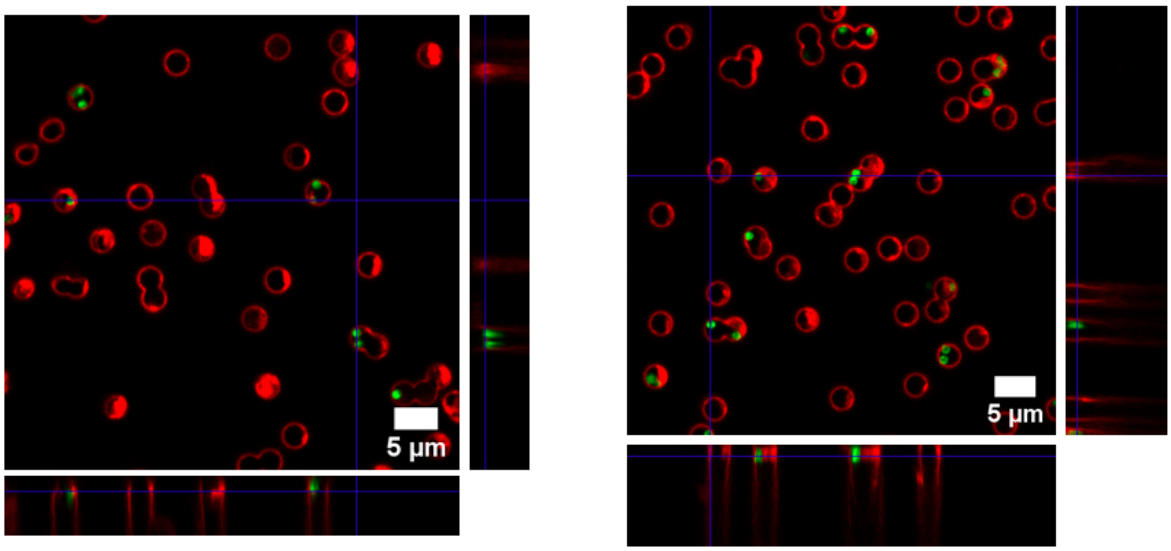

Figure 2.28: Top (left) and bottom (right) surfaces of the membrane for the passive diffusion process. Orthogonal views xz, at the bottom, and yz, on the side. Each view corresponds to a section of the Z-stack of xy images, taken at the location of the crosshair.

During the filtration process, a cake of microparticles formed on the top surface of the membrane by the microparticles that were retained on the membrane. The thickness of the cake increased with the amount of suspension filtered through the membrane. The thicker this cake, the more the resistance to the passage of microparticles in the pores of the membrane, resulting in a low fraction of microparticles encapsulated. In contrast, we can observe the absence of cake on the membrane when microparticles were loaded by passive diffusion. However, the amount of microparticles entrapped in the pores of the membrane was extremely low compared to the amount obtained for the forced filtration. In addition, passive diffusion was a very slow process in contrast to forced filtration. While the forced filtration only took a few minutes, the free diffusion required several hours to allow microparticles to reach the inner part of the pores. Given these results, it was decided to keep the forced filtration as the most suitable technology to load the microparticles into the microtubes.

2.5.4 Parameters of the filtration process

Setting up effective filtration involves finding a balance between different parameters such as the pore density of the membrane, concentration and volume of the suspension filtered through the membrane and the time used to push a given volume of suspension through the membrane. One of the critical problems governing the performance of the filtration process was the formation of microparticle aggregates and cake on the surface of the membrane. In order to find optimal experimental conditions to optimize the loading of microparticles into the pores of the membrane, different concentration, volumes to filter and pore density of the membrane were examined. The values of these parameters tested are listed in Table 2.29.

Pore diameter of the membrane [µm]	Pore density of the membrane [pores/cm2]	Initial concentration of the microparticle suspension [microparticles/mL]	Dilution factor	Final concentration of the microparticle suspension [microparticles/mL]	Filtered volume [mL]	Theoritical number of microparticles filtered through the membrane	Theoritical number of microparticles/pore
1.6	1.00E+07	1.50E+08	1X	1.50E+08	1	1.50E+08	15
			50X	3.00E+06	1	3.00E+06	0
					50	1.50E+08	15
2.0	2.00E+06	1.50E+08	10X	1.50E+07	10	1.50E+08	75
			20X	7.50E+06	20	1.50E+08	75
			50X	3.00E+06	1	3.00E+06	1
					50	1.50E+08	75
3.0	1.60E+06	1.50E+08	10X	1.50E+07	10	1.50E+08	93
			20X	7.50E+06	20	1.50E+08	93
			50X	3.00E+06	1	3.00E+06	1
					50	1.50E+08	93
5.0	8.00E+05	1.50E+08	1X	1.50E+08	1	1.50E+08	188
			50X	3.00E+06	50	1.50E+08	188

Figure 2.29: Values of the different parameters tested to optimize the loading of microparticles in microtubes by the filtration process.

Suspensions of bPEI/ALG coated microparticles with different concentrations (3.0×10^6, 7.5×10^6, 1.5×10^7 and 1.5×10^8 microparticles/mL) were prepared for these tests. Different volumes were filtered through the membranes, namely 10mL, 20mL and 50mL depending on the dilution factor. Figures 2.30, 2.31 and 2.32 show the top (left) and bottom (right) surfaces of the membrane (pore size of 3.0μm) obtained after filtration of 10mL of a suspension at the concentration of 1.5×10^7 microparticles/mL (10 fold-diluted), of 20mL of a suspension at the concentration of 7.5×10^6 microparticles/mL (20 fold-diluted) and of 50mL of a suspension at the concentration of 3.0×10^6 microparticles/mL (50 fold-diluted), respectively.

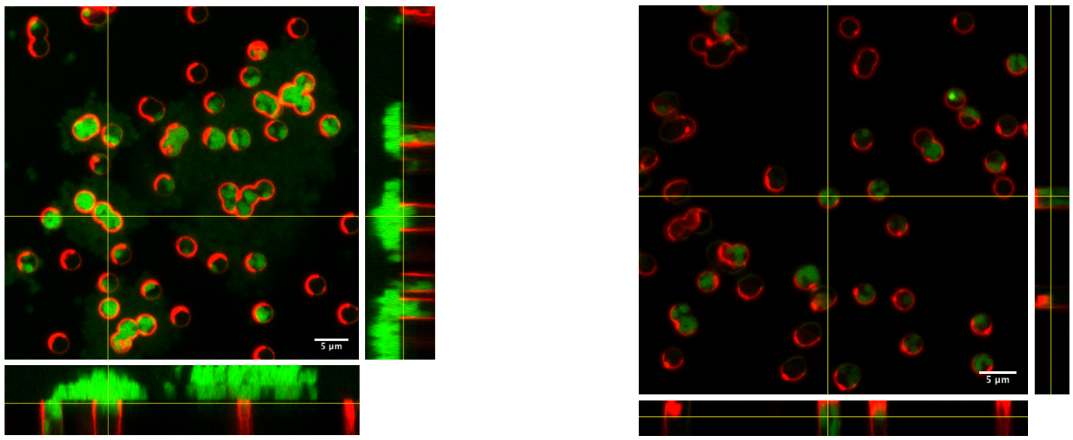

Figure 2.30: Top (left) and bottom (right) surfaces of a membrane after filtration of 10mL of a microparticle suspension at the concentration of 1.5×10^7 microparticles/mL. Orthogonal views xz, at the bottom, and yz, on the side. Each view corresponds to a section of the Z-stack of xy images, taken at the location of the crosshair.

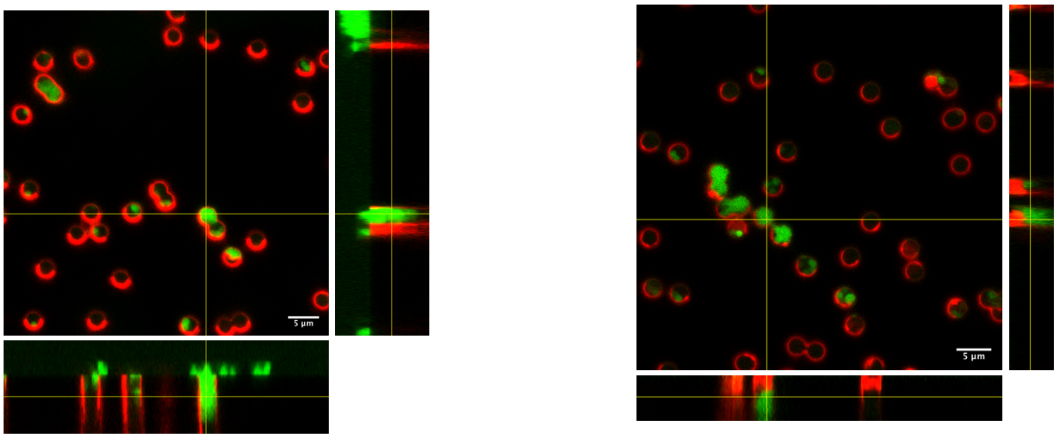

Figure 2.31: Top (left) and bottom (right) surfaces of the membrane after filtration of 20mL of a microparticle suspension at the concentration of 7.5×10^6 microparticles/mL. Orthogonal views xz, at the bottom, and yz, on the side. Each view corresponds to a section of the Z-stack of xy images, taken at the location of the crosshair.

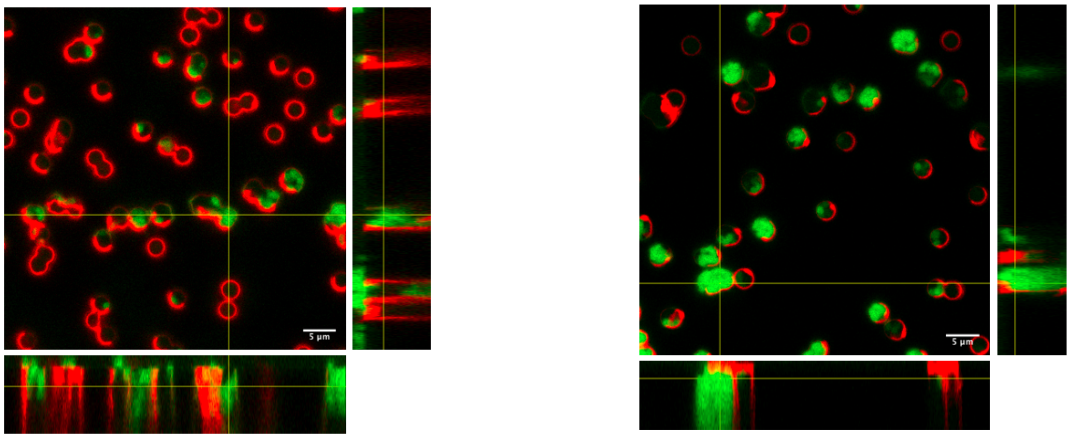

Figure 2.32: Top (left) and bottom (right) surfaces of the membrane after filtration of 50mL of a microparticle suspension at the concentration of 3.0×10^6 microparticles/mL. Orthogonal views xz, at the bottom, and yz, on the side. Each view corresponds to a section of the Z-stack of xy images, taken at the location of the crosshair.

On these figures, we observe that the fraction of encapsulated microparticles seems higher for the suspension at the concentration of 3×10^6 microparticles/mL. However, whatever the dilution factor used, the cake was always present on the surface of the membrane. This can be explained by the fact that the filtered volume being proportional to the dilution factor, the "theoretical" number of microparticles filtered (1.5×10^8) was kept constant. Therefore, we decreased the number of microparticles filtered by filtering only 1mL of a suspension at the concentration of 3×10^6 microparticles/mL and compared this result with that obtained for 50mL of filtered volume. Figures 2.33 and 2.34 show the top and bottom surfaces of membranes for the loading of 1mL and 50mL of a 50-fold diluted suspension, respectively. On the one hand, figure 2.33 reveals the absence of the cake but also the absence of microparticles inside the microtubes when 1mL of a microparticle suspension at the concentration of 3×10^6 microparticles/mL was filtered. On the other hand, figure 2.34 shows a much higher amount of microparticles inside the microtubes but a thick cake on the surface of the membrane when 50mL of the same suspension was filtered.

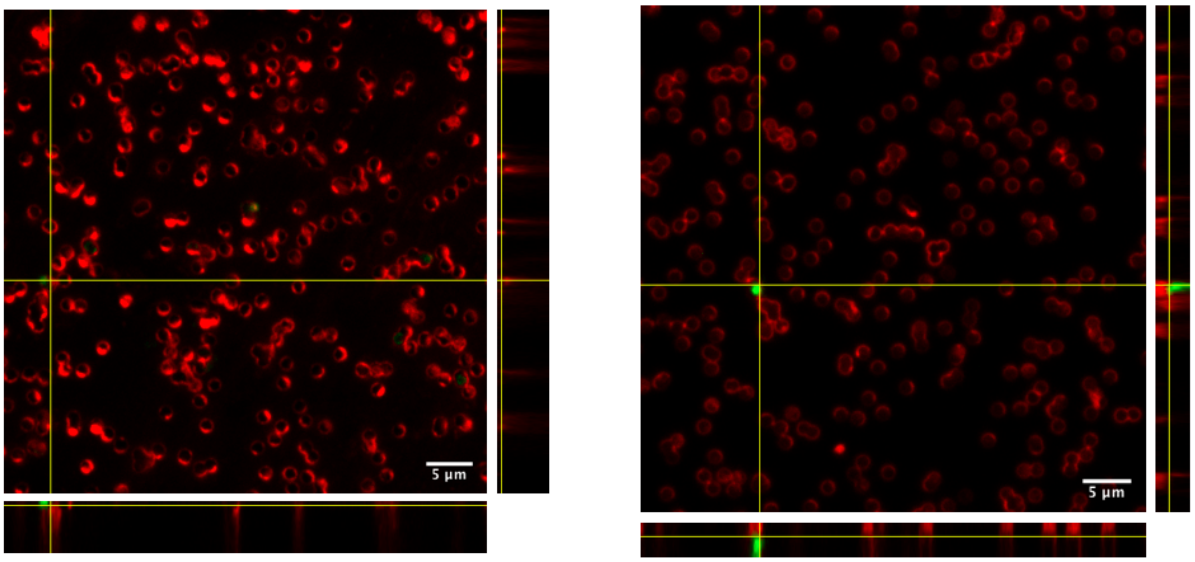

Figure 2.33: Top (left) and bottom (right) surfaces of membrane for the loading of 2% (1mL) of microparticle suspension at the concentration of 3.0×10^6 microparticles/mL. Orthogonal views xz, at the bottom, and yz, on the side. Each view corresponds to a section of the Z-stack of xy images, taken at the location of the crosshair.

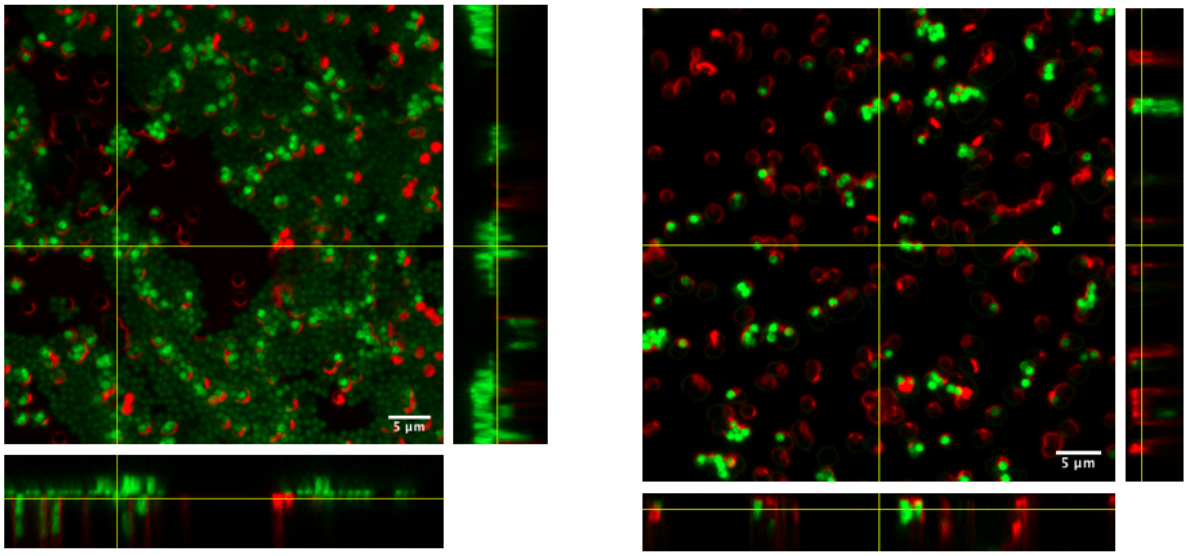

Figure 2.34: Top (left) and bottom (right) surfaces of membrane for the loading of 100% (50mL) of microparticle suspension at the concentration of 3.0×10^6 microparticles/mL. Orthogonal views xz, at the bottom, and yz, on the side. Each view corresponds to a section of the Z-stack of xy images, taken at the location of the crosshair.

In addition, we noticed that the filtration process was not uniform. As shown in figure 2.35, some regions of the membrane had a thick layer of microparticles while others had only a thin layer of microparticles. This problem could be solved by carrying out a filtration in several steps, for instance 5×10mL for 50mL of suspension, rather than a continuous filtration for which the 50mL are filtered in one step.

Figure 2.35: Top surface of membranes obtained after a continuous filtration process. The thick layers are delimited by the blue curves.

In conclusion, simple theoretical considerations (see Table 2.29) were not sufficient to determine the number of microparticles per pore because the filtration phenomenon is more complex than the simple regular passage of microparticles in pores. There is indeed a concentration gradient of the microparticles operating above the membrane which is not taken into account in the simple theoretical calculation. Furthermore, results obtained experimentally showed that the fraction of encapsulated microparticles increased as the concentration of the filtered suspension decreased. By filtering only a fraction of a diluted microparticle suspension, it prevented the formation of a thick cake of microparticles on the membrane surface. Because it was not possible to fully control the amount of microparticles loaded inside the microtubes regardless of the filtered volume, we opted for the filtration in 5 steps of 50mL of a microparticle suspension at the concentration of 3×10^6

microparticles/mL because these conditions gave the highest fraction of microparticles encapsulated despite the formation of a cake.

2.6 Conclusion of this chapter

The major objective of this first work was to optimize an encapsulation method starting from the work of Xu et al. on the fabrication of microtubes in biocompatible conditions. Different challenges were encountered during this study :

- The need to develop a biocompatible process that can be used to load bacteria while keeping their functions.
- The fact that the microtubes need to be closed after microparticle loading and before their release from the membrane in order to warrant the encapsulation process.
- The optimization of the loading process to obtain enough microparticles entrapped into the microtubes.

The optimization process was conducted on microparticles mimicking bacterial cells, and various parameters likely to influence the effectiveness of the encapsulation method were examined. By investigating the effect of these parameters, an "optimal" protocol could be established. The best conditions for the encapsulation of microparticles include :

- Use of a PC membrane with a pore size of 1.6μm and a pore density of $10^7 cm^{-2}$.
- Use of microtubes in which the inner wall is composed of ALG in order to have negatively charged inner walls in microtubes, which gives $(PVCL/PMAA)_{5.5}(ALG/CHI)_{6.5}$ microtubes.
- Use of microparticles surface-modified with bPEI/ALG in order to have negatively charged microparticles.
- Filter 50mL of a suspension of modified microparticles at the concentration of 3×10^6 microparticles/mL. It would have been interesting to try to filter other volumes, namely 12.5mL, 25mL and 37.5mL, of the microparticle suspension at the concentration of 3.0×10^6 microparticles/mL. However, this was not possible due to lack of time.
- A forced filtration process performed in 5 steps (5x10mL).

For this optimal protocol, a series of images were realized by SEM and CLSM in order to characterize the state of the membrane and microtubes after each step of the encapsulation method including the fabrication of microtubes, the loading of microparticles, the removal of the filter cake by decrusting, the closure of microtubes by depositing $(ALG/CHI)_{10}$ bilayers on the top surface of the membrane and the release of microtubes. These figures are shown in the Annex.

Since we demonstrated the feasibility of the encapsulation method in polyelectrolyte microtubes by using model microparticles, we decided to replace microparticles with bacteria for concrete application.

CHAPTER 3

Towards the fabrication of polymer microtubes entrapping bacteria

The previous chapter dealt with a method for the encapsulation of microparticles in polymer microtubes. In this chapter, the method is tested with *S. epidermidis* bacteria instead of microparticles. The encapsulation method should be adapted because microparticles are not perfect models of bacteria. The bacteria are indeed living entities, less rigid compared to PS microparticles, able to deform and interact with the microtubes. Moreover, the nature of the surface of bacterial cells differs from that of PS microparticles, which leads to differences in the interaction with microtubes. This chapter first describes conditions used for bacterial culture. Then, it presents the adaptation of the previously developed encapsulation method to bacteria. Finally, it finishes by addressing the remaining challenges and the possible ways of improvement.

3.1 Materials

Bacteria Freeze-dried *S.epidermidis* bacteria were obtained from ATCC (ATCC 12228, lot 70011848) and stored in the fridge at 4°C.

Broth and glycerol Nutrient Broth (BD 234000) used for the culture of bacteria was purchased from Becton, Dickinson and Company (BD). Glycerol (molar mass 92.094g/mol) used for low temperature storage of bacteria was purchased from Thermo-Fisher Scientific.

Polymers PMAA of average molar mass 100kg/mol was purchased from Polysciences, and PVCL of average molar mass 1.8kg/mol was purchased from Polymer Source Inc. Sodium ALG was obtained from Sigma-Aldrich and CHI of average molar mass 50-150kg/mol and deacetylation degree >90% was obtained from NovaMatrix. PAH-Rh of average molar mass 15kg/mol was purchased from Surflay Nanotec GmbH. All the polymer solutions were prepared at 1mg/mL, 150mM NaCl.

Track-etched membranes Track-etched membranes were supplied by it4ip (Belgium). As for the encapsulation of microparticles, track-etched membranes were used either as template for LbL deposition of microtubes or as filter for collecting microtubes while removing free bacteria. All membranes were sterilized before use. The characteristics of each track-etched membrane used are shown in Table 3.1.

Material	Pore diameter [μm]	Porosity [cm^{-2}]	Thickness [μm]
PC	1.6	1×10^7	24
PC	0.8	4×10^7	24
PET	0.2	5×10^8	23

Table 3.1: Track-etched membranes used during the encapsulation process of bacteria.

Water and other solvents Milli-Q water with a resistivity of 18.2MΩ·cm was obtained from a Merck Millipore system and sterilized in an autoclave prior to use. MES monohydrate (99^+%, for biochemistry, molar mass of 213.25g/mol) was purchased from Thermo Fischer Scientific. MES buffer (20mM MES, 150mM NaCl) with pH set to 6.5 was used to release microtubes fabricated in the pores of the membranes.

3.2 Protocols

3.2.1 Material sterilization

Working with bacteria requires strict sterile conditions. Therefore, all processes were performed in a safety cabinet. All solutions were autoclaved before use, except for ALG and CHI because they are biopolymers not stable at high temperature. Therefore, ALG and CHI solutions were filtered through low protein binding filters (0.8μm) in order to remove potential contaminants.

Membranes containing the $(PVCL/PMAA)_{5.5}(ALG/CHI)_{6.5}$ microtubes, as well as empty membranes used as filters were desinfected by fully dipping them in 70% ethanol for 2 minutes in a safety cabinet. Then, the membranes were rinsed three times in water at pH 5.0 and exposed to UV light for 1 minute in a safety cabinet. Finally, the membranes were left to dry overnight to ensure that all the ethanol liquid was evaporated. This process is shown in figure 3.1.

Figure 3.1: Scheme of the sterilization of the membrane before being loaded with bacteria.

All items were disinfected before being placed in the safety cabinet. After autoclaving, bottles were never opened except inside the safety cabinet. All items having been in contact with bacteria were immersed in a bleach solution, then cleaned and rinsed thoroughly before reuse or discard.

3.2.2 Bacterial culture

The experimental protocol for the revival and cryo-preservation of *S. epidermidis* was the following. First, bacteria were revived overnight in 6mL of sterilized broth (BD Difco Nutrient Broth 234000) at 37°C, in vented tubes, and under agitation (180 rpm). The next day, the broth was poured into 400mL of fresh broth in a vented culture flask, and cultured at 37°C/180 rpm. The OD_{540} of broth was monitored until the culture was in its exponential phase and an OD_{540} of $\pm$ 0.54 was reached. Then, the culture was collected in eight 50mL Falcon tubes and centrifuged at 4000 rpm for 10

minutes in order to remove the supernatant. After that, 10mL of fresh culture broth was added in each bacteria-containing Falcon tube and vortexed to well disperse bacteria. This suspension was poured in a second bacteria-containing Falcon tube, and additional 10mL of culture broth were added and vortexed. 20mL of glycerol/water solution were also added and the mixture was vortexed again. Finally, the tubes were stored in a freezer at -80°C for long term storage.

Bacteria growing in a given medium result, on the one hand, in the increase of the number of bacteria and, on the other hand, in a depletion of the culture medium in nutrients, as well as an enrichment in metabolites, possibly toxic. There are several phases which together constitute the bacterial growth curve. First, there is the "latency phase" where the growth rate is zero. The duration of this phase depends on the state of the bacteria and the composition of the medium. This is the time for bacteria to adapt to the culture medium. Secondly, there is the "exponential phase" in which the growth rate is constant. The bacterial mass is represented by viable microorganisms. During the exponential growth phase, cell multiplication is much greater than cell death. When the growth rate reaches the "stationary phase", the growth and death rates are equal. Therefore, no net increase in the number of bacteria is observed. Finally, the last phase is the "decline phase" characterized by a negative growth rate. Lack of nutritional resources and accumulation of toxic metabolites cause a decrease in the number of viable microorganisms [72].

A typical growth curve can be recorded simply by measuring the OD of the bacteria broth at regular time intervals. Figure 3.2 shows typical growth curves of *S. epidermidis* for OD_{540}.

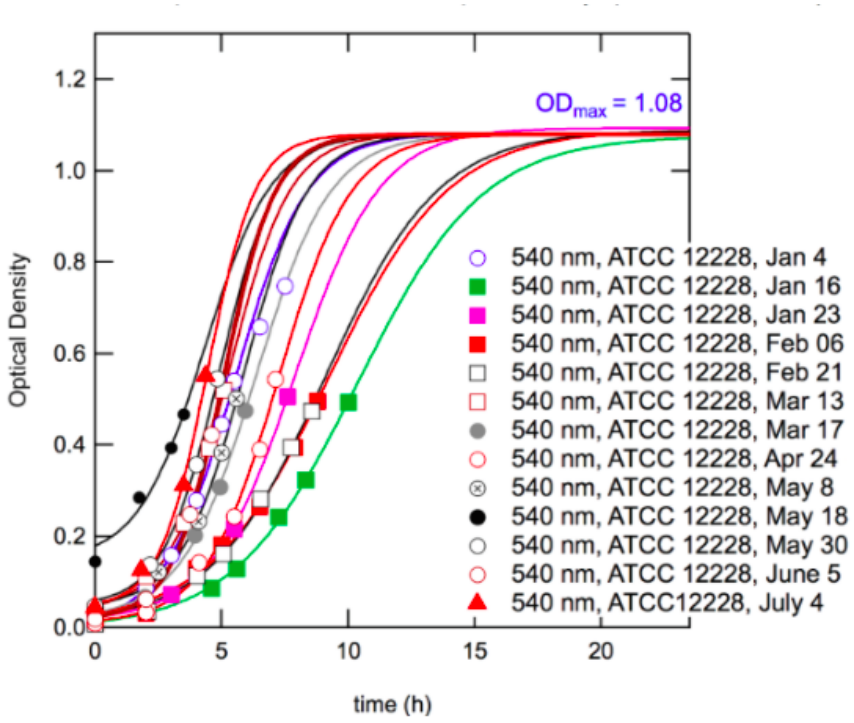

Figure 3.2: Typical growth curves of *S. epidermidis ATCC 12228*. OD_{540} as function of incubation time. Experiments from other researchers of our lab over a range of experiments. Note that there is a certain degree of variability from one culture to another.

3.2.3 Purification and concentration of bacteria

A small amount of cryo-preserved bacteria was added in 32mL of broth and pre-cultured overnight at 37°C, in air, and under agitation (180 rpm). The next morning, the pre-culture was centrifuged at 4000 rpm for 5 minutes and the supernatant was removed. Then, bacteria were rinsed by adding 30mL of salt water (150mM NaCl, pH 6.0) and a new centrifugation was carried out under the same conditions as the previous one. After removing the supernatant, bacteria were rinsed a second time by adding 12mL of salt water, then centrifuged and the supernatant was removed. Finally, bacteria were suspended in 8mL of salt water and stored in the fridge at 4°C before encapsulation in microtubes.

3.2.4 Determination of bacteria concentration

The OD of bacteria suspensions was measured at a wavelength of 540nm with a spectrometer (Tecan plate reader Infinite M Nano$^+$ PRO). The growth of bacteria during the culture was followed by monitoring the OD_{540}. To establish a relationship between the real bacterial concentration in the suspension and the measured OD_{540} value, a droplet of precise volume V_0 of bacteria suspension was placed on a glass slide. The area of the droplet (S) was estimated and the number of bacteria (N) was counted on optical microscopy images (area S_1). The concentration of bacteria (n) was obtained by :

$$n = \frac{NS}{S_1 V_0} [\text{cells}/mL]$$

The OD_{540} of a series of bacteria suspensions was measured and their corresponding bacteria concentration was calculated to obtain a calibration curve illustrating the relationship between OD_{540} and bacterial concentration. This curve is shown in figure 3.3.

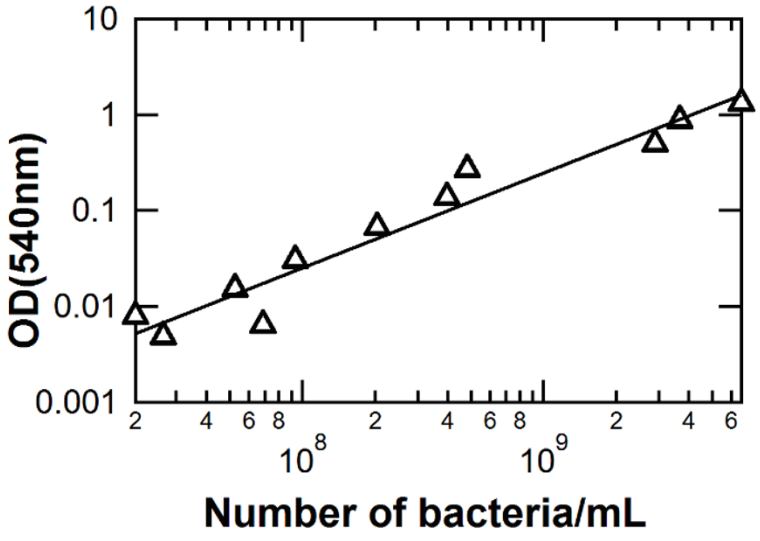

Figure 3.3: Calibration curve used to correlate the measured OD_{540} value with the bacteria concentration.

3.2.5 Determination of bacteria viability

The Live/Dead BacLight Bacterial Viability Kit was obtained from Thermo-Fisher Scientific and used to stain bacteria. This kit contains green-fluorescent SYTO 9 nucleic acid stain and red-fluorescent propidium iodide. The differences between these dyes are their spectral characteristics and their

capacity to penetrate bacteria. Indeed, the SYTO nucleic acid penetrates all bacteria, i.e., those with intact membranes and those with damaged membranes, while propidium iodide penetrates only bacterial cells with damaged membranes. When both dyes are present in the bacteria, the SYTO 9 stain fluorescence is quenched. Therefore, live bacteria are stained in green due to diffusion of the SYTO 9 stain through their membrane while dead cells are stained in red. Thus, the kit allows to quantitatively distinguish live and dead bacteria by providing two-color fluorescence assay of bacterial viability.

For epifluorescence microscopy, the bacteria were stained with a Live/Dead BacLight kit (SYTO 9 (3.34mM) and propidium iodide (20mM)). Because the microtubes were labelled with PAH-Rh and appear in red fluorescence in the same way as dead bacteria, only the SYTO 9 stain was used to have a good contrast. As mentioned, the SYTO 9 stains all bacteria in a population. Therefore, the Live/Dead kit was not used to study the viability of bacteria (rate of living bacteria versus rate of dead bacteria) in this case but rather to visualize the presence of the bacteria inside or outside microtubes. For this, 0.3μL of SYTO 9 dye solution were dissolved in 0.2mL of sterilized salt solution (150mM NaCl, pH 6.0). Then, the mixture was dropped on the track-etched membrane with microtubes collected on it, and incubated at room temperature in the dark for 20 minutes. After that, the stained membrane was placed on a glass slide with a cover slide. After staining, bacterial cells were observed with an Olympus IX71 epifluorescence microscope at 60x magnification[1].

3.2.6 Loading of bacteria in microtubes

Loading assays were carried out using sterilized membranes filled with $(PVCL/PMAA)_{5.5}(ALG/CHI)_{6.5}$ microtubes closed at their bottom end (see chapter 2, section 1.4). The concentration of bacterial suspension used for encapsulation assays was calibrated to be the same as the concentration of PS microparticles (1.5×10^8 microparticles/mL) illustrated in chapter 2. Then, the suspension of bacteria was 50-fold diluted in NaCl solution (150mM NaCl, pH 6.0) in order to achieve a final concentration of 3×10^6 bacteria/mL. A circular-shaped (12mm in diameter) membrane containing microtubes was placed in the Swinny filter unit and 50mL of the 50-fold diluted bacteria suspension were filtered through the membrane using the syringe fixed to the Swinny filter unit. This filtration process was carried out in 5 steps (5×10mL), each for 2 minutes. Then, the membrane was removed from the Swinny filter and decrusted three times on both sides to remove free bacteria that were not entrapped in the microtubes.

3.2.7 Closure of microtubes

To prevent the release of bacteria from microtubes, ALG/CHI bilayers were deposited on the top surface of the membrane by LbL deposition. In this process, the top surface of the membrane was floated on the surface of a filtered ALG solution (150mM NaCl, pH 6.0) for 2 minutes, then rinsed twice for 30 secondes in rinsing solutions of same NaCl concentration and same pH as the polymer solutions. Then, the membrane was floated on a filter-sterilized CHI solution (150mM NaCl, pH 6.0) for 2 minutes then twice rinsed. CHI is a bactericidal and bacteriostatic material. This means that CHI has the ability to kill bacteria or to hinder the growth of bacteria. However, the antibacterial potential of CHI decreases rapidly when CHI is complexed with ALG [8]. Therefore, the LbL deposition cycle started and ended with ALG deposition so that 9.5 bilayers were deposited. Every two cycles, the top surface of the membrane was decrusted with a cotton swab. After the last half-cycle, the membrane was decrusted on both sides and kept in a fresh 150mM NaCl solution before release of microtubes.

[1]The 60X objective has to be used with immersion oil to allow such magnification.

3.2.8 Release of microtubes

For the release of microtubes loaded with bacteria by disintegration of the sacrificial compartments, 120mL of an autoclaved buffer solution (20mM MES, 150mM NaCl, pH 6.5) were filtered through the membrane and the filtrate was recovered in an Erlenmeyer flask.

3.2.9 Collection of microtubes

The microtubes were collected by forced filtration of 10mL of the filtrate through a track-etched PC membrane of 1.6μm pore diameter to prevent the passage of microtubes while removing the residual non-entrapped bacteria or escaped from microtubes during the filtration process. Then, 5mL of fresh MES buffer solution were added to rinse the membrane and eliminate any remaining bacteria. This rinsing step was repeated three times.

3.3 Results and discussion

To visualize the entrapment of bacteria in the microtubes, the microtubes labelled with PAH-Rh were collected on a membrane and the resulting sample was exposed to the SYTO 9 dye in order to stain bacteria and observed them by epifluorescence microscopy. Figure 3.4 reveals a low density of encapsulated bacteria. The only microtube almost completely filled with bacteria is not representative of all the microtubes collected, most of them being empty.

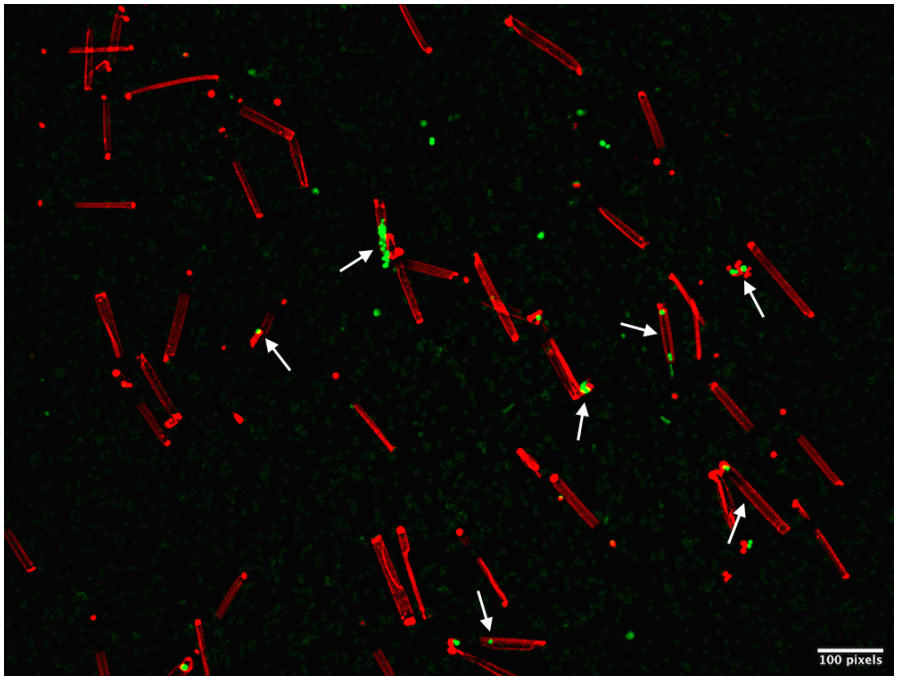

Figure 3.4: Epifluorescence microscopy image of microtubes entrapping bacteria: the wall of the microtubes was labelled with PAH-Rh (red) and bacteria were stained with SYTO 9 (green). The white arrows show the microtubes containing encapsulated bacteria.

Moreover, the filtration of the microtube suspension through a 1.6μm pore size filter was not sufficiently efficient to totally remove the free bacteria from the sample. We then attempted to increase the number of rinsing steps by filtering a larger volume of buffer solution after the collection of the

microtubes onto the membrane. Figure 3.5 shows the membrane after 5 rinsing steps (5×5mL). However, free bacteria are still visible in the sample.

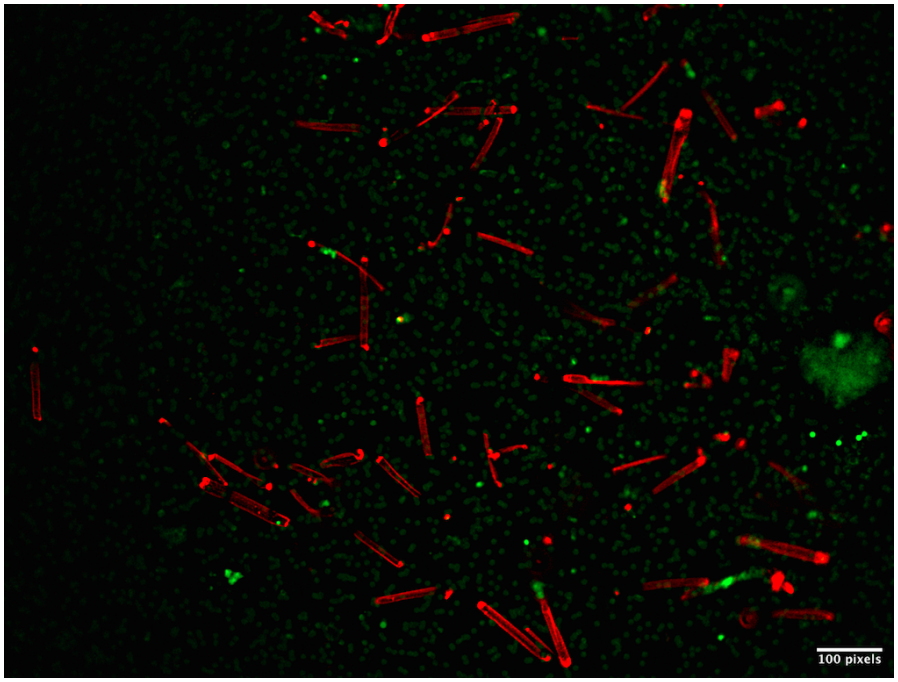

Figure 3.5: Epifluorescence microscopy image of microtubes entrapping bacteria with more rinsing steps: the wall of the microtubes was labelled with PAH-Rh (red) and bacteria were stained with SYTO 9 (green).

Another problem was that the SYTO 9 dye also stained the PC membrane, reducing the contrast between free bacteria and the membrane. Even if fluorescence intensity emitted by bacteria is higher than the one of the membrane, it remains difficult to conclude if free bacteria were fully removed.

3.4 Conclusion of this chapter

The objective of this chapter was to explore the encapsulation process, described in the previous chapter, to prepare polymer microtubes encapsulating bacteria of a biological interest, namely *S. epidermidis*. Results of this first assay of encapsulation reveal the need to consider a couple of improvements.

First, a method to avoid the fluorescence of the PC filtration membrane used to collect the microtubes has to be considered to better conclude about the presence of free bacteria in the sample. In this regard, bacteria could be stained before being loaded into the microtubes in order to avoid any interaction between the dye and the PC membrane. Then, the microtubes fabricated in the template membrane could be closed by depositing $(ALG/CHI)_{9.5}$ bilayers on the membrane, released and collected. However, all of these steps should be performed in the dark due to the light sensitivity of the SYTO 9 dye. Another possibility to avoid concomitant fluorescence is the use of a black membrane as a filter to collect the microtubes. This last alternative would be probably easier because it does not require any strict conditions.

Once we would be clearly able to distinguish stained bacteria from the membrane, we would need to improve the removal of non-encapsulated bacteria in the microtube sample. For this, we could try to filter microtubes on larger pore membranes, for example 2.0 and 3.0μm, in order to eliminate all

free bacteria from the sample. Increasing the number of ALG/CHI bilayers to be deposited on the membrane to close the ends of microtubes is also an option to consider to improve the efficiency of the encapsulation. However, the number of bilayers to be deposited should not be too high as the viability of bacteria may be affected by such treatment and the longer deposition time may cause the dissolution of sacrificial compartments.

CHAPTER 4

General conclusion

This last chapter briefly reminds the context and objective of this thesis and the strategy initially envisaged to achieve this objective. Then, it summarizes the main results according to the different parameters studied and discusses the improvements that could have been made to this work. Finally, it finishes by presenting the critical analysis and perspectives of the developed system.

4.1 Context, objective and strategy

Bacteria evolving on the skin are currently considered as potential components for skin-care products. However, considering the risks associated to their proliferation, it is crucial to develop solutions such as encapsulation. The objective of this thesis was to develop a method for the encapsulation of commensal skin bacteria in polymeric microtubes able to maintain their viability while controlling their development. For this, the encapsulation method developed by Xu et al. was first optimized on microparticles mimicking bacterial cells, then the method was tested on living bacteria.

This encapsulation method was based on the fabrication, in the micropores of a track-etched membrane, of bicompartmentalized microtubes with a sacrificial outer compartment that can be erased for the release of the inner compartment of microtubes in biocompatible conditions (no use of organic solvents for microtube recovery). The selected microtube fabrication methodology was LbL assembly on a microporous track-etched membrane, followed by the dissolution of the sacrificial compartment in a pH 6.5 aqueous solution and microtube collection by filtration. The different parameters studied were the pore size of the templating membrane, the interaction between the inner wall of microtubes and the surface of microparticles, the loading technology, and the filtration conditions. The strain of bacteria chosen within the framework of this thesis was *S. epidermidis* given its full clinical potential.

4.2 Results

The size of the pores of the track-etched membrane used as template for the fabrication of microtubes proved to be a determining parameter for improving the fraction of encapsulated microparticles. Indeed, the larger the pores, the larger the fraction of encapsulated microparticles. However, the use of membranes with larger pores made it longer and more difficult to close the microtubes at their extremities by decrusting.

The presence of an additional layer of ALG in the internal wall of the microtubes made it possible to slightly reduce the interactions between the internal wall of the microtubes and the surface of the microparticles so that they penetrate the microtubes more deeply and in a greater amount.

The forced filtration method showed to be much faster and more efficient than passive diffusion of microparticles into the pores of the membrane. However, the formation of a cake and aggregates of

microparticles were concomitant phenomena in the filtration process which created resistance to the passage of microparticles.

The conditions of the filtration process influenced the results of the filtration. The decrease in the concentration of the filtered microparticles suspension while keeping the same theoretical number of loaded microparticles showed a greater encapsulation rate but did not eliminate the filter cake. Incremental filtration in 5 steps rather than continuous filtration allowed a more homogeneous filtration.

Finally, commensal bacteria *S. epidermidis* were entrapped in $(PVCL/PMAA)_{5.5}(ALG/CHI)_{6.5}$ microtubes made by membrane-templated LbL according to the optimal protocol previously developed on the microparticles, then released from the membrane by disaggregation of the sacrificial PMAA/PVCL compartment and collected by filtration through a membrane. The interaction between the dye used to visualize the bacteria and the membrane used to collect the released microtubes did not allow to conclude definitively on the presence of the bacteria outside and inside the microtubes. It is very likely that many bacteria were not trapped and still managed to escape from the microtubes, hence the need to carry out additional work and make improvements.

4.3 Improvements

Given the health crisis that we are living due to the COVID-19, the federal government has adopted a series of measures, including those to suspend research activities and to close laboratories in order to limit the spread of the virus. Therefore, the optimization of the encapsulation process, as well as the behavior of the encapsulated bacteria could not be further studied.

If the context had been favorable for the continuation of this thesis, the influence of the volume of the filtered microparticle suspension would have been studied. For this research, volumes of 12.5mL, 25mL and 37.5mL of a microparticle suspension at the concentration of 3.0×10^6 microparticles/mL would have been filtered through a membrane with a pore size of 1.6μm and containing $(PVCL/PMAA)_{5.5}(ALG/CHI)_{6.5}$. Among the volumes tested, 37.5mL would probably have been the most promising, i.e., the volume that would have decreased the thickness of the cake, and therefore decreased the resistance of the passage of microparticles in the pores of the membrane, while providing a sufficiently high fraction of encapsulated microparticles.

With regard to the encapsulation of bacterial cells, the remaining time would have been devoted initially to solving the problems encountered, i.e., the limitation of interaction of the stain dye with the PC membrane to collect microtubes and the removal of all free bacteria. Once these issues resolved, we would have considered to fabricate mats of microtubes and to culture these mats in broth in the presence of an alamarBlue redox test in order to measure the growth, the proliferation and the metabolic activity of the so-trapped bacteria.

4.4 Perspectives

The final purpose of these mats of microtubes is to form soft patches directly applicable on the skin in order to restore the equilibrium of dysbiotic skin without risking adverse proliferation. At the end of the experiences conducted in this thesis, it is essential to question the strengths and weaknesses of the strategy to achieve the target purpose. Such an application indeed implies satisfying several criteria.

First, the encapsulation method has not to compromise the viability and functionality of bacteria. Bacteria should survive each step of the process and remain stable until they are used. The encapsu-

lation method developed within the framework of this thesis should normally satisfies this criterion since it takes place in soft and biocompatible conditions with living entities. It requires no organic solvent, no significant mechanical stress, no extreme pH or temperature. The encapsulation method is based only on the use of aqueous solutions, harmless to living entities. However, the preservation of the viability and functionality of trapped bacteria during the encapsulation method has not been proven due to lack of time.

Then, the encapsulation method has to be safe and not present a risk to the patient. In this regard, it is certain that if we do not manage to eliminate the non-encapsulated bacteria, the encapsulation method developed here will have to be abandoned.

Finally, the encapsulation method has to be transposable for use on an industrial scale and also adaptable to the encapsulation of other bioactive molecules. On this point, the method used present a severe limitation. It indeed requires laborious work for ultimately few results in terms of fraction of encapsulated material. The encapsulation method is currently unprofitable and too complex to envisage an application on an industrial scale.

Given the major limitations of this encapsulation method in microtubes, it seems normal to consider redefining a new strategy. Do we really need to work with well-defined microtubes? Should we consider using other encapsulating materials? The encapsulation method developed in this thesis has potential, in particular its biocompatibility and its high degree of control because of the possibility of compartmentalization, but there are many other options to explore which would probably give more promising results. For example, we can imagine incorporating the bacteria into a formulation containing crosslinkable hydrogels in response to environmental stimuli (temperature, concentration, pH,...) and nutrients to keep the bacteria alive. We can also think of other solutions such as the use of nanoporous membranes that we would weld together in order to retain bacteria while allowing secretion products to diffuse through. Finally, we can imagine to fabricate a nanoporous sheet of the desired material on which bacterial cells would be deposited and then roll it into a tubular structure.

Bibliography

[1] Ali Khademhosseini et al. Micromolding of photocrosslinkable hyaluronic acid for cell encapsulation and entrapment. *Journal of Biomedical Materials*, *Part A*:*522–532*, *2006*.

[2] John F. et al. Next generation, sequentially assembled ultrathin films: beyond electrostatics. *Chemical Society Reviews*, *5*:*707–718*, *2007*.

[3] Liyan Wang et al. Investigation into an alternating multilayer film of poly(4-vinylpyridine) and poly(acrylic acid) based on hydrogen bonding. *Langmuir*, *15*:*1360–1363*, *1999*.

[4] Charles R. Martin. Nanomaterials: A membrane-based synthetic approach. *Science*, *266 (5193)*:*1961–1966.*, *1994*.

[5] George M. Weinstock. Genomic approaches to studying the human microbiota. *Nature*, *489*:*250–256*, *2012*.

[6] Aaron C. Anselmo et al. Layer-by-layer encapsulation of probiotics for delivery to the microbiome. *Advanced Materials*, *2016*.

[7] Karine Glinel et al. Nanofibrillar patches of commensal skin bacteria. *Biomacromolecules*, *2018*.

[8] Alain M. Jonas et al. Controlling the growth of staphylococcus epidermidis by layer-by-layer encapsulation. *ACS Applied Materials and Interfaces*, *2018*.

[9] Marina Vemmer et al. Review of encapsulation methods suitable for microbial biological control agents marina vemmer. *Biological Control*, *67*:*380–389*, *2013*.

[10] Wanlin Xu et al. Hydrogen-bonded multilayers for the release of polyelectrolyte nanotubes in biocompatible conditions. *ACS Applied Polymer Materials*, *2019*.

[11] Saghi Saghazadeh et al. Universal method to transfer membrane-templated nano-objects to aqueous solutions. *Langmuir*, *31*:*7264–7273*, *2015*.

[12] Andrés Felipe et al. Studies in Surface Science and Catalysis, volume *178*. *2019*.

[13] Yasmine Belkaid. Dialogue between skin microbiota and immunity. *Science Magazine*, *346*:*954–959*, *2014*.

[14] Michael R. Williams et al. The role of the skin microbiome in atopic dermatitis. *Curr. Allergy Asthma Rep.*, *15 (11)*:*1–10*, *2015*.

[15] Mariana Rosenthal et al. Skin microbiota: Microbial community structure and its potential association with health and disease. *Infect Genet Evol.*, *6*:*839–848*, *2011*.

[16] Michael R. Williams et al. The role of the skin microbiome in atopic dermatitis. *Springer*, *15: 65*:*1–10*, *2015*.

[17] Richard L. Gallo. S. epidermidis influence on host immunity: More than skin deep. *Cell Host Microbe*, *17 (2)*:*143–144*, *2015*.

[18] Marina Sabaté Brescó et al. Pathogenic mechanisms and host interactions in staphylococcus epidermidis device-related infection. *Front. Microbiol.*, *8*:*1–24*, *2017*.

[19] Michael Otto. Staphylococcus epidermidis. *Staphylococcus epidermidis*, *7*:*555–567*, *2009*.

[20] Rawil F. Fakhrullin et al. "face-lifting" and "make-up" for microorganisms: Layer-by-layer polyelectrolyte nanocoating. *ACS Nano*, *6*:*557–4564*, *2012*.

[21] Yang S. H. et al. Bioinspired functionalization of silica-encapsulated yeast cells. *Angew. Chem.*, *50*:*61156118*, *2011*.

[22] Fakhrullin R. F. et al. Hybrid cellularinorganic coreshell microparticles: Encapsulation of individual living cells in calcium carbonate microshells. *Langmuir*, *25*:*66176621*, *2009*.

[23] Wang B. et al. Yeast cells with an artificial mineral shell: Protection and modification of living cells by biomimetic mineralization. *Angew. Chem.*, *47*:*35603564*, *2008*.

[24] Liang K. et al. Metal-organic framework coatings as cytoprotective exoskeletons for living cells. *Adv. Mater.*, *28*:*79107914*, *2016*.

[25] AhRan Kang et al. Cell encapsulation via microtechnologies. *Biomaterials*, *35*:*2651–2663*, *2014*.

[26] Kuen Yong Lee et al. Alginate: properties and biomedical applications. *Prog Polym Sci.*, *37 (1)*:*106–126*, *2012*.

[27] Wen Fan et al. Formation mechanism of monodisperse, low molecular weight chitosan nanoparticles by ionic gelation technique. *Bioninterfaces*, *90*:*21–27*, *2012*.

[28] Eng-Seng Chan et al. Prediction models for shape and size of ca-alginate macrobeads produced through extrusion–dripping method. *Journal of Colloid and Interface Science*, *338*:*63–72*, *2009*.

[29] Connick W.J. Formulation of living biological control agents with alginate. in: Pesticide formulations. *American Chemical Society*, :*241–250*, *1988*.

[30] Lifeng Qi et al. Preparation and antibacterial activity of chitosan nanoparticles. *Carbohydrate Research*, *339*:*2693–2700*, *2004*.

[31] Patel A.V. et al. Fermentation and microencapsulation of the nematophagous fungus hirsutella rhossiliensis in a novel type of hollow beads. *Applied Microbiology Biotechnology*, *89*:*1751–1760*, *2011*.

[32] A. Bidoret et al. Cell Microencapsulation : Methods and Protocols. *Springer Nature*, *Emmanuel C. Opara (ed)* edition, *2017*.

[33] Gaëlle Roudaut et al. Applications of spray-drying in microencapsulation of food ingredients: An overview. *Macromolecules*, *40*:*1107–1121*, *2007*.

[34] J. Burgain et al. Encapsulation of probiotic living cells: From laboratory scale to industrial applications. *Journal of Food Engineering*, *104*:*467–483*, *2011*.

[35] María Chávarri et al. Probiotcs. *Intech*, everlon cid rigobelo (ed) edition, *2012*.

[36] Gardiner G.E. et al. Comparative survival rates of human-derived probiotic lactobacillus paracasei and l salivarius strains during heat treatment and spray drying. *Applied and Environmental Microbiology*, *66*:*2605–2615*, *2000*.

[37] Solmaz Behboudi-Jobbehdar et al. Optimization of spray-drying process conditions for the production of maximally viable microencapsulated l. acidophilus ncimb 701748. *Applied and Environmental Microbiology*, *31*:*1274–1283*, *2013*.

[38] M.C. et al. Raymond. Encapsulation of brewers yeast in chitosan coated carrageenan microspheres by emulsification/thermal gelation. *Artificial Cells, Blood Substitutes and Biotechnology*, *32*:*275–291*, *2004*.

[39] K. et al. Nilsson. Preparation of immobilized animal cells. *FEBS Letters*, *118*:*145–150*, *1980*.

[40] Herbert B. Scher. Controlled-release delivery systems for pesticides. *Dekker*, *1999*.

[41] Eyal Zussman. Encapsulation of cells within electrospun fibers. *Polym. Adv. Technol.*, *22*:*366–371*, *2010*.

[42] Jingwei Xie et al. Putting electrospun nanofibers to work for biomedical research. *Macromol.*, *29*:*1775–1792*, *2008*.

[43] Zussman et al. Encapsulation of bacteria and viruses in electrospun nanofibres. *Nanotechnology*, *17*:*4675–4681*, *2006*.

[44] Alvarez et al. Immobilization of bacteria in silica matrices using citric acid in the sol–gel process. *Appl Microbiol Biotechnol*, *73*:*1059–1064*, *2007*.

[45] Alvarez et al. Effect of various parameters on viability and growth of bacteria immobilized in sol–gel-derived silica matrices. *Appl Microbiol Biotechnol*, *82*:*639–646*, *2009*.

[46] Coiffier et al. Sol–gel encapsulation of bacteria: a comparison between alkoxide and aqueous routes. *J Mater Chem*, *11 (8)*:*2039–2044*, *2001*.

[47] Uiyoung Han et al. Effect of ph on the structure and drug release profiles of layer-by-layer assembled films containing polyelectrolyte, micelles, and graphene oxide. *Scientific Reports*, *6*, *2016*.

[48] Joao Borges. Molecular interactions driving the layer-by-layer assembly of multilayers. *American Chemical Society*, *114*:*8883–8942*, *2014*.

[49] Stephan T. Dubas et al. Factors controlling the growth of polyelectrolyte multilayers. *Macromolecules*, *32*:*8153–8160*, *1999*.

[50] Christian Ringwald et al. Layer-by-layer deposition of tannic acid and fe3+ cations is of electrostatic nature but almost ionic strength independent at ph 5. *Journal of Colloid and Interface Science*, *450*:*119–126*, *2015*.

[51] El Haitami et al. Tunable synthesis of prussian blue in exponentially growing polyelectrolyte multilayer films. *Langmuir*, *25*:*2282*, *2009*.

[52] You-Hao Yang et al. Super gas barrier of all-polymer multilayer thin films. *Macromolecules*, *44*:*1450–1459*, *2011*.

[53] Aliaksandr Zhuk et al. Hydrogen-bonded layer-by-layer temperature-triggered release films. *Langmuir*, *25 (24)*:*14025–14029*, *2009*.

[54] Svetlana A. et al. Layered, erasable polymer multilayers formed by hydrogen-bonded sequential self-assembly. *Macromolecules*, *35*:*301–310*, *2002*.

[55] Susan E et al.. ph-responsive properties of multilayered poly(l-lysine)/hyaluronic acid surfaces. *Biomacromolecules*, *4*:*1773–1783*, *2003*.

[56] Sukhishvili et al. Hydrogen-bonded multilayers of a neutral polymer and a polyphenol. *Macromolecules*, *41*:*39623970*, *2008*.

[57] Veronika Kozlovskaya et al. Hydrogen-bonded lbl shells for living cell surface engineering. *Soft Matter,*, 7:*2364–2372*, *2011*.

[58] Tengfei Liu et al. Biomedical applications of layer-by-layer self-assembly for cell encapsulation: Current status and future perspectives. *Adv. Healthcare Mater.*, *8*:*1–16*, *2019*.

[59] P. Apel. Track-etching technique in membrane technology. *Radiation Measurements*, *34*:*559–566*, *2001*.

[60] R. C. Furneaux et al. The formation of controlled-porosity membranes from anodically oxidized aluminium. *Nature*, *337 (12)*:*856–866*, *1989*.

[61] Ilaria Ghidoni. Alginate cell encapsulation: new advances in reproduction and cartilage regenerative medicine. *Springer*, *58*:*49–56*, *2008*.

[62] T. Jankowski et al. Encapsulation of lactic acid bacteria with alginate/starch capsules. *Biotechnology Techniques*, *11*:*31–34*, *1997*.

[63] Riccardo Muzzarelli et al. Antimicrobial properties of n-carboxybutyl chitosan. *Antimicrobial Agents and Chemotherapy*, *34 (10)*:*2019–2023*, *1990*.

[64] Michael T. Cook et al. Production and evaluation of dry alginate-chitosan microcapsules as an enteric delivery vehicle for probiotic bacteria. *Biomacromolecules*, *12*:*2834–2840*, *2011*.

[65] Jing Zhang et al. Synthesis and characterization of ph- and temperature-sensitive poly(methacrylic acid)/poly(n-isopropylacrylamide) interpenetrating polymeric networks. *Macromolecules*, *33*:*102–107*, *2000*.

[66] Elena A. Markvicheva et al. Immobilized enzymes and cells in poly(n-vinyl caprolactam)-based hydrogels. *Applied Biotechnology and Medicine*, *88*:*145–157*, *2000*.

[67] Fluorescence microscope. `https://en.wikipedia.org/wiki/Fluorescence_microscope` [Accessed: 26.10.19].

[68] Confocal microscopy. `https://en.wikipedia.org/wiki/Confocal_microscopy` [Accessed: 26.10.19].

[69] Joseph R. Lakowicz. Principles of fluorescence spectroscopy. *Springer Science Business Media*, *2013*.

[70] Scanning electron microscope. `https://en.wikipedia.org/wiki/Scanning_electron_microscope` [Accessed: 26.10.19].

[71] Xuedong Zhou and Yuqing Li. Atlas of Oral Microbiology. *Healthy Microflora to Disease*, *2015*.

[72] Friedrich Widdel. Theory and measurement of bacterial growth. *Grundpraktikum Mikrobiologie*, *4*:*1–11*, *2010*.

Annex

SEM images

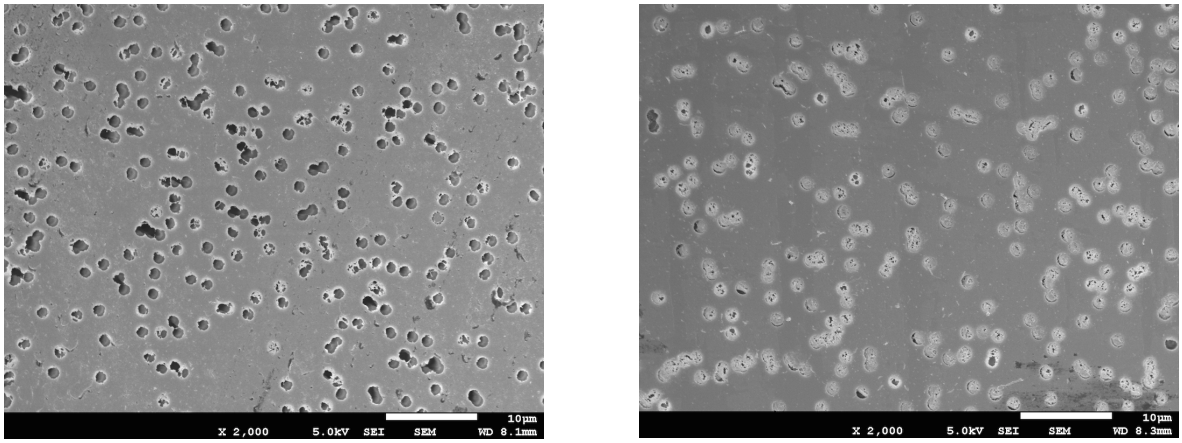

Figure 4.1: Top (left) and bottom (right) surfaces of the membrane after the LbL deposition of microtubes and decrusting of the top surface in a 3M salt solution.

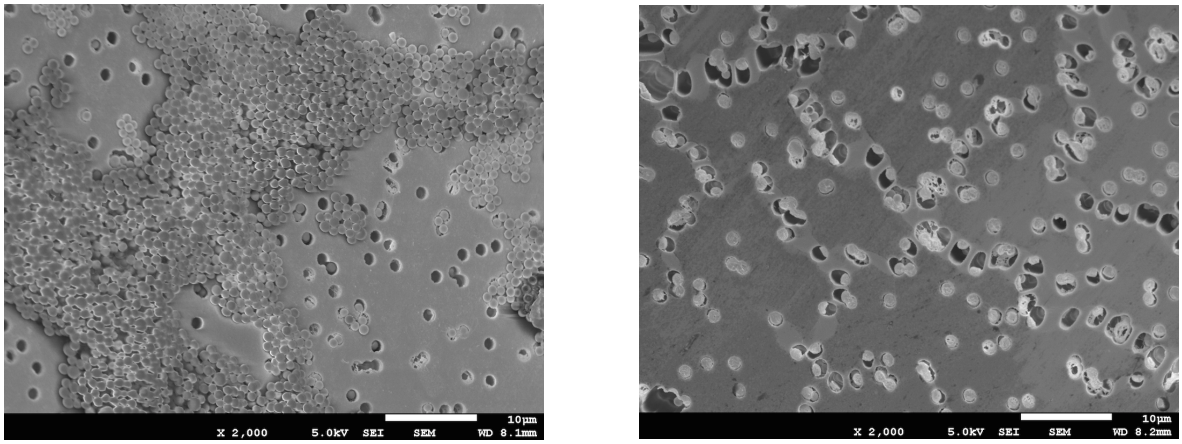

Figure 4.2: Top (left) and bottom (right) surfaces of the membrane after the loading of microparticles by forced filtration.

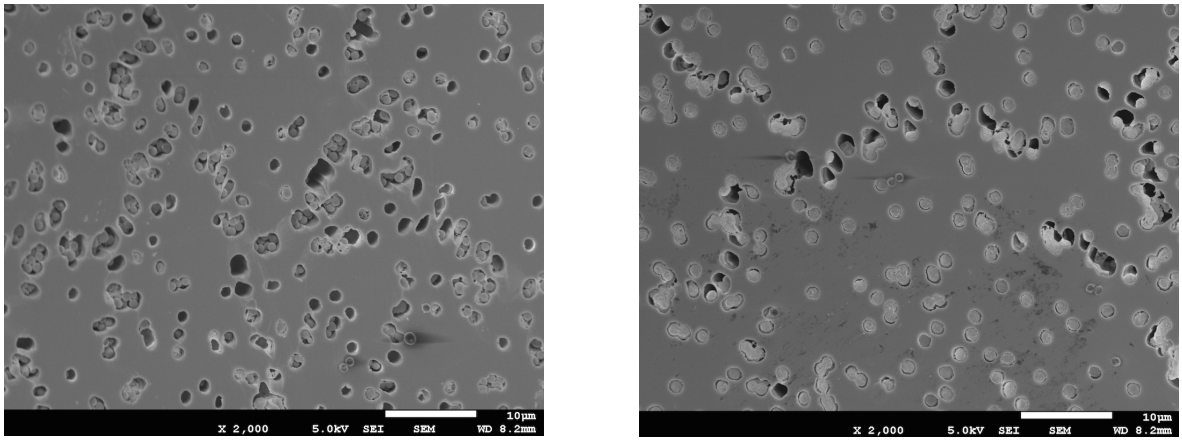

Figure 4.3: Top (left) and bottom (right) surfaces of the membrane after decrusting of the cake of microparticles.

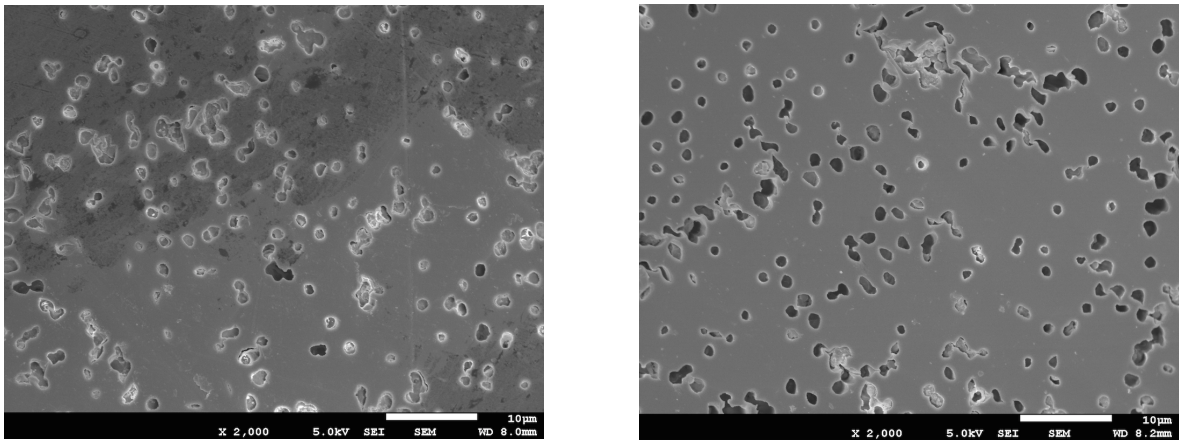

Figure 4.4: Top (left) and bottom (right) surfaces of the membrane after the LbL deposition of 10 ALG/CHI bilayers on the top surface of the membrane.

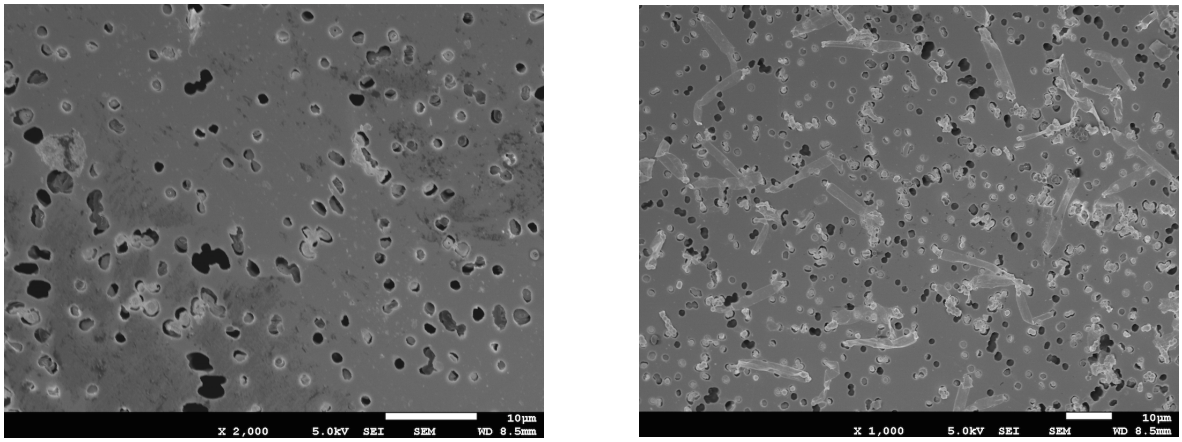

Figure 4.5: Top (left) and bottom (right) surfaces of the membrane after release of the microtubes at pH 6.5.

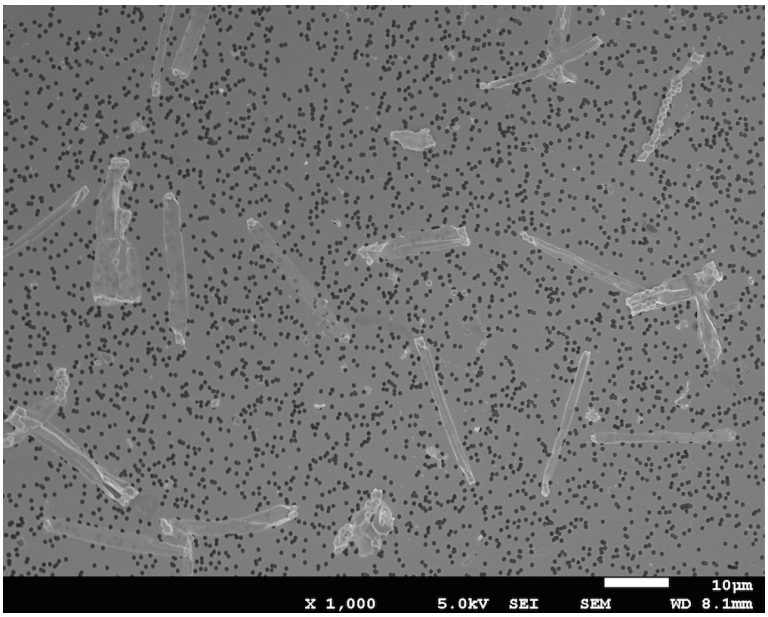

Figure 4.6: Released microtubes.

CLSM images

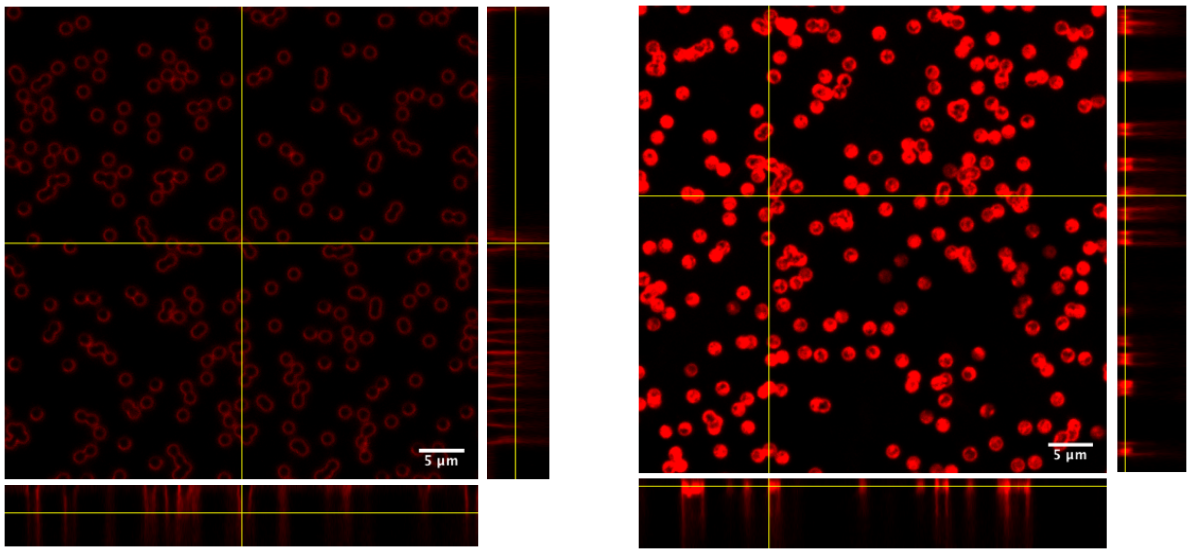

Figure 4.7: Top (left) and bottom (right) surfaces of the membrane after the LbL deposition of microtubes and decrusting of the top surface in a 3M salt solution.

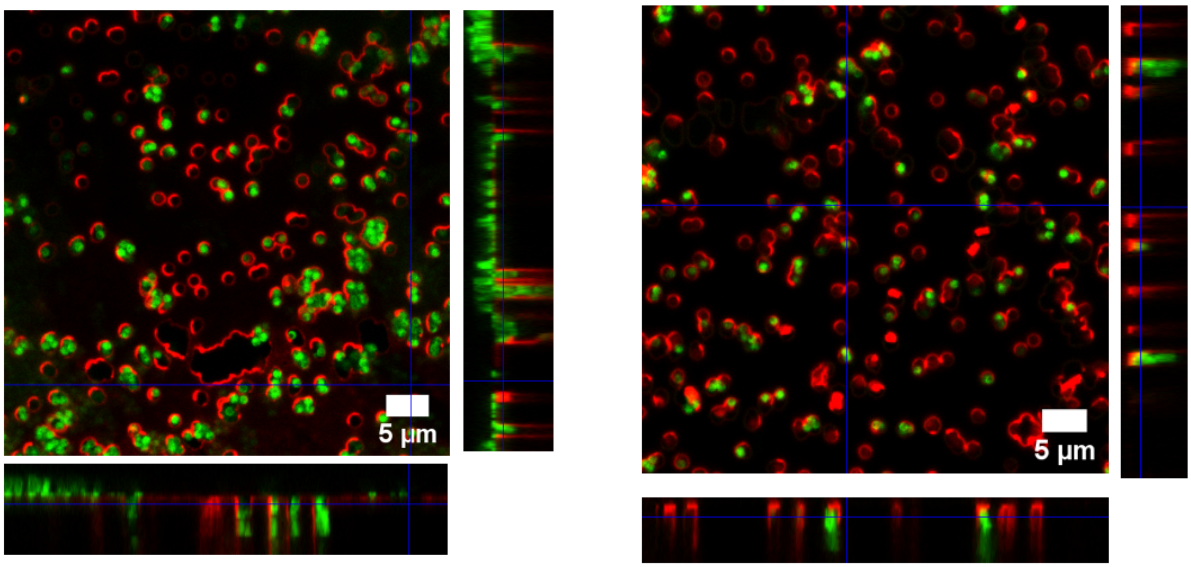

Figure 4.8: Top (left) and bottom (right) surfaces of the membrane after the loading of microparticles by forced filtration.

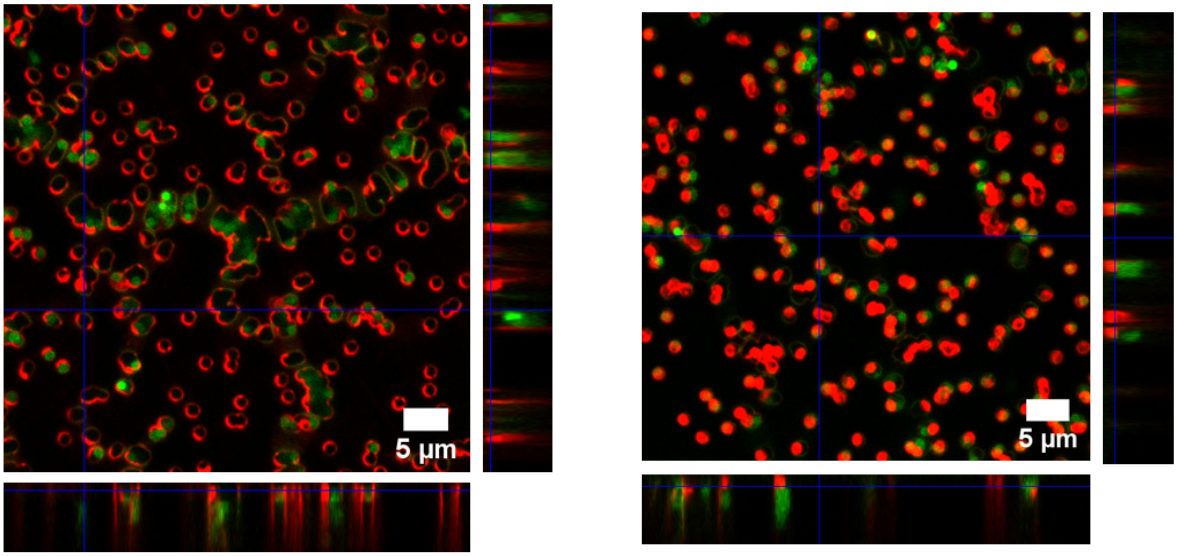

Figure 4.9: Top (left) and bottom (right) surfaces of the membrane after decrusting of the cake of microparticles.

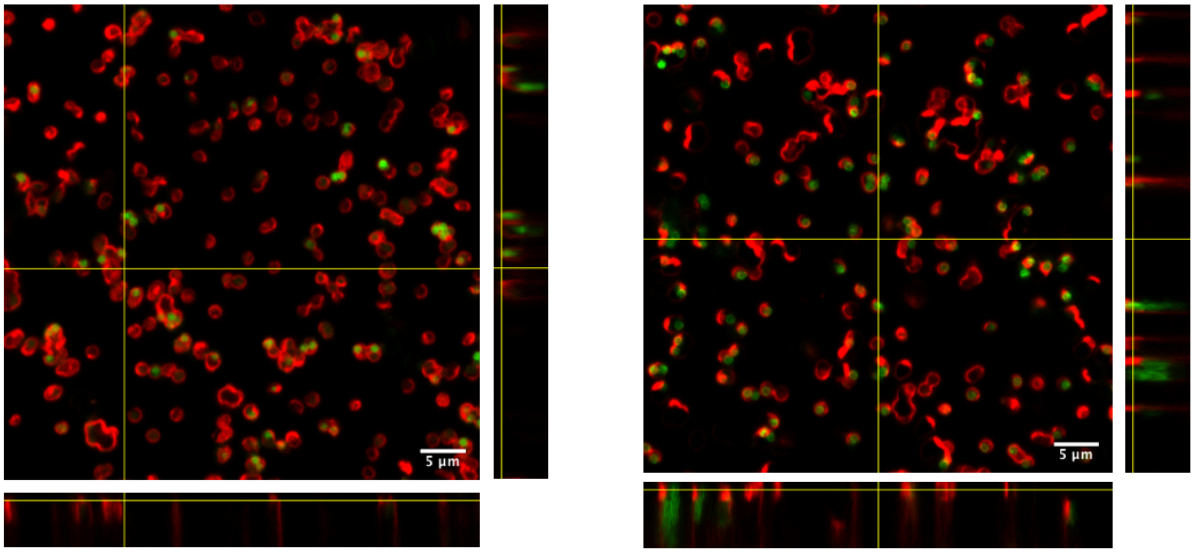

Figure 4.10: Top (left) and bottom (right) surfaces of the membrane after the LbL deposition of 10 ALG/CHI bilayers on the top surface of the membrane.

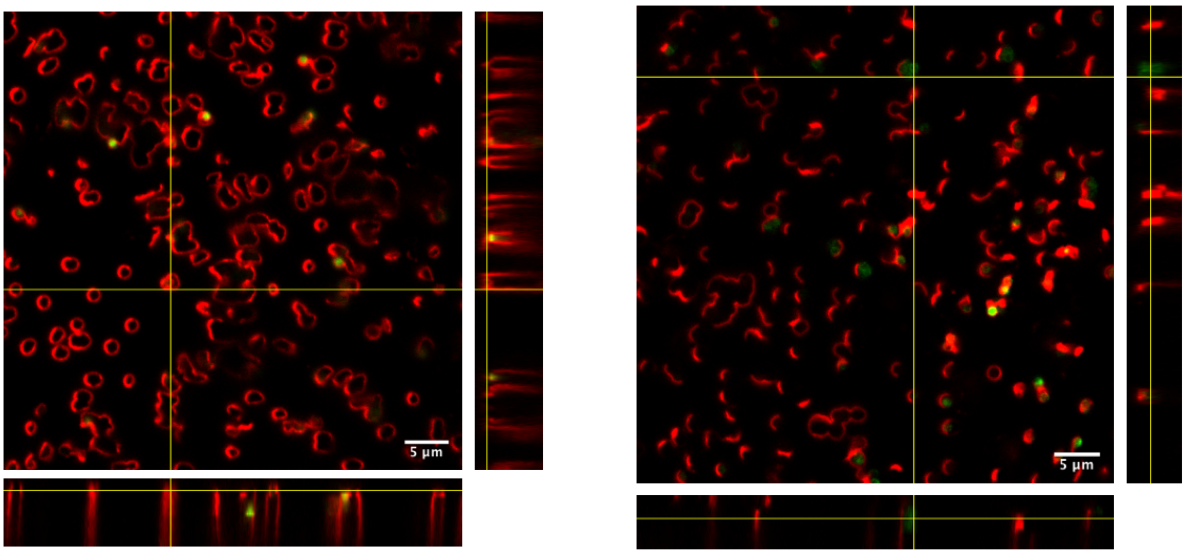

Figure 4.11: Top (left) and bottom (right) surfaces of the membrane after release of the microtubes at pH 6.5.

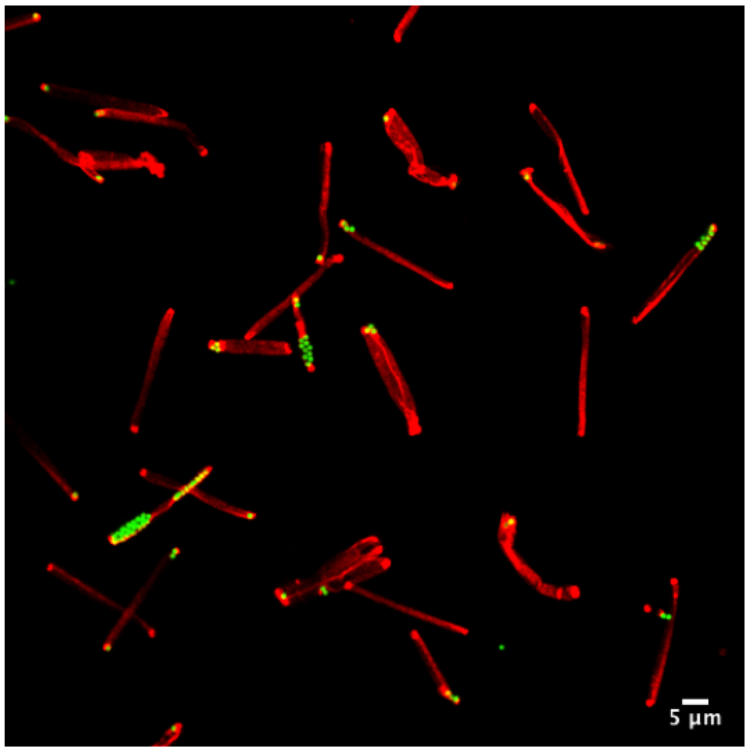

Figure 4.12: Released microtubes.

UNIVERSITÉ CATHOLIQUE DE LOUVAIN
École polytechnique de Louvain
Rue Archimède, 1 bte L6.11.01, 1348 Louvain-la-Neuve, Belgique | **www.uclouvain.be/epl**